2014-09-30

Mechanical, Rheological and Thermal Properties of Polyethylene (PE)/Clay Nanocomposite for Rotomolded Containers

Jamshidi, Shadi

UNIVERSITY OF CALGARY

Mechanical, Rheological and Thermal Properties of Polyethylene (PE)/Clay Nanocomposite for Rotomolded Containers

by

Shadi Jamshidi

A THESIS SUBMITTED TO THE FACULTY OF GRADUATE STUDIES AND RESEARCH

IN PARTIAL FULLFILLMENT OF THE REQUIREMENTS FOR THE

DERGREE OF MASTER OF ENGINEERING

DEPARTMENT OF CHEMICAL AND PETROLEUM ENGINEERING

CALGARY, ALBERTA

September 2014

Abstract

Polyethylene (PE) is widely used to make bulk containers via rotational molding process. Adding 2 wt % and 4 wt % organo-modified clay improved the thermal, barrier and mechanical properties of PE. Clay layers create a tortuous path against the permeant, yielding better barrier properties. Due to the non-polar hydrophobic nature of PE and polar hydrophilic structure of clay minerals, a compatibilizer (PE-g-Maleic Anhydride) was required to enhance the dispersion level of clay in the matrix. In this study High Density Polyethylene (HDPE) and Linear Low Density Polyethylene (LLDPE) layered silicate nanocomposites were melt-compounded with two concentrations of organo-modified clay (2 and 4 weight %). The interaction between nanoclay, compatibilizer and rotomolding grade of PE were examined using X-ray diffraction (XRD), transmission electron microscopy (TEM), mechanical and rheological tests. The XRD results revealed an enhanced basal spacing of layered silicates within both LLDPE nanocomposites at low nanoclay loadings, in agreement with the TEM observations; TEM images showed a uniformly dispersed layered silicates. Through thermal and rheological characterization techniques, the results illustrated that the thermal resistance, elastic and viscous modulus of nanocomposites improved significantly with incorporation of layered silicates. Analyzing all the data showed enhanced properties of LLDPE nanocomposites, which can be attributed to a strong interfacial interaction between the compatibilizer with LLDPE backbone and LLDPE matrices compared with HDPE matrices. The influence of in-house organo-modification of layered silicates on the properties of nanocomposites was compared to that of nanocomposites prepared with commercially available nanoclay (Cloisite 20A). LLDPE nanocomposites prepared by the in-house organo-modified clay showed better mechanical properties, elastic and viscous modulus due to good dispersion of layered silicates as determined by the XRD patterns. In addition, the

complex viscosity measurements and sintering experiments allowed us to obtain a general understanding of the behavior of pure PE and nanocomposites at low shear rate processing conditions. The results showed only a modest decrease in sintering rate of LLDPE (8555)/clay nanocomposites which is ascribed to an enhanced miscibility and interaction of the nanocomposite components. Thus, processing times for LLDPE/clay nanocomposites should be comparable to pure LLDPE.

Acknowledgements

I would like to express my sincere appreciation to my supervisor, Dr. Uttandaraman Sundararaj, for having given me the opportunity to work under his supervision. I very much appreciate his continuous support and tutelage, without which this work would have been far more difficult.

I am thankful to Imperial Oil Ltd. for funding this project and supplying the materials. Specially, I want to express my gratitude for the several valuable comments provided with Mr. Ronald Cooke, Imperial Oil Ltd.

I am so grateful to all the members of Polymer Processing Group (PPG) for their kind help particularly, Dr. Maryam Khajehpour and Dr. Mehdi Mahmoodi who have helped me in different ways for this project. I would like to thank my committee members: Dr. Mahinpey, Dr. Nassar and Dr. Sudak for their insights and comments. I would also like to acknowledge Dr. Tobias Fürstenhaupt and Dr. Wei-Xiang Dong, Mr. Kent Paulson and Mr. Brandon Ferguson for their contributions in TEM images and tensile tests.

Last but not least, I am indebted the deepest gratitude to my father for his support in all ups and downs; my brothers Arash and Payam, and their beautiful spouses Sara and Sanam for their unconditional support and love; also, my mother whose her memories are my perennial motivation and inspiration and pave the way to my success. At the end, I am thankful to my friend, Vahid Hoghooghi, for his precious help and guidance.

Dedicated to my beloved Parents and Brothers

for their unconditional love and endless support

Table of contents

List of tables

List of figures

List of symbols, abbreviation and nomenclature

ΔH_C^0	Enthalpy of 100 % crystalline polymer
ΔH_C	Enthalpy of polymer
ΔH_C	Enthalpy of cooling
ΔH_m	Enthalpy of melting
a_T	Shift factor
C_1, C_2	Constants in WLF equation
C20A	Cloisite 20A
CEC	Cation exchange capacity
Co	Cobalt
Cu	Copper
$d_{(001)}$	Basal spacing
DDAB	dimethyldioctadecylammonium bromide
DSC	Diffraction scanning calorimeter
e	Strain
G’	Storage modulus
G”	Loss modulus
HDPE	High density polyethylene
He	Helium
HMW	High molecular weight
HRR	Heat release rate
HT	Hydrogenated tallow
L/D	Length/diameter

LLDPE	Linear low density polyethylene
LMW	Low molecular weight
LS	Layered silicates
MA	Maleic anhydride
MFI	Melt flow index
MMT	Montmorillonite
MMW	Medium molecular weight
N6	Nylon-6
O	Oxygen
OMLS	Organo modified layered silicates
PCL	Polycaprolactone
PE	Polyethylene
PE-g-MA	Polyethylene grafted maleic anhydride
PEO	Polyethylene oxide
PNC	Polymer nanoclay
PP	Polypropylene
PS	Polystyrene
PVA	Polyvinyl alcohol
Si	Silicone
$T_{0.5}$	Temperature at 50 % degradation of initial weight
$T_{0.9}$	Temperature at 10 % degradation of initial weight

T_c	Crystallinity temperature
TEM	Transmission electron microscopy
T_g	Glass transition temperature
TGA	Thermo gravimetric analysis
T_m	Melting temperature
T_S	Reference temperature
wt	Weight
XRD	X-ray diffraction
η*	Complex viscosity
σ	Stress
X_C	Degree of crystallinity
ω	Frequency
ω_S	Reference frequency

Chapter 1 – Introduction

1-1. General Background

Polyethylene (PE) is widely used in the rotational molding industry due to its good flow properties, thermal stability and impact properties (1). However its poor permeation resistance to hydrocarbon solvents and gases, such as oxygen, nitrogen and volatile fuel, remains a challenge. Several techniques have been used to improve the barrier properties of PE, including surface treatment, co-extrusion, and blending (2, 3). Unfortunately, high cost and lack of compatibility between materials make each of these methods less appealing for industry. Recently, the incorporation of organo-modified layered silicates (OMLS), as an impermeable phase, into the PE matrix has attracted much attention. In fact, clay layers create a tortuous path against the permeant, yielding better barrier properties, especially for gases (4, 5). Due to the non-polar hydrophobic nature of PE and the polar hydrophilic structure of clay minerals, compatibilizer plays a crucial role in enhancing the dispersion level of layered silicates in the matrix (6). In addition, organo-modification of the layered silicates, through ion exchange reactions with a cationic surfactant, can decrease the cohesive forces between the layered silicates. Consequently, this enhances the interaction between the layered silicates and PE matrix (4). Furthermore, the barrier properties of the PE/clay nanocomposites depend not only on the dispersion of layered silicates, but also on the interaction between the compatibilizer and both the matrix and layered silicates surface. A good dispersion of layered silicates, along with a strong interaction between nanocomposite components can pave the way for a reduction in the diffusion rate of the permeant.

In the case of PE/clay nanocomposites, although they have been extensively studied in high-pressure industrial plastic processes such as extrusion and injection molding (7, 8), their properties and the behaviors have not been investigated in low-shear processes, such as rotational molding. Indeed, very few attempts have been reported in the literature about using polymer nanocomposites for the rotational molding process. In one study, lamellar graphite was incorporated into ethylene–propylene copolymer to increase the thermal conductivity of polyolefin and, consequently, reduced the processing cycle time (9). To match the surface energy of the graphite and polyolefin, graphite's surface was treated using acid solutions. In another study, polyamide-6 (PA6) and its nanocomposites were used in the rotational molding process (10). It was found that without a thermal stabilizer, the PA6 nanocomposites had a narrower processing temperature window than the pure PA6. The key aspects to consider are the effects of the layered silicates on processing at the very low shear rates for rotomolding. Therefore, the study of the rheological behavior, along with the sintering behavior, of nanocomposites can be used as fundamental information to understand the rotational molding processing cycle and the properties of the final product (11).

1-2. Objectives and Thesis Outline

The current study is part of a project with the objective of investigating the effects of using various types of organo-modified layered silicates (OMLS) at different concentrations, along with compatibilizer, on the thermal, rheological, mechanical and barrier properties of rotomolded polyethylene (PE) nanocomposites. The effect of very low shear rates for rotomolding - essentially zero shear viscosity - is also considered in the sintering behavior of the PE nanocomposites. Performing rotational molding on the best PE nanocomposite samples, according to the above studies, also will take place. To carry out the objectives, three rotational

molding grades of LLDPE and HDPE, along with an injection molding grade of HDPE, from Imperial Oil Ltd., were used as the polymer matrices, due to their vast industrial usage.

This thesis comprises six chapters, including this introduction (Chapter 1). A review of relevant literature of nanoclay and polymer/clay nanocomposites' characteristics is presented in Chapter 2. At the end of this chapter, several important aspects of the rotational molding process are also reviewed. In Chapter 3, the material properties, as well as the experimental and characterization setups used in this study are presented. The nanocomposites' characterization results are also discussed. Chapter 4 focuses on the synthesis of in-house organo-modified clay and their nanocomposites' characterizations as compared with those nanocomposites prepared with commercial organo-modified clay. Sintering experiments and a discussion of their results are presented in Chapter 5. Finally, Chapter 6 gives the conclusions and recommendations for future work.

1-3. References

1. Crawford RJ, Crawford RJ, Throne JL. Rotational molding technology: William Andrew; 2001.

2. Yeh JT, Huang SS, Chen HY. Barrier resistance of polyethylene, polyethylene/modified polyamide, and polyethylene/blends of modified polyamide and ethylene vinyl alcohol bottles against permeation of polar and nonpolar mixed solvents. Journal of applied polymer science. 2005;97(3):1333-44.

3. Flodberg G, Hellman A, Hedenqvist MS, Sadiku ER, Gedde UW. Barrier properties of blends based on liquid crystalline polymers and polyethylene. Polymer Engineering & Science. 2000;40(9):1969-78.

4. Sinha Ray S, Okamoto M. Polymer/layered silicate nanocomposites: a review from preparation to processing. Progress in polymer science. 2003;28(11):1539-641.

5. Ray SS. Clay-containing polymer nanocomposites: from fundamentals to real applications: Newnes; 2013.

6. Reichert P, Nitz H, Klinke S, Brandsch R, Thomann R, Mülhaupt R. Poly (propylene)/organoclay nanocomposite formation: influence of compatibilizer functionality and organoclay modification. Macromolecular Materials and Engineering. 2000;275(1):8-17.

7. Zhang M, Sundararaj U. Thermal, rheological, and mechanical behaviors of LLDPE/PEMA/clay nanocomposites: effect of interaction between polymer, compatibilizer, and nanofiller. Macromolecular Materials and Engineering. 2006;291(6):697-706.

8. Shah RK, Paul DR. Organoclay degradation in melt processed polyethylene nanocomposites. Polymer. 2006;47(11):4075-84.

9. Planes E, Duchet J, Maazouz A, Gerard JF. Characterization of new formulations for the rotational molding based on ethylene–propylene copolymer/graphite nanocomposites. Polymer Engineering & Science. 2008;48(4):723-31.

10. Dasari A, Yu Z-Z, Mai Y-W, Liu S. Flame retardancy of highly filled polyamide 6/clay nanocomposites. Nanotechnology. 2007;18(44):445602.

11. Bellehumeur CT, Bisaria MK, Vlachopoulos J. An experimental study and model assessment of polymer sintering. Polymer Engineering & Science. 1996;36(17):2198-207.

Chapter 2 – Literature review

The present chapter reviews several unique structural aspects and properties of nanoclay along with the methods for improving the interaction between polymer and nanoclay. This is followed by a discussion of the morphology, preparation, properties and melt rheology of polymer/clay nanocomposites. A brief introduction to rotational molding process, with its advantages and disadvantages are included. Finally, powder sintering is introduced as a dominant step in rotational molding.

2-1. Nanoclay

2-1-1. Structure and Properties of Nanoclay

Clay, a widely popular compound in modern times, has been used in building materials, paints, plastics, rubbers, cosmetics and medicines. As defined by the Clay Mineral Society, clay is a "naturally occurring material composed primarily of fine-grained minerals, which is generally plastic at appropriate water contents and will harden when dried" (1).

Recently, using nanoclay in polymer nanocomposites attracts great interest, both in industry and academia, since it is possible to achieve remarkable property enhancements as compared to pure polymer or conventional microcomposites (2). These improvements include high moduli increased strength and heat resistance, decreased gas permeability and flammability, and increased biodegradability of biodegradable polymers (1-3).

Phyllosilicates with a silicone to oxygen ratio of 2:5 (Si_2O_5), are the most important type of clays for the preparation of polymer nanocomposites. Phyllosilicates mineral have layers, or sheet-like structures that create clays commonly referred to as layered silicate (LS) (3). The crystal structure of layered silicates is built up of two tetrahedral sheets and one octahedral sheet.

The structure 2:1 layered silicates are shown in Figure 2-1. The thickness of each layer is around 1 nm and the lateral dimension may vary from 30 nm to several microns(3). These stacked layers have a van der Waals gap between layers, which is called the *interlayer* or *gallery*.

Isomorphous substitution within the layers can cause the formation of negative charges on clay layers, as seen, for example, in the substitution of Al^{3+} by Mg^{2+} and Fe^{2+} or Mg^{2+} by Li^{1+}. These charges are counterbalanced by alkali and alkaline earth cations situated inside the galleries (3). This type of layered silicate is characterized by a moderate surface charge known as the cation exchange capacity (CEC), and is generally expressed as mequiv/100 g of clay. This charge is not locally constant, but varies from layer to layer, and must be considered as an average value over the whole crystal (3).

Among all types of layered silicates, montmorillonite (MMT), saponite and hectorite are the most commonly used clays for the production of polymer nanocomposites. Two types of structure for layered silicates are tetrahedrally and octahedrally substituted. The polymer can react or interact more easily with the tetrahedral structure compared with the octahedral type, because negative charges are located on the surface of silicate layers (2, 4), as shown in Figure 2-1.

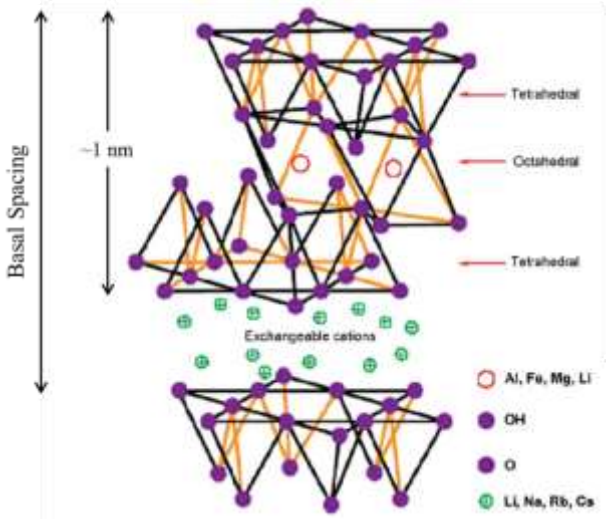

Figure 2-1 – Crystal structure of 2:1 layered silicates, reproduced from (4)

Layered silicates have two particular characteristics that make them perfect for mixing with polymer to prepare polymer nanoclay (PNC) nanocomposites. The first characteristic is the dispersion of layered silicates into individual layers in the polymer matrix and the second is the finely tuned surface made through cation exchange reactions with organic and inorganic cations. Both characteristics are dependent on each other, since the dispersion of layered silicate in a particular polymer is related to the interlayer cation (3).

2-1-2. Structure and Properties of Organically Modified Nanoclay

As mentioned above, the isomorphous substitution within the layers of silicates produces clays with a net negative charge. Thus, sodium, and potassium ions may be attracted to the surface to neutralize layer charges. In this state, LS are only miscible with hydrophilic polymers, such as Polyethylene Oxide (PEO) (5) and Polyvinyl Alcohol (PVA) (6). Mixing hydrophilic LS with other polymers such as polyethylene (PE) and polypropylene (PP), however, still remains a challenge for scientists (7) due to the non-polar nature of these polymers and the highly hydrophilic structure of layered silicates. To make LS compatible with a nonpolar polymer

matrix, therefore, an ion exchange reaction can be used for converting hydrophilic LS to organophilic LS. Through this reaction, the LS are modified by cationic surfactants (3, 4) such as primary, secondary, tertiary and quaternary alkylammonium or alkylphosphonium compounds (3, 4), which results in an organo modified layered silicate (OMLS). The cation exchange reactions lower the surface energy of inorganic silicate layers and improve the wetting characteristic of polymer matrix. OMLS can also increase the basal spacing (d_{001}) of silicate layers. Consequently, higher basal spacing, together with an organophilic surface, makes the OMLS a good candidate for mixing with PE.

2-1-3. Cation Exchange Mechanism

As mentioned above, clay layers consist of negative charges due to the substitution of Al^{3+} by Mg^{2+} and Fe^{2+} or Mg^{2+} by Li^{1+}. The negative charges can be replaced by Na^{+} and Ca^{2+}on the surface of layers. The size and degree of hydration energy of these cations affect the attraction between the layers of nanoclay; for instance, K^{+}, NH_4^{+} and Cs^{+} are large and less hydrated monovalent cations, while Na^{+}, Li^{+} and P^{+} have a higher hydration energy, which decreases the attraction between the silicate layers and increases the basal spacing between the layers (3). Alkyl-ammonium or phosphonium salt, replaced by the "intergallery cations", can improve the basal spacing between the layers but may also enhance the interaction of the polar nanoclay and nonpolar polymer matrix. It is believed that a good interaction between the nanoclay and polymer matrix is essential for dispersion in nanoscale. Otherwise, organic and inorganic components of the polymer nanocomposite will have poor adhesion, leading to poor mechanical and thermal properties.

The concentration of the modifier is determined based on the cation exchange capacity (CEC) of nanoclay. In general, the common concentration of the modifier is 1.1 CEC (8).

Research by Seyidoglu and Xi, who studied the effects of higher concentrations of modifier reveals that using an excess amount of surfactant in the cation exchange reaction is not necessary for increasing the basal spacing of layered silicates (8, 9).

2-2. Polymer/Nanoclay Nanocomposites

2-2-1. Morphology of Polymer/Clay Nanocomposite

The structure and properties of polymer/clay nanocomposite are governed mainly by the interfacial interaction of layered silicates and the polymer matrix. They are divided into two groups: microcomposite and nanocomposite. The conventional type of microcomposite is the *immiscible* structure in which the polymer matrix and layered silicates formed separated phases and the basal spacing remains unchanged (10). Another group is polymer layered silicates nanocomposite (PLS) that are classified based on the strength of the interactions. These have three types of structure which are thermodynamically achievable (2, 4). In an *intercalated* structure, polymer chains intercalate between the layered structures of the clay and effectively expand the distance between the layers. Polymer chains penetrate inside the galleries of layered silicates and make a "crystallographically regular fashion" structure (3, 4). A *flocculated* structure conceptually, is similar to an intercalated one; however in this structure, silicate layers become flocculated due to the hydroxilated edge-edge interaction. The last type is the *exfoliated* structure in which layered silicates are separated to their individual layers. The layers disperse continuously in the polymer matrix at random orientation and have an average distance with a value that is dependent on the amount of nanoclay loading. All structures of polymer layered silicates nanocomposites are shown in Figure 2-2.

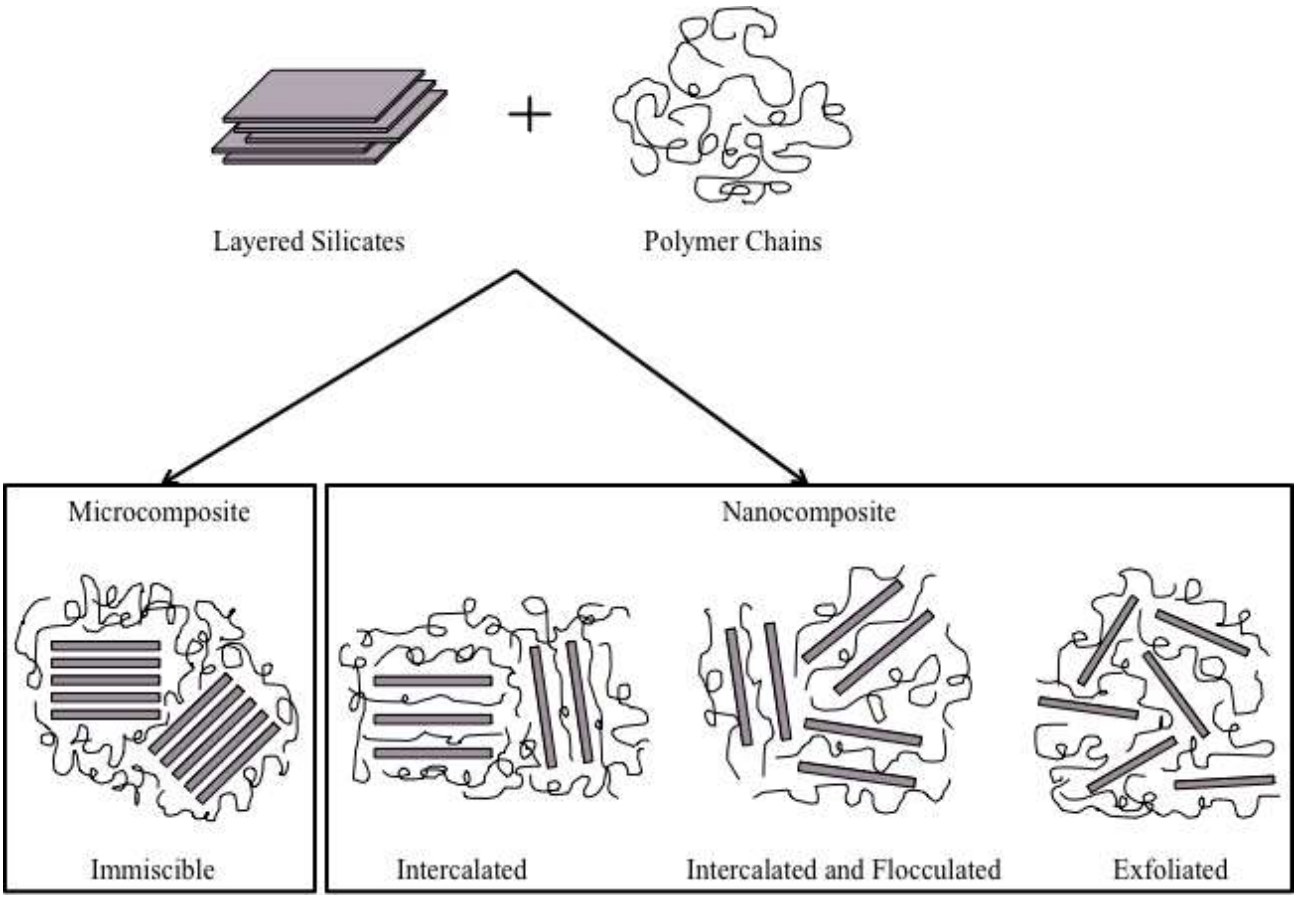

Figure 2-2 – Different structures of polymer layered silicates (PLS) nanocomposite, reproduced from (10)

2-2-2. Preparation Method of Polymer/Clay Nanocomposite

In this section, three main methods for preparation of polymer layered silicate nanocomposites are explained. The differences between these methods are the result of the initial materials and the processing techniques used (3, 4, 10).

Intercalation of polymer or pre-polymer from solution: Basically, polymer or pre-polymer is dissolved in a solvent (e.g. water, chloroform or toluene), which is appropriate for the dispersion of the silicate layers. The polymer chains intercalate into the interlayer silicates in the solution phase and remain in the intercalated structure after removal form the solvent.

Polyethylene Oxide (PEO) (5) and polyvinyl alcohol (PVA) (6) nanocomposites are examples of materials that result from using this process.

This method is limited to a limited number of polymers, which have a suitable and available solvent that is also suitable for the clay. It is useful for producing polymer nanocomposites with little or no polarity (3). However this method is not commercially viable because of high cost of solvent recovery, that making it environmentally unfriendly (3).

In situ intercalative polymerization method: In this method, the silicate layers disperse within the liquid monomer or monomer solution. The polymerization process can be initiated by heat or radiation, suitable initiator or fixed catalyst, which leads to the formation of an exfoliated structure.

Many studies have shown some interesting results for the preparation of PLS nanocomposite, such as nylon-6 (11) and polycaprolactone (PCL) (12) nanocomposites. Most factors, including the requirement for separate production lines or major changes to existing production facilities, limit the commercialization of this method.

Melt intercalation method: Structurally, polymer/layered silicates are prepared under annealing polymer glass transition or melting temperature conditions, as well as shear mixing. Above their softening point polymer chains move easily, and can intercalate between silicate layers. In Figure 2-3, a schematic of the melt intercalation method is shown.

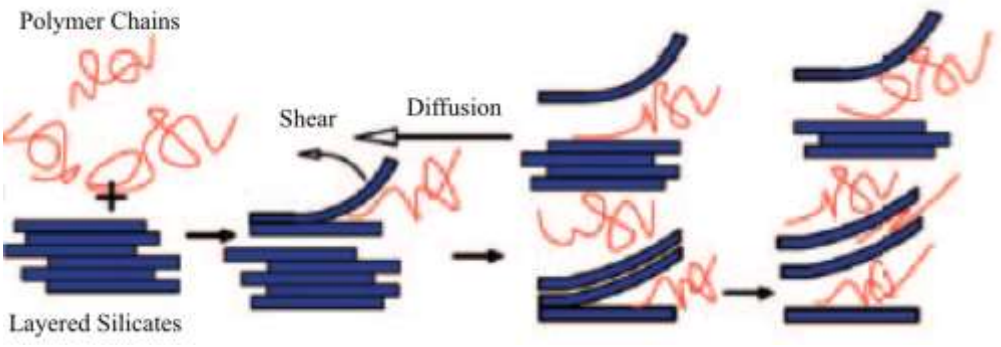

Figure 2-3 – Schematic of melt intercalation method, reproduced from (10)

This preparation method is environmentally friendly and economically favorable compared to other methods because of the absence of solvents in this technique. In addition, evidence suggests that a conventional processing technique, such as the twin-screw extruder, is an effective way for the dispersion of layered silicates within the polymer (13, 14). A range of nanocomposite structures, from intercalated to exfoliated, can be obtained by this method. Vaia and coworkers (15) produced the first Polystyrene (PS)/layered silicate nanocomposite using the melt intercalation method, suggesting that if the organoclay is compatible with the polymer matrix, even the exfoliated structure may be achieved by melt intercalation.

2-2-3. Advantages of Polymer/Clay Nanocomposite

Despite the fact that producing nanocomposites with a polymer and inorganic fillers improves properties of the material due to changes in structure and chemistry, poor interaction between polymer and inorganic fillers leads to "conventional filler-reinforced systems" without property improvement. In contrast to conventional composites, properties' enhancement can be achieved by adding a small amount of layered silicates to the polymer. The properties' improvements include enhanced modulus, strength and heat resistance, as well as decreased gas permeability and flammability.

2-2-3-1. Mechanical Properties

The tensile test (stress-strain curve) is a common method used to determine the mechanical properties of polymer nanocomposites, such as *Young's modulus*, *yield strength*, and *elongation at break*. Figure 2-4 shows an idealized stress-strain for a semi-crystalline polymer (16). The slope of the initial linear part of the stress (σ) – strain (e) curve is used to measure *Young's modulus*, an indicator of the material stiffness or rigidity. There is an elevation in the strain measure while the slope of the curve decreases, until the stress reaches to a maximum. The maximum point is identified as the *yield point*; the corresponding stress and strain are depicted in Figure 2-4. At this point, the process of necking starts in the gauge length then continues until it extends along the sample. Afterwards, the whole sample necks down; the increasing strain, as a response to the stress, is referred to as strain hardening. This process continues until the sample breaks down at a high strain. The strain corresponding to the breaking point is described as *elongation at break*. Another important value calculated from the stress-strain curve is the area under the curve, defined as the *toughness* of the sample (16).

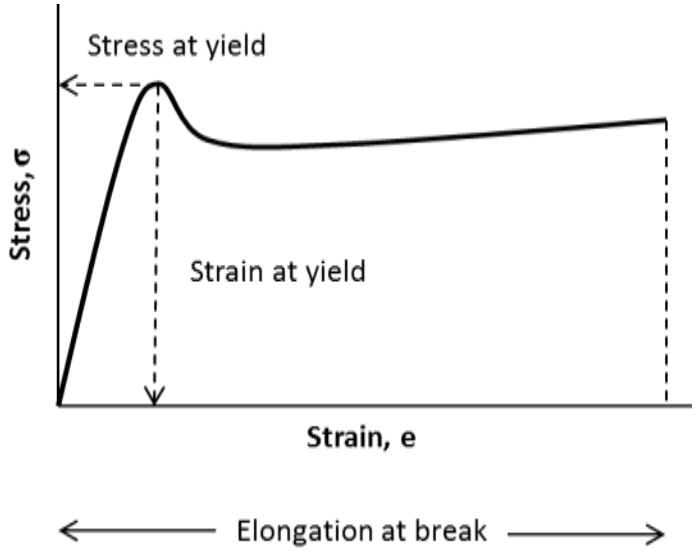

Figure 2-4 – Schematic of the stress-strain curve for semi-crystalline polymer matrix, reproduced from (16)

The mechanical properties of polymeric materials have been shown to be enhanced with incorporation of a small amount of OMLS in the polymer. With a higher interaction between the polymer and OMLS, the nanocomposites exhibit drastic improvement in tensile modulus since the stress transfers much more effectively from the polymer chains to the silicate layers. Kojima and his colleagues demonstrated significant enhancement in the mechanical properties of N6/clay nanocomposite prepared by in-situ polymerization. These drastic improvements are the result of a good interaction between the polymer chain and nanoclay via the formation of hydrogen bonds (17). In addition, they studied the effect of the aspect ratio of dispersed nanoclay within the N6 nanocomposite. The mechanical properties of the nanocomposite improved directly by using a higher aspect ratio filler (17). In summery, the proper interaction between layered silicates and polymer can significantly improve the final mechanical properties of nanocomposites in comparison with neat polymers.

In recent years, a number of the studies have investigated the function of layered silicates upon the mechanical properties of polyolefin. For instance, Manias et al., using the melt

intercalation method, examined the effect of layered silicates on the mechanical properties of polypropylene (PP)/nanoclay nanocomposites (18). Through increasing the amount of nanoclay, the mechanical properties enhanced rapidly; however, after an optimum increase, the enhancement is less pronounced. Moreover, Reichert et al., studying PP/nanoclay nanocomposite systems, found that without favorable thermodynamic interactions between the polymer, compatibilizer (e.g. PP grafted MA) and layered silicates, the structure and tensile properties change significantly by process conditions (19). Inducing good interaction between layered silicates and specific polymers, particularly non-polar polymers such as polyolefin, remains a challenge for researchers.

2-2-3-2. Barrier Properties

Many research studies show the improvement of gas barrier properties by the incorporation of nanoclay in the polymer matrix (3). The clay platelets construct a "tortuous path", as shown in Figure 2-5, which hinders the permeation of small molecule gases, such as O_2, H_2O, CO_2, Helium (He), and ethylacetate vapors, through the polymer matrix (20). The gas molecules' passage involves a longer diffusive path in the nanocomposite as compared to macrocomposites.

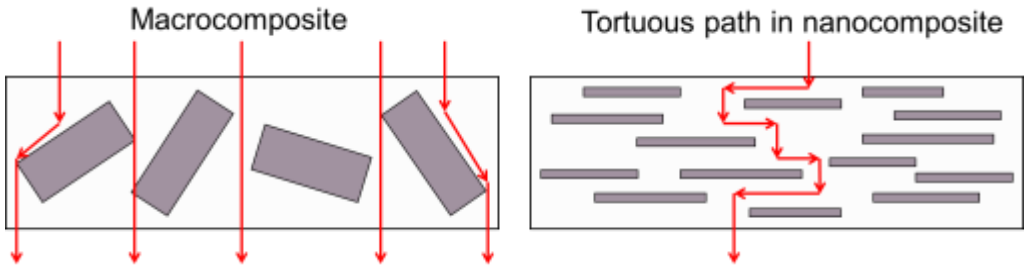

Figure 2-5 – Formation of tortuous path in polymer layered silicate nanocomposite, reproduced from (3)

Yano and Bharadwaj deciphered the improvement of gas barrier properties, which are dependent on various factors such as the relative orientation of clay platelets, the concentration

of nanoclay and the dispersion through the matrix and sheet length. These factors play important roles in producing more efficient barrier nanocomposites (20, 21).

2-2-3-3. Thermal Properties

Thermal properties are generally enhanced by the incorporation of layered silicates into the polymer matrix, since nanoclay hinders the diffusion of volatiles during thermal decomposition. Favorable thermodynamic interactions between the polymer and the surface of LS are crucial for a significant enhancement in the thermal properties of nanocomposites (22). Thermogravimetric Analysis (TGA) is usually implemented to investigate the thermal degradation rate of nanocomposites.

The thermal stability of Polyethylene (PE)-nanoclay nanocomposite has been widely studied. As above mentioned, PE and LS are not thermodynamically attracted to each other; hence, a compatibilizer, such as PE grafted maleic anhydride (PE-g-MA), can be used to improve the interaction between the polymer and layered silicates. Stoeffler and Shyh-shin investigated the effect of compatibilizer on the thermal properties of PE/layered silicate nanocomposite (23, 24). Interestingly, they found that even a small amount of compatibilizer (MA) can increase the thermal stability of nanocomposites. There is, however, an optimum for the concentration of clay to enhance the thermal stability of the nanocomposite, which is 4 wt % of the nanoclay. This is because the nanoclay agglomerates act as a heat source to increase the speed of the decomposition process (24).

In some other studies, the effect of different organically modified nanoclay on thermal properties of PS nanocomposite was investigated. They showed that the phosphonium clays have a greater thermal stability than the ammonium salts, and these results are important if the

polymer nanocomposite will be processed at high temperature (25). All of these findings suggest that using layered silicate in polymer plays a pivotal role in the thermal stability of nanocomposites.

2-2-3-4. Fire Retardant Properties

Polymer layered silicates are recognized as an enhancer in fire relevant properties, such as heat release rate (HRR), heat peak HRR and smoke production, as compared to the neat polymer materials (3, 26). A nano dispersion of layered silicates in the polymer matrix reduces the flammability due to the formation of silicate char on the surface of the nanoclay during burning. Through the decomposition, the silicate char insulates the material preventing the mass and energy diffusion within the nanocomposite. Thus, burned nanoclay, acts as a fire retardant, decreasing the rate of mass loss in the polymer layered silicates nanocomposites (27).

2-3. Rheology of Polymer/Clay Nanocomposite

Rheology is defined as "a science dealing with deformation and flow of matter" (28), and is used to understand the processability of molten material, and to explain the relationship between the structure and properties of the material. Rheological properties, such as storage and loss modulus, are significantly improved by the incorporation of layered silicates within the polymer (19, 29, 30). Improvement of rheological properties, however, is related to the degree of interaction between the polymer and nanoclay. Studying the rheological behavior of polymer layered silicate nanocomposite is important to determine the structure of PLS nanocomposites and the degree of interaction between the polymer and nanoclay (3).

2-3-1. Effect of Nanoclay on rheological properties

One of the important effects of nanoclays in polymer nanocomposites is increasing the storage modulus (G'), loss modulus (G") and viscosity at low frequency or zero shear rate (19, 29, 30). In addition, polymer nanocomposites show solid-like behavior at low frequency due to the presence of nanoclay within the polymer matrix. Ren et al. suggested that the solid-like behavior of nanocomposites at low frequency is derived from the anisotropic nature of silicate layers that cause the physical squeezing or percolation of the randomly distributed silicate layers in the polymer matrix, even at a very low fraction of nanoclay (31). The flow curve of pure polymer has a transition from a Newtonian region to a power law (shear-thinning) region (Figure 2-6). At low frequency, the viscosity of the polymer is independent of frequency, which is the Newtonian region. Furthermore, by increasing the frequency, the viscosity decreases as a power law which is the sign of shear-thinning behavior occurring in the polymer material (32). Nanocomposites sample also can show shear-thinning behavior at a higher frequency; however, this phenomenon is faster for nanocomposites as compared with pure polymer. This shear-thinning is present at low frequencies too. Hence, as the frequency increases, the rheological behavior of all nanocomposites becomes more similar to that of pure polymers. This is a result of the domination of the polymer matrix in the nanocomposite at high frequency (32). In addition, the rheological properties of nanocomposite enhance at a low frequency, due to increasing the amount of nanoclay in the nanocomposite. For instance, Fornes et al. have shown that nanocomposites have a solid-like behavior at a low frequency with the incorporation of nanoclay into polymer matrix; this behavior is primarily dependent on the amount of nanoclay (29).

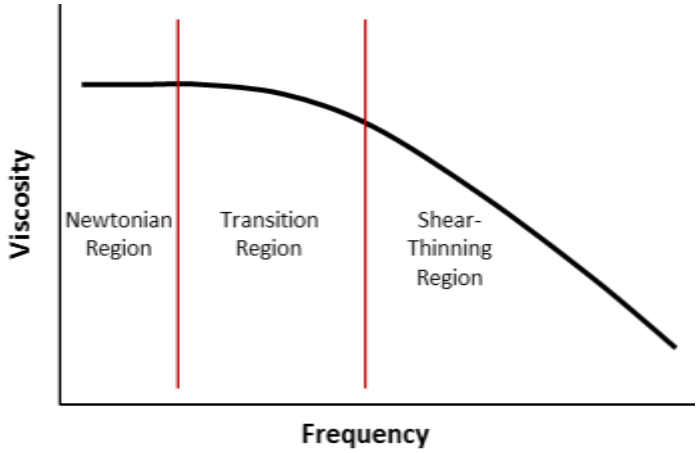

Figure 2-6 – Typical flow curve for polymer melts

Overall, improvements in the rheological properties of polymers are expected with the incorporation of nanoclay. The degree of improvement is mainly dependent on the level of interaction between all components of the nanocomposites.

2-3-2. Time-Temperature Superposition

The rheological properties of polymer are greatly dependent on the testing temperature. It is possible to interrelate the dependency of time and temperature on the viscoelastic polymer. For example, the polymer can show a glassy behavior at lower temperatures or at a higher frequency or shear rate (16). It is demonstrated that all the rheological curves can be brought together by keeping one specific temperature's curve fixed and shifting all the others by using the principles of "time-temperature superposition" (16, 28). Thus, the rheological behavior of polymer can be shown at a wide range of frequency by measuring the rheological properties at different temperatures and using "time-temperature superposition".

The amount of shift required can calculated by superposition of two curves in a plot of rheological properties versus time dependent units such as frequency, and it can be defined by shift factor (a_T). The shift factor can be calculated from using a rheological property at the

particular frequency (ω_S) point at a reference temperature T_s with the same value of rheological property at different temperature T (16). Shift factor (a_T), which is a function of temperature, is defined as follows (16):

$$\log a_T = \log \omega_S - \log \omega = log\ \omega_S/\omega \qquad \text{Eq. 2-1}$$

Williams, Landel and Ferry have shown that the shift factor can also be calculated by the WLF equation (Eq. 2-2). The WLF is defined as follows:

$$\log a_T = \frac{-C_1(T - T_s)}{C_2 + (T - T_s)} \qquad \text{Eq. 2-2}$$

C_1 and C_2, are constants and T_S is the reference temperature. This equation is usually applicable to temperatures close to the glass transition temperature of the polymer.

2-4. Rotational Molding Process

Rotational molding is a rapidly growing process for the production of large, hollow objects in one piece. The advantages of this process compared to other processes (such as injection molding, blow molding, etc.) are simplicity, less expensive molds and the production of stress-free parts (33). Rotational molding is used for the production of chemical tanks, toys, leisure crafts, and complex medical instruments (33).

Figure 2-7 – Examples of rotational molding products a) marine equipment (www.risingsunkayaks.com) b) chemical storage tanks (www.esemag.com) c) floor scrubber (www.vipercleaning.com)

Generally, rotational molding comprises the following four steps (Figure 2-8):

1) A fixed amount of thermoplastic polymer in powder, granular, or viscous liquid form is loaded in one half of a hollow metal mold.
2) The loaded mold is placed in an isothermal oven. When the polymer reaches its melting point, polymer particles sinter layer by layer, to the mold wall. During heating in the oven, the mold rotates biaxially to ensure that the polymer melts uniformly distribute on the inner surface of the mold.
3) After sufficient time for densification of the polymer, the mold is moved to the cooling section where the mold is cooled by air or water, while still rotating.
4) Finally, the solidified product, with the desired shape, is removed from the mold.

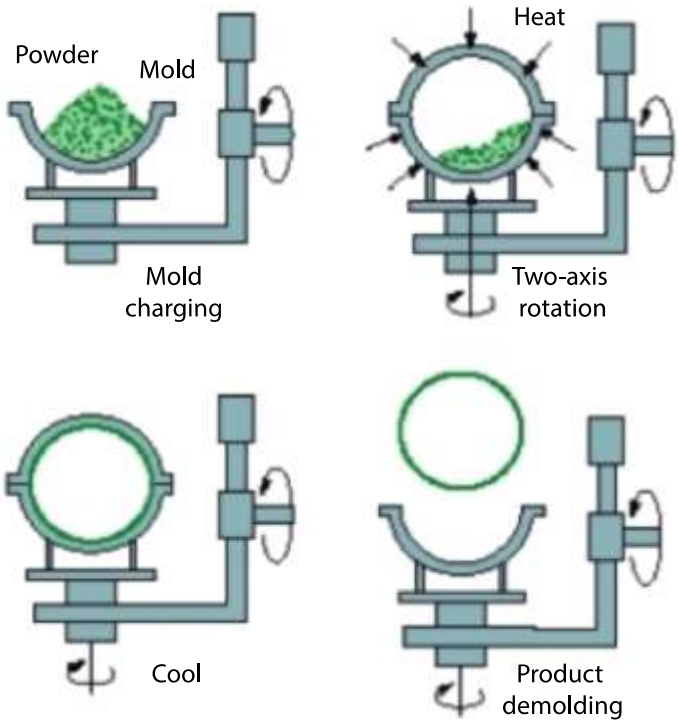

Figure 2-8 – Rotational molding process, reproduced from (www.sarmi-rotomolding.com)

2-4-1. The Material Used for Rotational Molding

Polyethylene (PE) is the dominant thermoplastic polymer for rotational molding. As shown in Figure 2-9, different forms of PE consist of more than 85 % of plastic usage for rotational molding products in North America (33).

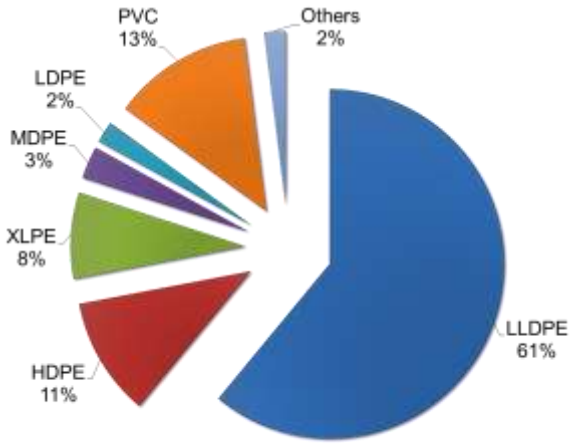

Figure 2-9 – Usage of plastics in North American rotational molding industry, reproduced from (33)

The major reasons for using PE for rotational molding are good thermal stability, modest melting point and more important, the ability to coalescence under zero shear stress. In addition, the low cost of PE makes this polymer a proper choice in the industry.

2-4-2. Powder Sintering

Sintering of the polymer powder is a dominant step in the rotational molding process. During sintering, two solid particles, at high temperature and/or pressure, form a homogenous melt (34). The surface tension between the two particles is the important drive for the coalescence of the two particles. Rao and Throne (35) found that sintering happens in two steps: first, the powder particles stick, or fuse together, at the point of contact. The diffusion point grows until the mass becomes a porous three-dimensional network. This step is referred to as sintering. Second, at some point in the diffusion process, the network begins to collapse into the void spaces. These spaces are filled with molten polymer that is drawn into the region by capillary forces. This step is interpreted as densification.

The sintering model is used to predict the rotomoldability and coalescence behavior of different grades of polymer powders. Frenkel's model is the first theoretical model derived to evaluate the early stage of the viscous coalescence of two identical spherical particles of amorphous polymer (36). A modified Frenkel's model was studied by Bellehumeur et al. (36). The model includes the surface tension as well as viscous dissipation. Through this model, analytical results showed strong agreement with experimental data.

Polymer viscosity plays an important role in the formation of neck and the rate of coalescence. On the one hand, polymers with a lower viscosity sinter with a higher rate, which is beneficial for our process. On the other hand, lower viscosity means a lower molecular weight and molecular weight distribution, which gives poor mechanical and chemical resistance. This dual character has been found in polyethylene (36).

Only Martin et al (37) studied the sinterability of polyethylene/layered silicate nanocomposite via hot-stage optical microscopy. The sinterability of nanocomposite declined in comparison to neat polyethylene, since the viscosity of the nanocomposite increases, as the rheological results showed.

2-4-3. Advantages and Disadvantages of Rotational Molding

The rotational molding process has some special advantages and disadvantages as compared to other processes, such as injection molding, blow molding, etc.

The advantages of rotational molding process are (33):

- ✓ It can produce a large hollow part in one piece without weld lines and waste scrap. Furthermore, because the end products are stress-free, they are stronger.

- ✓ It has a relatively low-cost mold since the mold has a relatively thin wall and can be made in a short time. The mold is not necessarily strong because rotational molding is accomplished through a low pressure process.
- ✓ It is possible to produce complex shape parts and multilayer products with high quality graphics (Figure 2-7).
- ✓ It is possible to design the place for inserts inside the molded parts easily.

The disadvantages of rotational molding are (33):

- ✓ It is a relatively time-consuming process due to the long heating and cooling cycles. Thus, the process is not economical for production of small parts in a large scale.
- ✓ There are limited material's choices for this process due to the high temperature and zero-shear stress process. Materials are limited to those with high thermal stability and the ability to flow easily through the mold.
- ✓ It is expensive to get a high quality polymer powder for the process.

2-5. References:

1. Bergaya F, Theng BKG, Lagaly G. Handbook of clay science: Elsevier; 2011.

2. Utracki LA. Clay-containing polymeric nanocomposites: iSmithers Rapra Publishing; 2004.

3. Ray SS. Clay-containing polymer nanocomposites: from fundamentals to real applications: Newnes; 2013.

4. Sinha Ray S, Okamoto M. Polymer/layered silicate nanocomposites: a review from preparation to processing. Progress in polymer science. 2003;28(11):1539-641.

5. Aranda P, Ruiz-Hitzky E. Poly (ethylene oxide)-silicate intercalation materials. Chemistry of Materials. 1992;4(6):1395-403.

6. Greenland DJ. Adsorption of polyvinyl alcohols by montmorillonite. Journal of Colloid Science. 1963;18(7):647-64.

7. Wang KH, Choi MH, Koo CM, Choi YS, Chung IJ. Synthesis and characterization of maleated polyethylene/clay nanocomposites. Polymer. 2001;42(24):9819-26.

8. Seyidoglu T, Yilmazer U. Production of modified clays and their use in polypropylene-based nanocomposites. Journal of Applied Polymer Science. 2013;127(2):1257-67.

9. Xi Y, Frost RL, He H, Kloprogge T, Bostrom T. Modification of Wyoming montmorillonite surfaces using a cationic surfactant. Langmuir. 2005;21(19):8675-80.

10. Albdiry MT, Yousif BF, Ku H, Lau KT. A critical review on the manufacturing processes in relation to the properties of nanoclay/polymer composites. Journal of Composite Materials. 2013;47(9):1093-115.

11. Usuki A, Kojima Y, Kawasumi M, Okada A, Fukushima Y, Kurauchi T, et al. Synthesis of nylon 6-clay hybrid. Journal of Materials Research. 1993;8(05):1179-84.

12. Messersmith PB, Giannelis EP. Polymer-layered silicate nanocomposites: in situ intercalative polymerization of. epsilon.-caprolactone in layered silicates. Chemistry of materials. 1993;5(8):1064-6.

13. Vaia RA, Giannelis EP. Polymer melt intercalation in organically-modified layered silicates: model predictions and experiment. Macromolecules. 1997;30(25):8000-9.

14. Dintcheva NT, Al-Malaika S, La Mantia FP. Effect of extrusion and photo-oxidation on polyethylene/clay nanocomposites. Polymer degradation and stability. 2009;94(9):1571-88.

15. Vaia RA, Ishii H, Giannelis EP. Synthesis and properties of two-dimensional nanostructures by direct intercalation of polymer melts in layered silicates. Chemistry of Materials. 1993;5(12):1694-6.

16. Young RJ, Lovell PA. Introduction to polymers: CRC press; 2011.

17. Kojima Y, Usuki A, Kawasumi M, Okada A, Fukushima Y, Kurauchi T, et al. Mechanical properties of nylon 6-clay hybrid. Journal of Materials Research. 1993;8(05):1185-9.

18. Manias E, Touny A, Wu L, Strawhecker K, Lu B, Chung TC. Polypropylene/montmorillonite nanocomposites. Review of the synthetic routes and materials properties. Chemistry of Materials. 2001;13(10):3516-23.

19. Reichert P, Nitz H, Klinke S, Brandsch R, Thomann R, Mülhaupt R. Poly (propylene)/organoclay nanocomposite formation: influence of compatibilizer functionality and organoclay modification. Macromolecular Materials and Engineering. 2000;275(1):8-17.

20. Yano K, Usuki A, Okada A, Kurauchi T, Kamigaito O. Synthesis and properties of polyimide–clay hybrid. Journal of Polymer Science Part A: Polymer Chemistry. 1993;31(10):2493-8.

21. Bharadwaj RK. Modeling the barrier properties of polymer-layered silicate nanocomposites. Macromolecules. 2001;34(26):9189-92.

22. Gilman JW. Flammability and thermal stability studies of polymer layered-silicate (clay) nanocomposites. Applied Clay Science. 1999;15(1):31-49.

23. Stoeffler K, Lafleur PG, Denault J. Effect of intercalating agents on clay dispersion and thermal properties in polyethylene/montmorillonite nanocomposites. Polymer Engineering & Science. 2008;48(8):1449-66.

24. Hwang S-s, Hsu PP, Yeh J-m, Yang J-p, Chang K-c, Lai Y-z. Effect of clay and compatibilizer on the mechanical/thermal properties of microcellular injection molded low density polyethylene nanocomposites. International Communications in Heat and Mass Transfer. 2009;36(5):471-9.

25. Zhu J, Morgan AB, Lamelas FJ, Wilkie CA. Fire properties of polystyrene-clay nanocomposites. Chemistry of Materials. 2001;13(10):3774-80.

26. Gilman JW, Kashiwagi T, Brown JET, Lomakin S, Giannelis EP, Manias E. Flammability studies of polymer layered silicate nanocomposites. Materials and Process Affordability: Keys to the Future. 1998;43:1053-66.

27. Gilman JW, Jackson CL, Morgan AB, Harris R, Manias E, Giannelis EP, et al. Flammability properties of polymer-layered-silicate nanocomposites. Polypropylene and polystyrene nanocomposites. Chemistry of Materials. 2000;12(7):1866-73.

28. Malkin AI, Malkin AY, Isayev AI. Rheology: concepts, methods, and applications: ChemTec Publishing; 2006.

29. Fornes TD, Yoon PJ, Keskkula H, Paul DR. Nylon 6 nanocomposites: the effect of matrix molecular weight. Polymer. 2001;42(25):09929-40.

30. Zhang M, Sundararaj U. Thermal, rheological, and mechanical behaviors of LLDPE/PEMA/clay nanocomposites: effect of interaction between polymer, compatibilizer, and nanofiller. Macromolecular Materials and Engineering. 2006;291(6):697-706.

31. Ren J, Silva AS, Krishnamoorti R. Linear viscoelasticity of disordered polystyrene-polyisoprene block copolymer based layered-silicate nanocomposites. Macromolecules. 2000;33(10):3739-46.

32. Hyun YH, Lim ST, Choi HJ, Jhon MS. Rheology of poly (ethylene oxide)/organoclay nanocomposites. Macromolecules. 2001;34(23):8084-93.

33. Crawford RJ, Crawford RJ, Throne JL. Rotational molding technology: William Andrew; 2001.

34. Bellehumeur CT, Kontopoulou M, Vlachopoulos J. The role of viscoelasticity in polymer sintering. Rheologica acta. 1998;37(3):270-8.

35. Rao MA, Throne JL. Principles of rotational molding. Polymer Engineering & Science. 1972;12(4):237-64.

36. Bellehumeur CT, Bisaria MK, Vlachopoulos J. An experimental study and model assessment of polymer sintering. Polymer Engineering & Science. 1996;36(17):2198-207.

37. Martin D, Halley P, Truss R, Murphy M, Jackson O, Kwon OY. Polyethylene-layered silicate nanocomposites for rotational moulding. Polymer international. 2003;52(11):1774-9.

Chapter 3 – Materials, Processing and Characterization of Polymer/Clay Nanocomposite

This chapter begins with a discussion of the materials used in this study and their characteristics. Following is a description of the various experimental techniques used for characterizing PE/clay nanocomposites along with the technical specifications of instruments. The chapter then presents the various experimental results and their analysis.

3-1. Experimental

3-1-1. Materials

Polyethylene (PE):

Linear low density polyethylene (LLDPE) and high density polyethylene (HDPE) (hexene copolymer) were kindly provided by Imperial Oil as the base polymer for this project. The characteristics of different grades of polyethylene are listed in Table 3-1.

Table 3-1 – Polyethylene (PE) characteristics

Material	Density (g/cm^3)	Melt Flow Index (MFI) (g/10min)
LLDPE (8460) (LL 8460.29)	0.938	3.3
LLDPE (8555) (LL 8555.25)	0.936	6.8
HDPE (6719) (HD 6719.17)	0.952	19
HDPE (8660) (HD 8660.29)	0.942	2

The melt flow index (MFI) of PE was measured at 190 ^{0}C, with 2.16 kg loading based on ASTM D1238. The density was measured based on ASTM D4883.

Grafted modified polyethylene:

In this study, OREVAC 18340 was used as a commercially available compatibilizer from Arkema Inc., France. OREVAC 18340 is linear low density polyethylene (LLDPE) modified with grafted maleic anhydride. This compatibilizer creates a strong bonding between the polyethylene and mineral fillers, such as nanoclay. LLDPE grafted maleic anhydride (LLDPE-g-MA) has a density of 0.913 g/cm^3 (ASTM D1505) and MFI of 2.5 g/10min (ASTM D1238). The reasons for choosing this compatibilizer were that the MFI of OREVAC 18340 closely matches with the MFI of the base polymer, so it should have minimal effect on the viscosity of the final product; also, low MFI may provide more shear viscous forces, resulting in more delaminated structures of clay. Additionally, this compatibilizer was chosen to compare the compatibility of LLDPE-g-MA with LLDPE and HDPE matrices.

Organo-modified clay:

Cloisite 20A (C20A) was used as the available commercial organo-modified clay. C20A is a natural montmorillonite modified with a quaternary ammonium salt. The structure of the modifier is shown schematically in Figure 3-1, where HT is a hydrogenated tallow with a mixture of C_{14}-C_{18} alkyl chains (~65% C_{18}, ~30% C_{16} and ~5% C_{14}). For C20A, the concentration of the modifier is 95 meq/100 g clay and d-spacing is 2.42 nm, based on X-ray diffraction results (Southern Clay Products, Inc.).

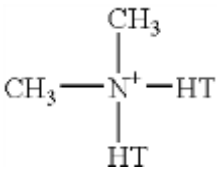

Figure 3-1 – Chemical structure of modifier: dimethyl, dihydrogenated tallow, quaternary ammonium salt

3-1-2. Sample Polyethylene/Clay Nanocomposite Preparation

Twin-screw extruder:

The samples were prepared by a Coperion 25mm ZSK co-rotating twin-screw extruder. The screw diameter is 25 mm with a barrel length/diameter (L/D) ratio of 37. The melt compounding was performed at a specific barrel temperature profile (190, 190,195, 195 ^{0}C) and die temperature (200 ^{0}C) with 100 rpm screw speed (Figure 3-2 (b)). All the materials were used without drying and further purification. PE and PE-g-MA pellets were hand-mixed and fed to the extruder through a single feeder; nanoclay was fed from a separate micro feeder. Figure 3-2 (a) shows the twin-screw extruder machine used in this study.

(a)

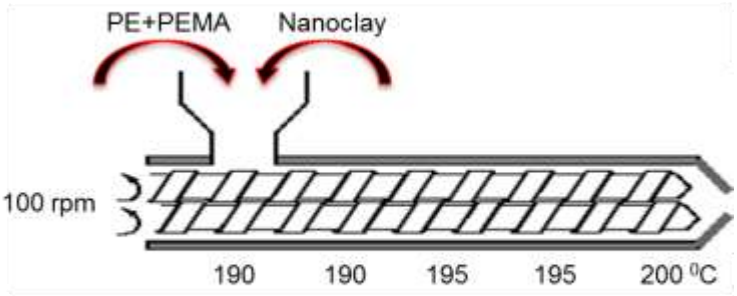

(b)

Figure 3-2 – (a) Coperion 25mm ZSK co-rotating twin-screw extruder (b) schematic of melt compounding and process conditions in twin-screw extruder, reproduced from (www.polymerprocessing.com)

The extrudates were quenched in a water bath and then guided to a rotating disk pelletizer to create granules as the final samples. The granular samples were then fed into post processes, such as compression molding and injection molding. Samples' compositions prepared by the twin-screw extruder are listed in Table 3-2.

Table 3-2 – PE nanocomposite compositions and sample name

Material	Sample Name	Composition (wt %)
LLDPE (8460) (LL 8460.29)	LL(8460)/PEMA/C20A	82/16/2
	LL(8460)/PEMA/C20A	80/16/4
LLDPE (8555) (LL 8555.25)	LL(8555)/PEMA/C20A	82/16/2
	LL(8555)/PEMA/C20A	80/16/4
HDPE (6719) (HD 6719.17)	HD(6719)/PEMA/C20A	82/16/2
	HD(6719)/PEMA/C20A	80/16/4
HDPE (8660) (HD 8660.29)	HD(8660)/PEMA/C20A	82/16/2
	HD(8660)/PEMA/C20A	80/16/4

Injection molding:

The mechanical test samples were prepared with a BOY 35E injection molding machine, shown in Figure 3-3 (a). All the injection molding processes were controlled automatically by the control panel of the injection molding machine. The injection process was done using a specific temperature profile of 170, 170, 180, 180 and 190 ^{0}C, a mold temperature of 18 ^{0}C, a holding pressure of 120 bars and a screw speed of 200 rpm. A schematic of the process conditions are shown in Figure 3-3 (b).

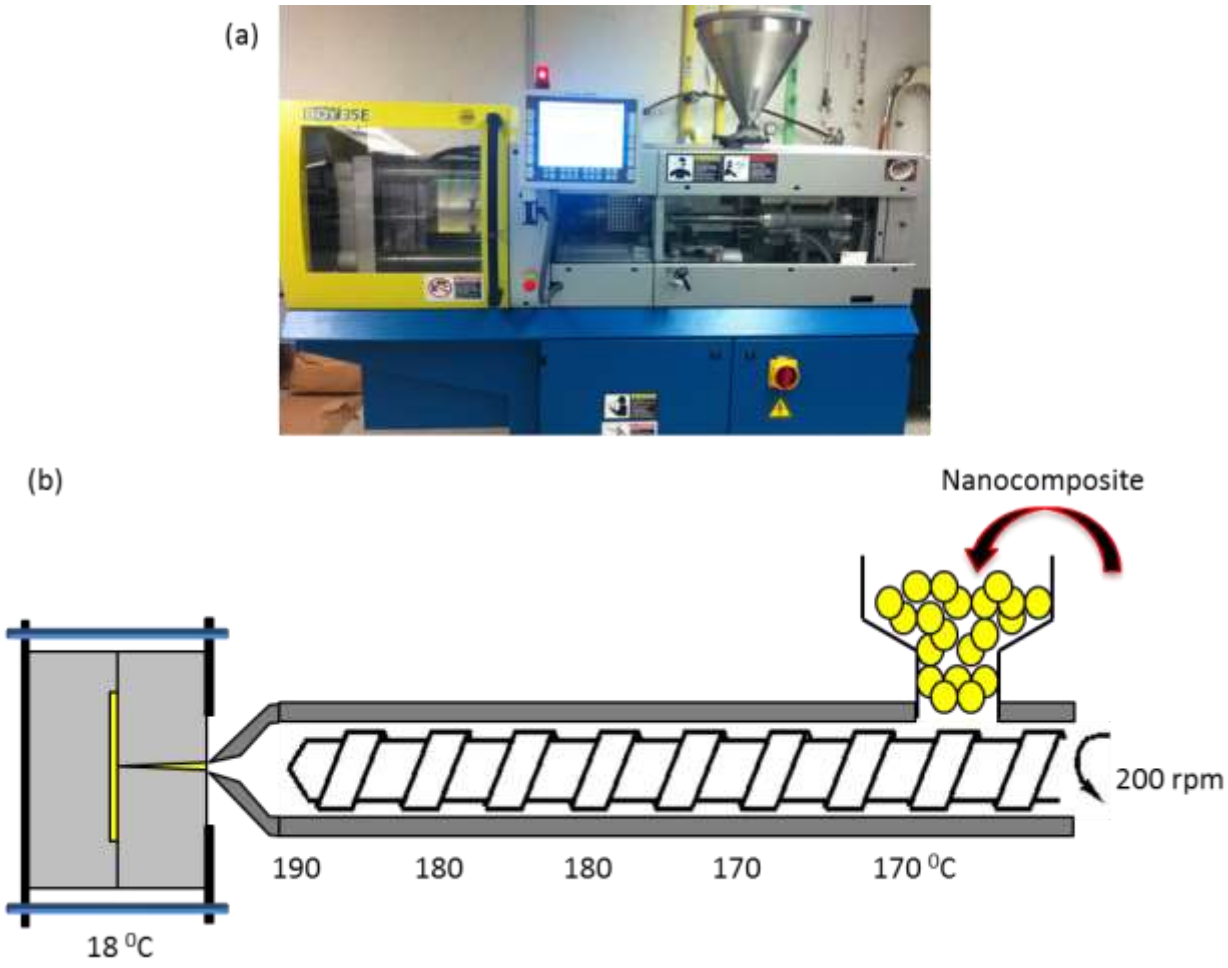

Figure 3-3 – (a) injection molding machine (BOY 35E) (b) schematic of melt compounding and process conditions in injection molding, reproduced from (www.toolcraft.co.uk)

Compression molding:

A manually operated compression molding machine, made by Carver, was used in this study to prepare the compression molded nanocomposite. The machine is shown in Figure 3-4. Both platens in the compression molding machine were equipped with a controlled heater. The cooling line was designed and installed on the machine to cool down the nanocomposites to room temperature under pressure.

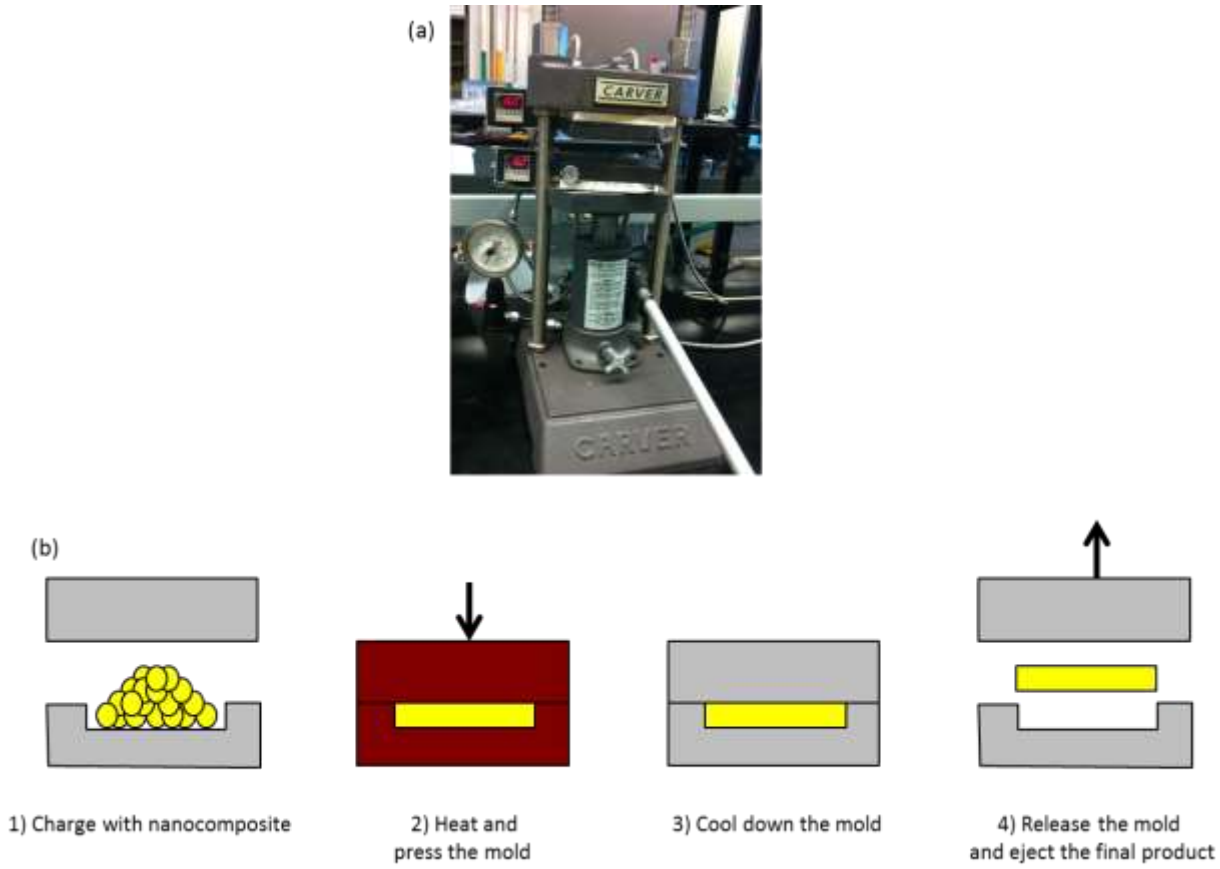

Figure 3-4 – (a) Carver compression molding machine (Carver Inc., Wabash, IN, USA) (b) schematic of compression molding process

3-1-3. X-Ray Diffraction (XRD) and Transmission Electron Microscopy (TEM)

X-ray diffraction (XRD) is the most commonly used test to identify the structure of polymer/clay nanocomposite. Generally, XRD has specific peaks, which appear at an initial angle (1-10 ^{0}) corresponding to the dispersion of the layered silicate in the nanocomposite (1, 2). Much information can be deduced about the structure of the nanocomposite (dispersion of silicate layers) through analyzing the peak position, intensity and shape (1, 2). For instance, the peak at the initial angle shifts to a lower diffraction angle and becomes less strong in the intercalated structure. The exfoliated or highly intercalated structure, however, can cause the disappearance of the corresponding peak in the XRD plots. The characteristic XRD peaks are

associated with the crystallinity of the pure polymer and do not rely on the incorporation of the layered silicates in the polymer.

The peaks in the XRD pattern are directly related to atomic distances based on Bragg's Law described as a relationship between the distance among the silicate layers in the nanocomposite, identified wavelength and scattering angle 2θ. The Bragg's Law is defined as follows:

$$2d.sin\theta = n\lambda \qquad \text{Eq. 3-1}$$

where, λ is the wavelength of the XRD, d is the d-spacing between the silicate layers, θ is the scattering angle and n is an integer representing the order of the diffraction peak (1).

For the XRD characterization, the rectangular samples with 2 mm thickness were prepared using compression molding at about 160 ^{0}C and 15 MPa for 5 minutes. The XRD was performed using two XRD machines for two different experiments. The first XRD was the X-ray diffractometer (CoKα, λ=0.154 nm) operated at room temperature, in the 2θ range from 1.5 to 40^0, at a scanning rate of 1^0/min. The second XRD was a Rigaku Multiflex X-ray diffractometer (Cu Kα, λ=0.179 nm) with an X-ray tube at a voltage of 40 kV and a current of 20 mA, operated at room temperature in the 2θ range, from 1.5 to 40^0, at scanning rate of 1^0/min.

Although the XRD is an effective method for identifying the intercalated structure of nanocomposites and the effect of the surfactant on the basal spacing of organo-modified layered silicates (1-4 nm periodic spacing) (3), XRD results cannot be used solely to determine the structure of exfoliated nanocomposite. Transmission electron microscopy (TEM), therefore, is also used to analyze nanocomposites qualitatively (2). Moreover, TEM images, accompanied by XRD results can show a wider view of dispersion of nanoclay within the polymer matrix.

The TEM analysis of the nanocomposites was carried out on ultramicrotomed sample sections using a Tecnai TF20 G2 FEG-TEM at 200 kV acceleration voltages with the standard single tilt holder. The samples were cryo-ultra-microtomed in a Leica ultramicrotome at a temperature of -90 ^{0}C. The thickness of the microtomed samples was ~ 100 nm.

3-1-4. Thermal Stability Tests

Thermo gravimetric analysis (TGA) is usually used to investigate the thermal stability and thermal degradation rate of the polymer and polymer/clay nanocomposites. Differential scanning calorimetry (DSC) is also another thermo analytical technique that can be used to determine the crystallinity and kinetics of crystallization in polymer/clay nanocomposites.

Differential Scanning Calorimetry (DSC): Differential Scanning Calorimetric (DSC) measurements were performed on a TA Q100 Instrument. The weights of the DSC samples were ~4 mg. The DSC tests were carried out in 3-cycles (melting-crystallization-melting), first heated from -90 to 150 ^{0}C at a heating rate of 10 ^{0}C/min and subsequently cooled to -90 ^{0}C, at the same rate. The second heating cycle was performed right after the first cycle at the same rate. The thermal characteristics, including melting temperature, crystallization temperature and enthalpy of crystallization, were analyzed using TA2200 software.

Thermal Gravimetric Analysis (TGA): Thermal Gravimetric Analysis (TGA) measurements were carried out via a TA Q500 instrument. The microbalance was calibrated with a reference weight of 100 mg (the calibration procedures are listed in the TGA TA Q500 manual). Sample weights ranging from 10 to 15 mg were heated from room temperature to 600 ^{0}C at the rate of 10 ^{0}C/min under nitrogen gas. The data from the TGA were analyzed with TA2200 software.

3-1-5. Mechanical Test

Tensile tests were used to measure the effect of nanoclay on the mechanical properties of polymer/clay nanocomposites. The mechanical properties of the polymer nanocomposite rely directly upon the dispersion of the layered silicates in the polymer matrix and the adhesion between the layered silicates' surface and polymer chains. To examine the mechanical properties of the samples, two tensile tests were conducted in this study: one for extruded samples and the other for batch mixer samples. First, the Tinius Olson model H25kS, with digital data acquisition, was used to test the samples from the injection molding. The tensile properties were measured based on the ASTM D638 standard, with a 1kN load cell at 500 mm/min cross-head speed. Five samples of each material were tested at 21 ^{0}C and 18 % relative humidity. The specimens' dimensions are those of type IV specimens, as described in the ASTM D638 standard. The exact dimensions of our specimens are also shown in Figure 3-5.

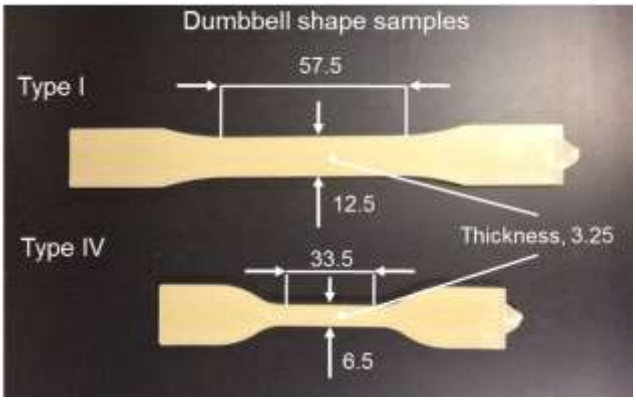

Figure 3-5 – Injection molding samples (type I and IV from ASTM D638), dimensions are in mm

The second tensile test machine used was the Tinius Olson model H1KT with digital data acquisition. The tensile properties were measured based on the ASTM standard D638, with a 1kN load cell at 100 mm/min cross-head speed. Five samples of each material were tested similar to the first mechanical test, at 21 ^{0}C and 18 % relative humidity. A sheet of each sample

was prepared by compression molding at 160 ^{0}C and pressed for 7 minutes under 20 MPa. Subsequently the specimens were cut by the mold, which was a design based on type V of the ASTM D638 standard. The mold and the exact dimensions of samples are illustrated in Figure 3-6.

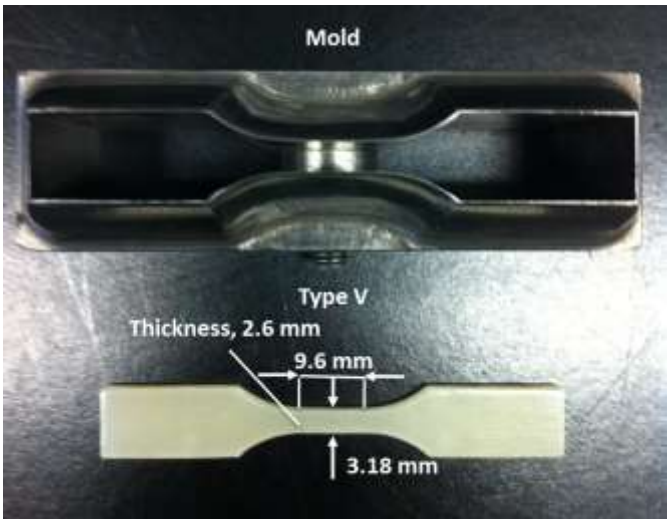

Figure 3-6 – Compression molding samples and mold (type V from ASTM D638)

3-1-6. Rheology

The rheological behavior of nanocomposites provides a fundamental knowledge of their processability at molten state. In addition, studying the rheological behavior is helpful to understand the structure-property relationships of the nanocomposites (2). To measure the rheological properties of the PE nanocomposite, a MCR-302 Rheometer (Anton Paar) was used in this study. The storage modulus (G'), loss modulus (G") and complex viscosity (η*) were measured at 160, 180 and 200 ^{0}C, in an oscillatory mode with parallel plate geometry, with 25 mm diameter and a gap of 1 and 1.5 mm. Time – temperature superposition principles were applied and the reference temperature (T_S) was taken as 200 ^{0}C. Each sample was examined at a minimum of two different gaps to ensure data reproducibility.

3-2. Results and discussions

3-2-1. X-Ray Diffraction (XRD) and Transmission Electron Microscopy (TEM)

The X-ray diffraction (XRD) patterns, with a characteristic peak, are shown in Figure 3-7 and 3-8 for 2 wt % nanoclay and 4 wt % nanoclay nanocomposite, respectively. As mentioned previously, the angle of initial peaks (range of 1-10 ^{0}) are the indication of the level of dispersion of the nanoclay and are used for measuring the basal spacing of silicate layers (Figure 3-9 and 3-10). Intensity, position and shape analysis of the silicate layers' peak can be used to identify the nanocomposite structure and basal spacing of the silicate layers (1, 2). The XRD peaks broadened and shifted to a lower diffraction angle in 2 wt % nanoclay nanocomposites. An almost intercalated structure was obtained for both LLDPEs at a lower nanoclay loading (2 wt %). To obtain a quantitative overview of the dispersion of layered silicates, the basal spacing of silicate layers from the XRD results was determined using Bragg's Law. For instance, the LLDPE (8460) reveals a peak at 2θ around 3.4^0, which corresponds to the basal spacing (d_{001}) of 2.6 nm. Also, the HDPE (8660) has a basal spacing of 2.49 nm. An increase in the distance of silicate layers indicates a very high intercalation of the LLDPE (8460) and layered silicates. Layered silicates, however, may not have a good interaction with the HDPE (8660) chains since the basal spacing of layered silicates only slightly increases. On the other hand, the peaks become stronger and shift to a higher diffraction angle by increasing the amount of nanoclay (4 wt %), as shown in Figure 3-10. Consequently, the distance between the silicate layers decreased. Again, Bragg's Law was used to determine the basal spacing of the LLDPE (8460), which revealed a peak at 2θ around 3.6^0, equal to 2.49 nm. The basal spacing for the HDPE (8660) with 4 wt % nanoclay is equal to 2.39 nm.

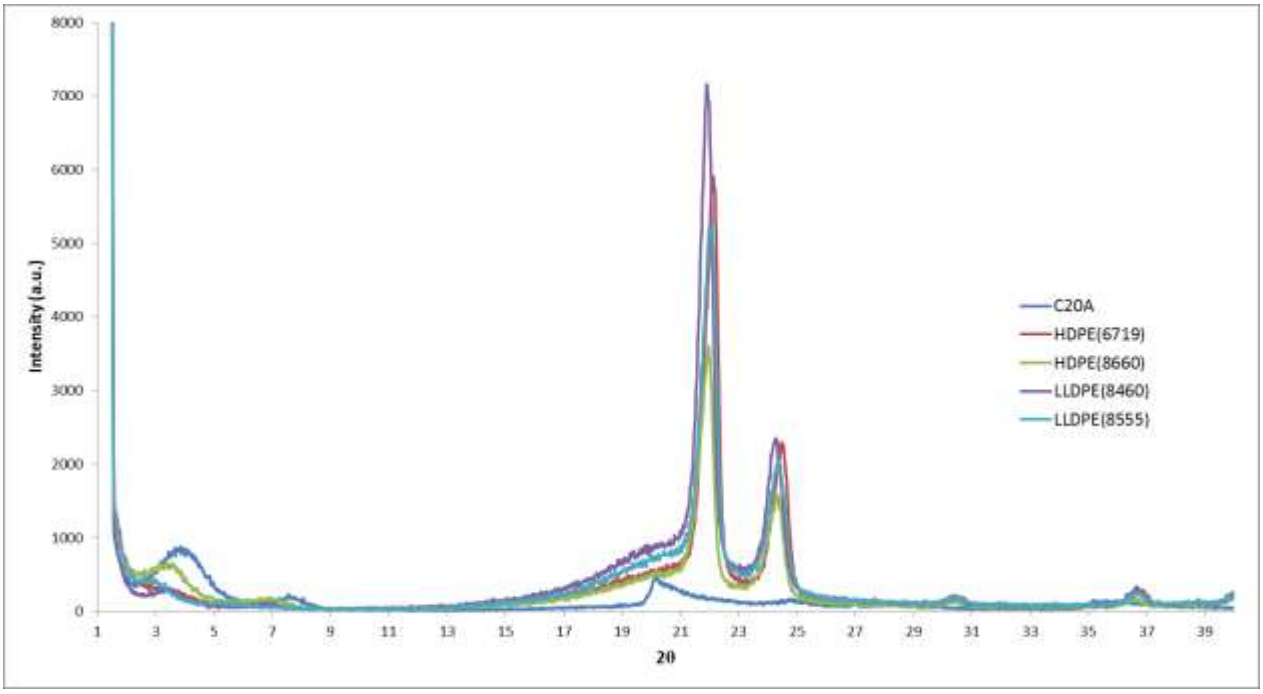

Figure 3-7 – XRD pattern of polyethylene nanocomposite (PE/PEMA/C20A, 82/16/2 wt %)

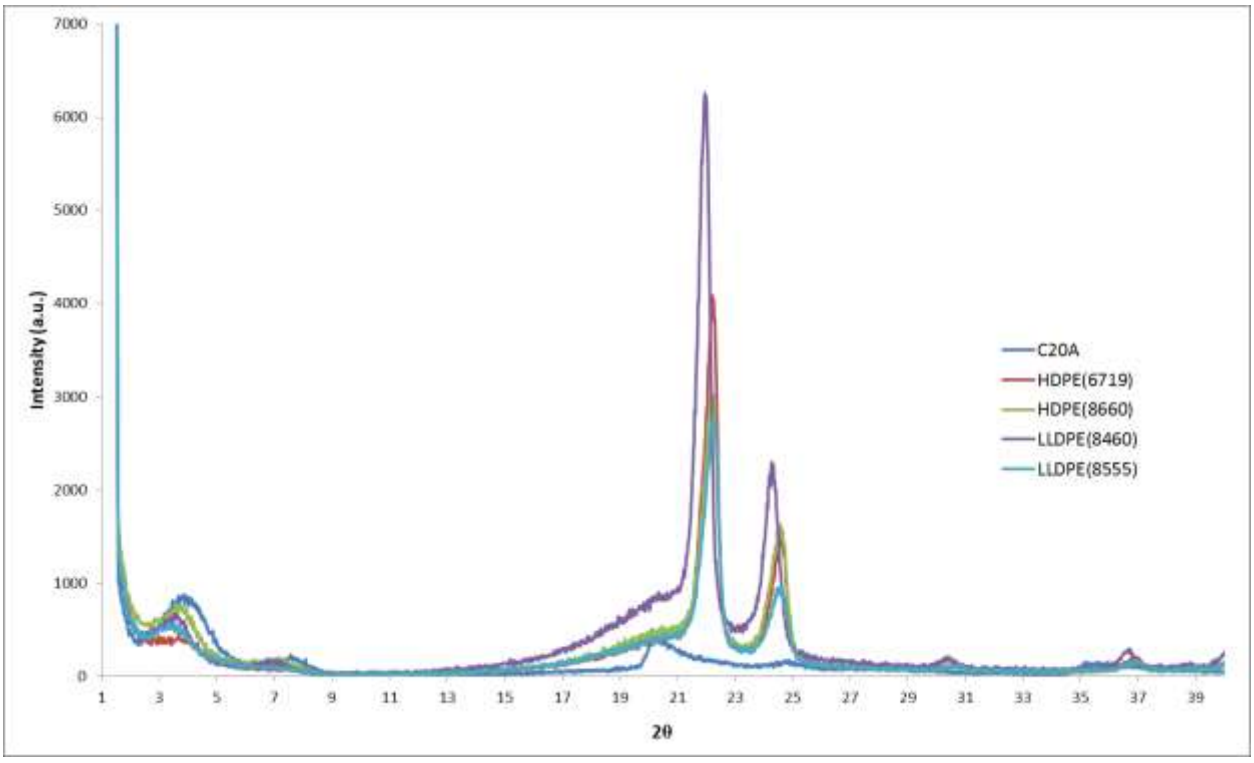

Figure 3-8 – XRD pattern of polyethylene nanocomposite (PE/PEMA/C20A, 80/16/4 wt %)

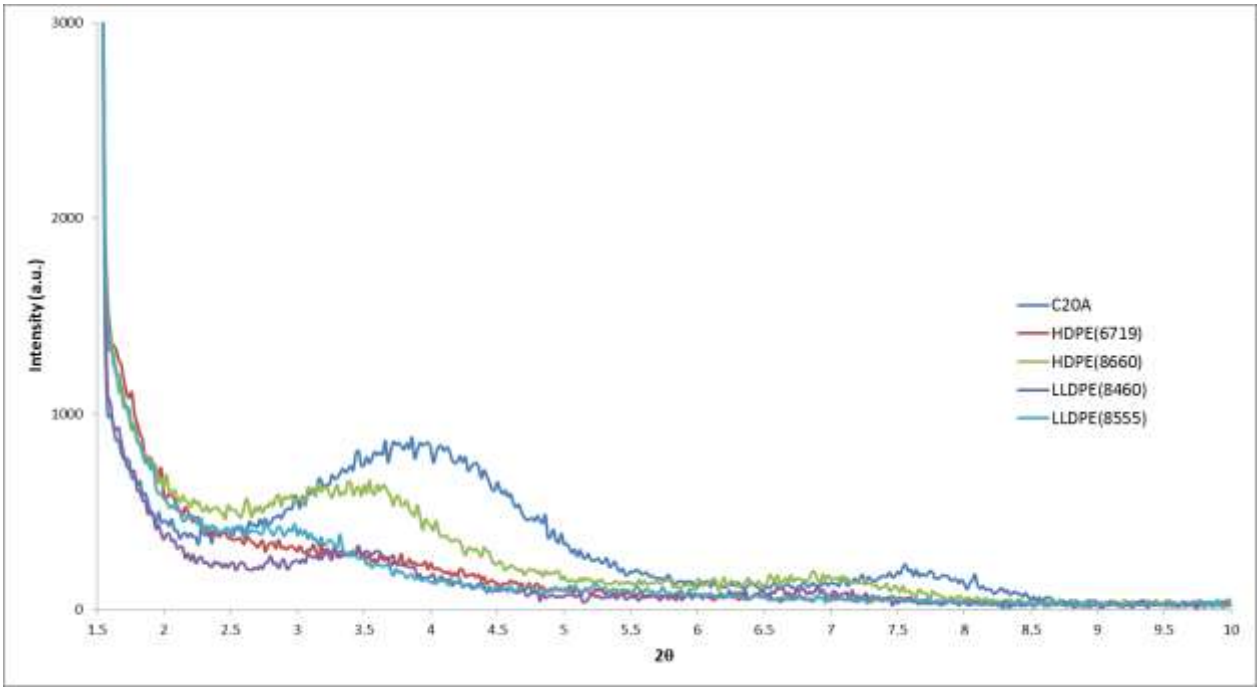

Figure 3-9 – XRD pattern for initial angle of polyethylene nanocomposite (PE/PEMA/C20A, 82/16/2 wt %), $d_{(001)}$ (C20A)= 2.31 nm

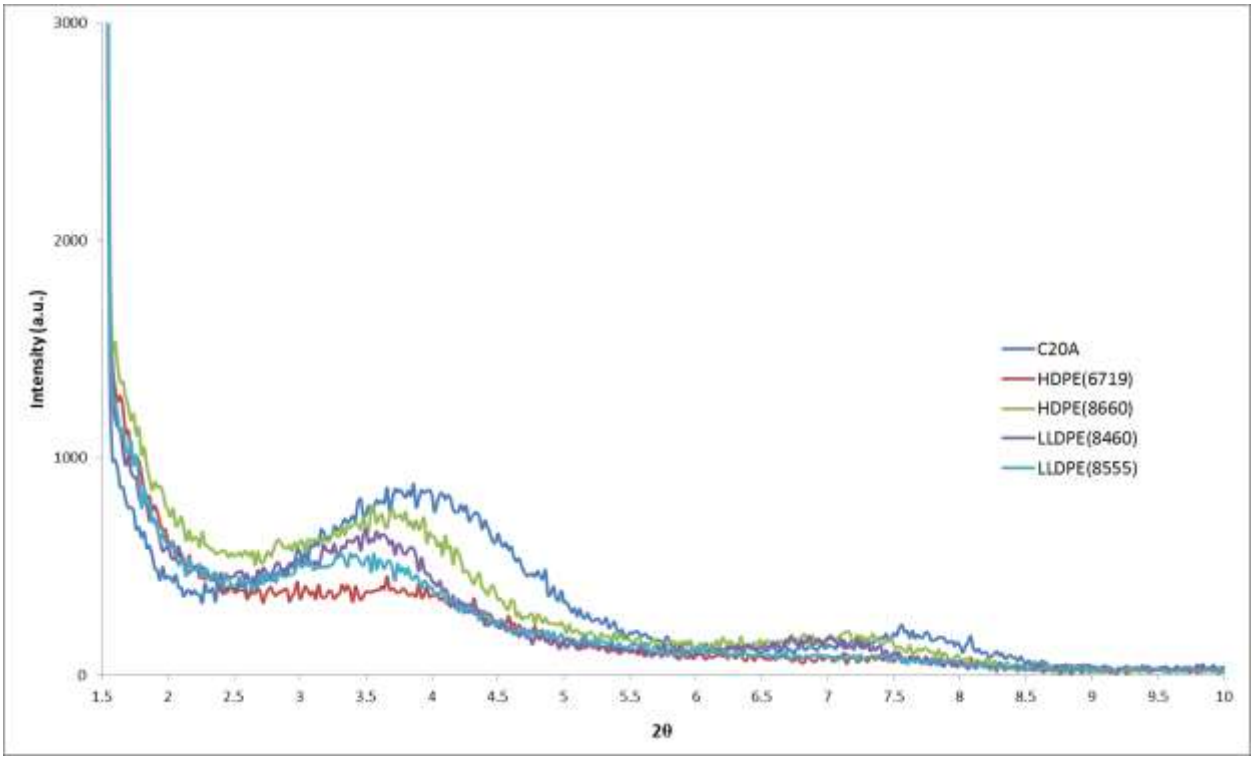

Figure 3-10 – XRD pattern for initial angle of polyethylene nanocomposite (PE/PEMA/C20A, 80/16/4 wt %)

TEM images were used, along with XRD results, to attain a qualitative understanding about the internal structure of the nanocomposites. The TEM images of nanocomposites with high and low intensity peaks from XRD (HDPE (8660) and LLDPE (8460)), are represented, at different magnifications, in Figure 3-11 to 3-14. In the case of LLDPE (8460) nanocomposites, individual silicate layers are stacked together and nicely dispersed in the LLDPE (8460) matrix (Figure 3-11), which was consistent with the XRD data. In the LLDPE (8460) nanocomposite with 4 wt % nanoclay (Figure 3-12), the layered silicates have started delaminating by the polymer chains; thus, a complete intercalated structure was achieved in the LLDPE (8460) nanocomposites.

On the other hand, in the case of the HDPE (8660) nanocomposites, big clusters, with many stacked silicate layers, even at 2 wt % nanoclay, are dispersed in the HDPE (8660) matrix (Figure 3-13). In addition, the stacked layered silicates become bigger and denser by increasing the nanoclay content to 4 wt % (Figure 3-14). The difference in the final structure of the nanocomposite can be attributed to the difference between the compatibility of the LLDPE-g-MA with the LLDPE and HDPE matrices (4). Overall, the presence of individual silicate layers in the LLDPE (8460) nanocomposites introduces a tortuous path for a penetrant. The gas barrier properties of nanocomposites, therefore, are expected to improve, as compared to the neat polymer's barrier properties.

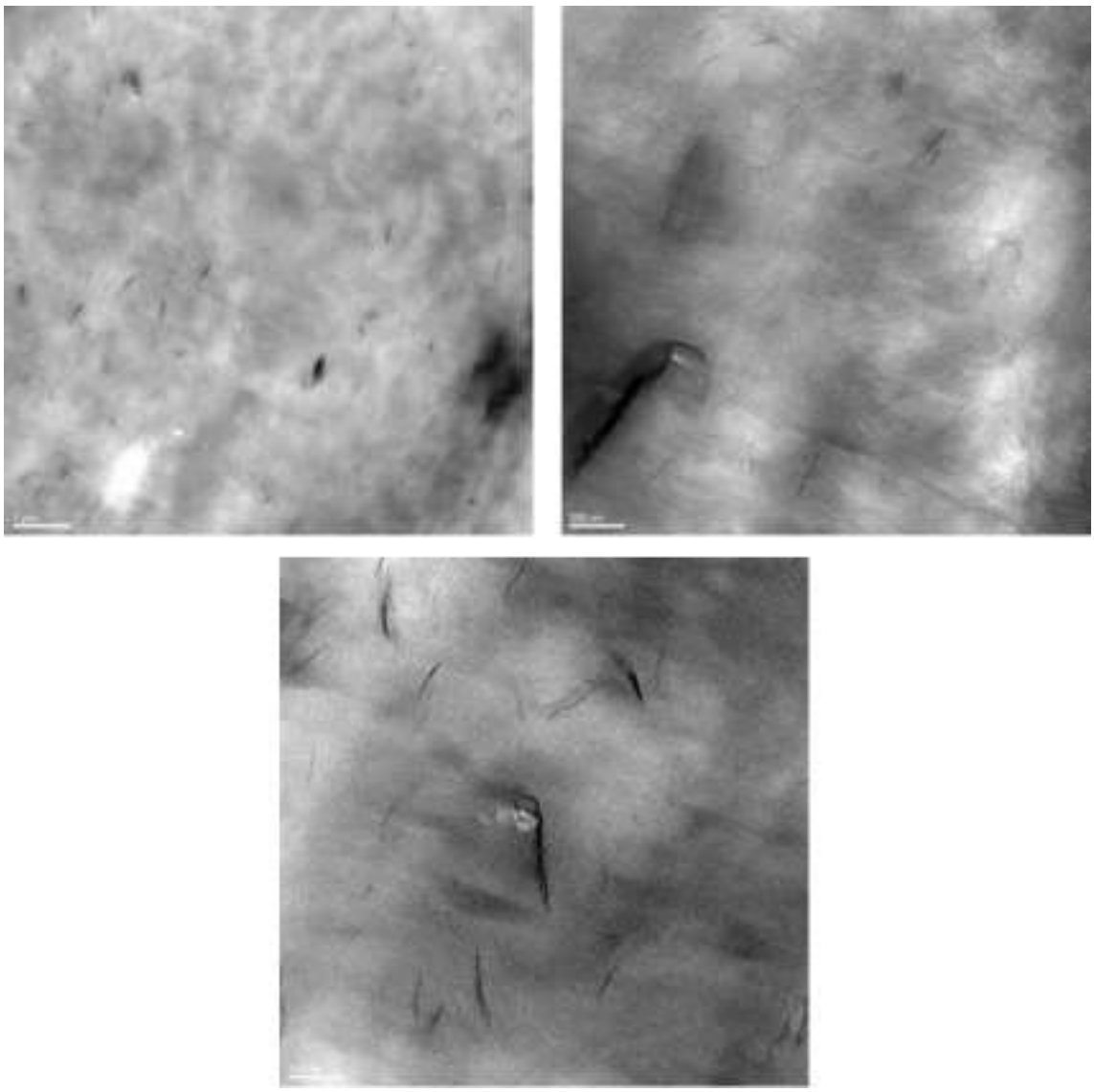

Figure 3-11 – TEM images of LLDPE (8460) nanocomposite (PE/PEMA/C20A, 82/16/2 wt %) at three different magnifications

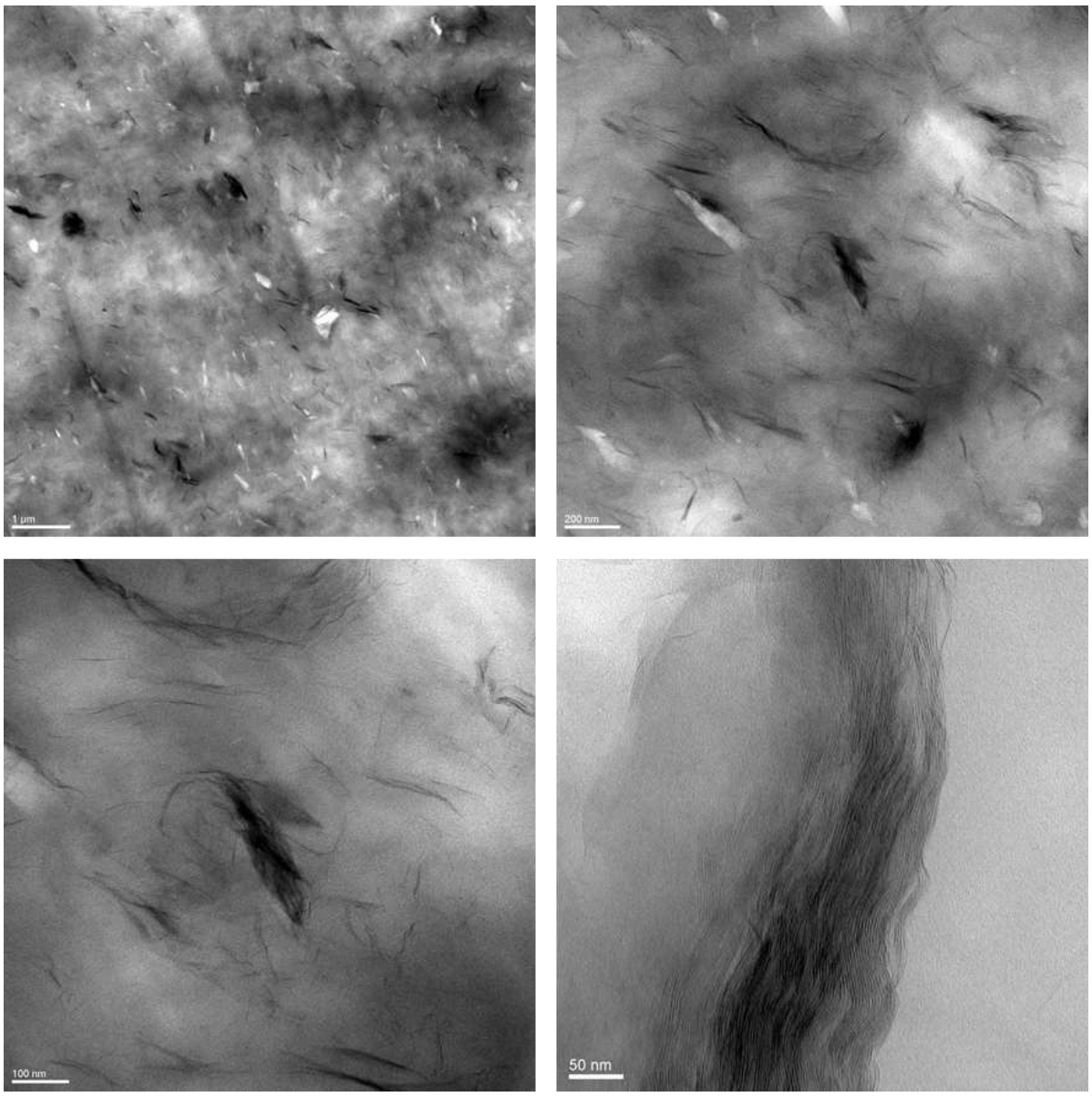

Figure 3-12 – TEM images of LLDPE (8460) nanocomposite (PE/PEMA/C20A, 80/16/4 wt %) at four different magnifications

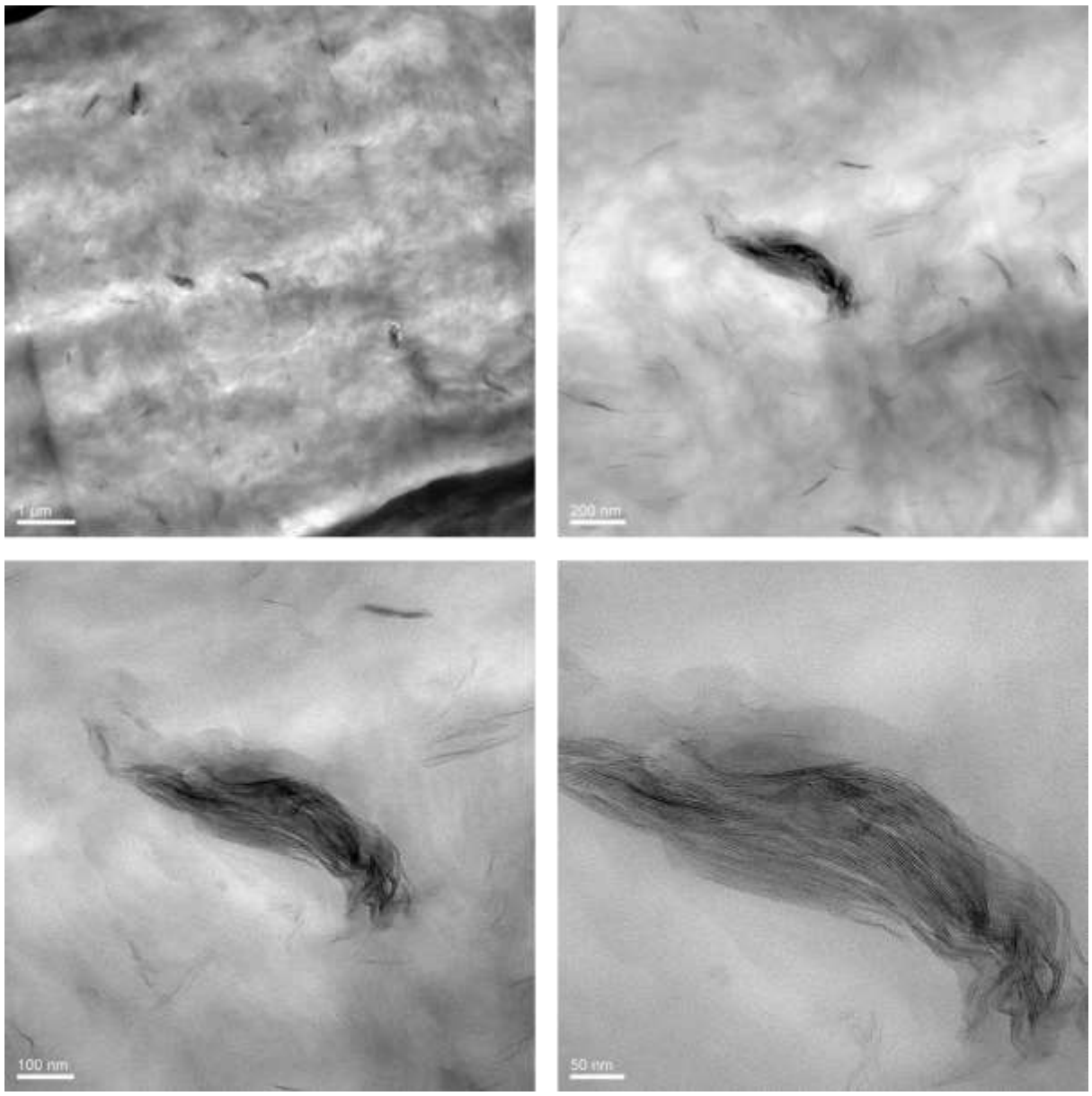

Figure 3-13 – TEM images of HDPE (8660) nanocomposite (PE/PEMA/C20A, 82/16/2 wt %) at four different magnifications

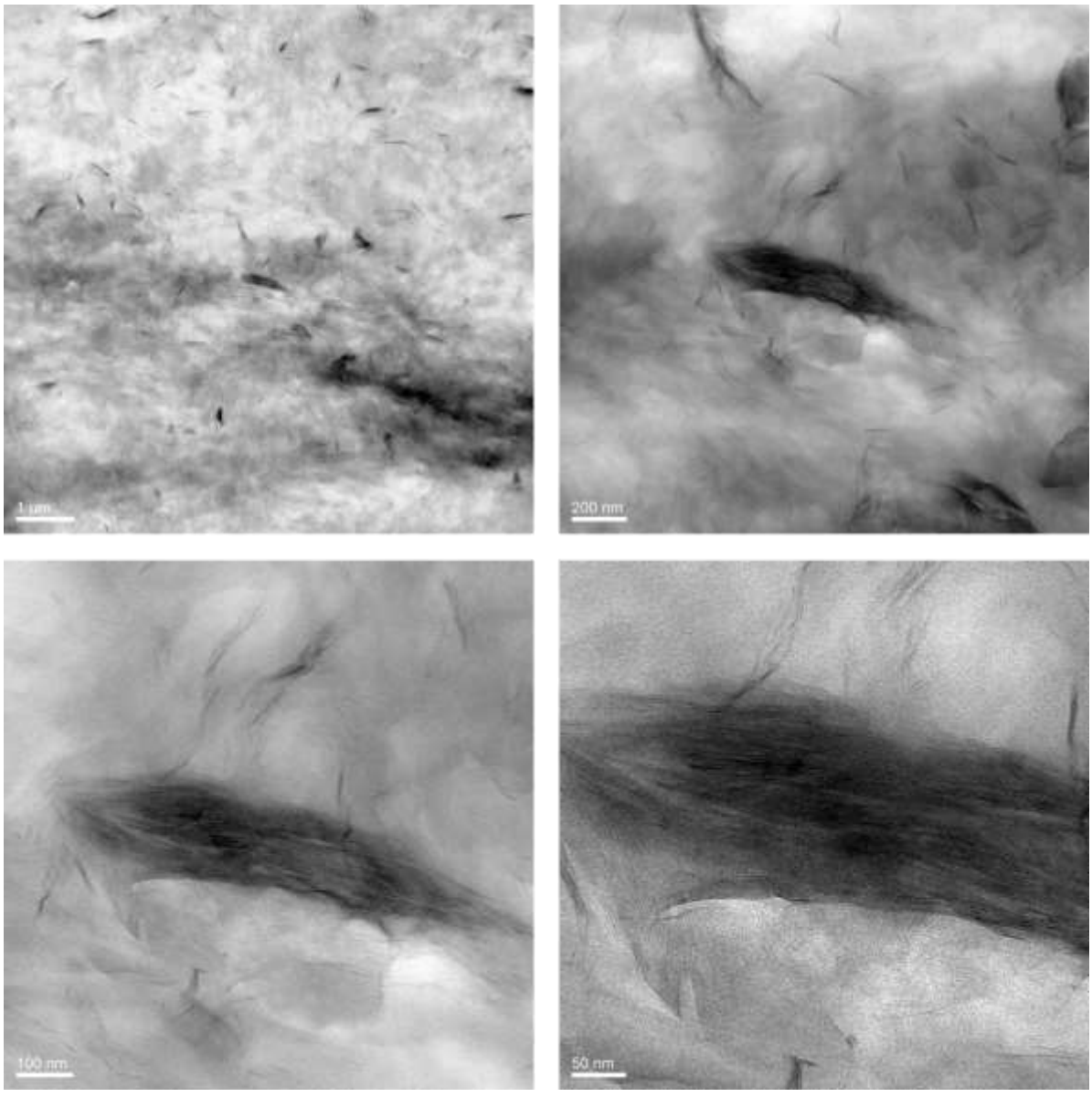

Figure 3-14 – TEM images of HDPE (8660) nanocomposite (PE/PEMA/C20A, 80/16/4 wt %) at four different magnifications

3-2-2. Thermal Stability

Differential Scanning Calorimetry (DSC):

The thermal characteristics, including the melting temperature (T_m), crystallization temperature (T_c), enthalpy of melting (ΔH_m), enthalpy of crystallization (ΔH_c) and degree of crystallinity (X_c) of pure PE and PE/clay nanocomposites were determined using DSC cycles

consisting of melting-crystallization-melting. The thermal characteristics of pure PE and PE/clay nanocomposite are summarized in Table 3-3. There was no significant difference in the melting temperature for both heating cycles; these results are in agreement with the previous studies for intercalated nanocomposites (5, 6). All the samples have the melting temperature in the range of 127-130 ^{0}C. The addition of nanoclay to both the LLDPE and HDPE matrices, however, caused a decrease in the heat of fusion, ΔH_m. The crystallization temperature of the PE/clay nanocomposite did not change significantly, as compared to neat PE. Adding nanoclay to the PE matrices decreased the enthalpy of melting. The data from the enthalpy of fusion can be used to calculate the degree of crystallinity, (X_C), using the formula:

$$X_C = \frac{\Delta H_m}{\Delta H_m^0} \times 100 \qquad \text{Eq. 3-2}$$

where, ΔH_m^0 is the enthalpy of the 100 % crystalline form of PE. The value of ΔH_m^0 for the LLDPE and HDPE, as found in the literature, is equal to 279 and 293 (J/g) respectively (7, 8).

Although the nanoparticles act as nucleating sites, the degree of crystallinity for all nanocomposites decreased, as compared to that of pure PE (Table 3-3). The reason for the reduction of the degree of crystallinity is explained by Perrin-Sarazin et al. They referred to this phenomenon as interactions between the maleic anhydride groups of the compatibilizer and the layered silicates, which can hinder the mobility of crystallisable chain segments. The result is a limitation in the nucleation effect of the nanoclay (9). The decrease in the degree of crystallinity becomes less intense as the nanoclay content increases.

Table 3-3 – Thermal characteristics of pure PE and PE/clay nanocomposite determined by DSC

Sample	DSC						
	First Heating		Cooling		Second Heating		X_C (%)
	ΔH_m (J/g)	T_m (^{0}C)	ΔH_c (J/g)	T_c (^{0}C)	ΔH_m (J/g)	T_m (^{0}C)	
LLDPE (8460)	117.3	126.8	121.9	114.0	113.7	127.8	40.8
LLDPE (8460)/PEMA/ C20A 82/16/2	110.2	127.1	102.7	115.1	107.3	127.6	38.5
LLDPE (8460)/PEMA/ C20A 80/16/4	108.7	127.6	99.9	114.9	104.7	127.9	37.5
LLDPE (8555)	123.5	126.6	108.7	112.9	122.3	127.6	43.8
LLDPE (8555)/PEMA/ C20A 82/16/2	101.1	127.7	79.0	115.8	88.8	129.8	31.8
LLDPE (8555)/PEMA/ C20A 80/16/4	99.7	126.4	83.7	114.7	90.2	127.1	32.3
HDPE (6719)	174.8	130.0	155.8	116.3	166.5	130.0	56.8
HDPE (6719)/PEMA/ C20A 82/16/2	143.5	129.8	129.8	117.6	130.9	130.3	44.7
HDPE (6719)/PEMA/ C20A 80/16/4	141.5	129.3	126.5	117.5	131.6	129.5	44.9
HDPE (8660)	138.3	128.9	121.9	115.0	129.8	129.0	44.3
HDPE (8660)/PEMA/C20A 82/16/2	134.2	128.3	118.6	115.9	124.2	128.3	42.4
HDPE (8660)/PEMA/C20A 80/16/4	131.0	129.16	113.7	114.57	119.5	129.6	40.8

Thermal Gravimetric Analysis (TGA):

The TGA curves for all pure PE and PE/clay nanocomposites are plotted in Figure 3-15 and 3-16. The temperatures, at 10% and 50% degradation of the initial weight ($T_{0.9}$ and $T_{0.5}$, respectively), are two important data obtained from the TGA curves, which provide a general understanding of the thermal properties of nanocomposite. The $T_{0.9}$ and $T_{0.5}$ for each sample are listed in Table 3-4.

Analyzing the TGA results shows that the degree of dispersion of the nanoclay in the PE matrix can affect the thermal stability of the nanocomposite. A good interaction between the

nanoclay and PE improves the heat barrier properties and consequently, enhances the thermal stability of the nanocomposite at the early stages of decomposition ($T_{0.9}$). This phenomenon can be impaired with a poor dispersion of the nanoclay. Afterwards, the stacked layered silicates hold accumulated heat and will use this as a heat source for the rest of the process, leading to an increased rate in the decomposition process. As a result, adding nanoclay increases the temperature of 50% decomposition ($T_{0.5}$); however, the rate of this increment is slower with increasing nanoclay concentration. All the nanocomposites, with 4 wt % nanoclay, show higher thermal stability, while the rate of increase in both $T_{0.9}$ and $T_{0.5}$ are not as high as samples with 2 wt % nanoclay. Hence, it is concluded there are more agglomerates than individual silicate layers in the nanocomposites with a higher clay content. Interestingly, in HDPE (8660) nanocomposites, which exhibited poor dispersion of layered silicates, the $T_{0.5}$ actually decreases with nanoclay addition. This conclusion parallels previous data, portrayed in the XRD results and TEM images.

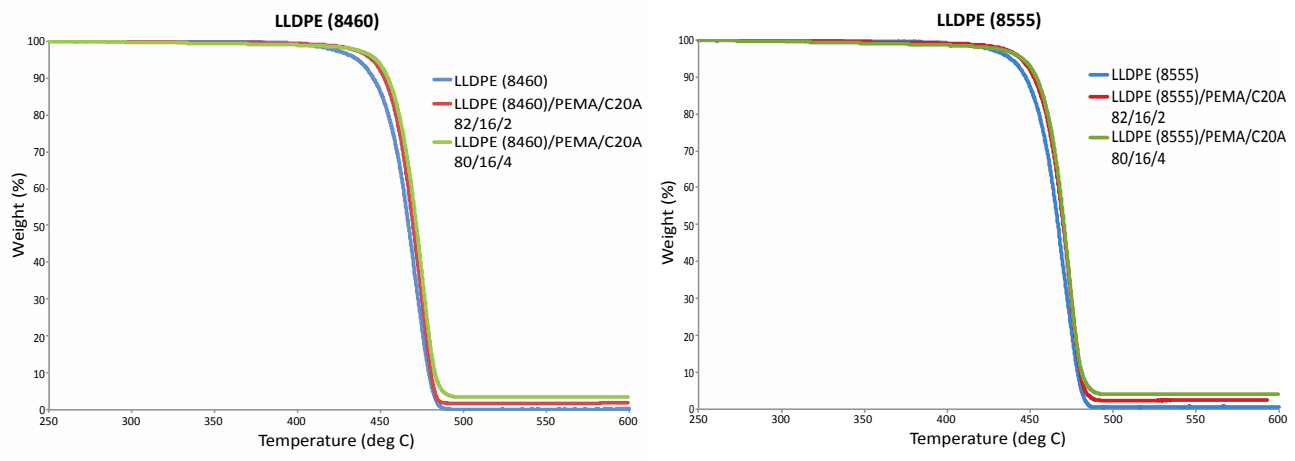

Figure 3-15 – TGA curve of pure LLDPE and LLDPE nanocomposite containing different concentrations of nanoclay (Cloisite 20A)

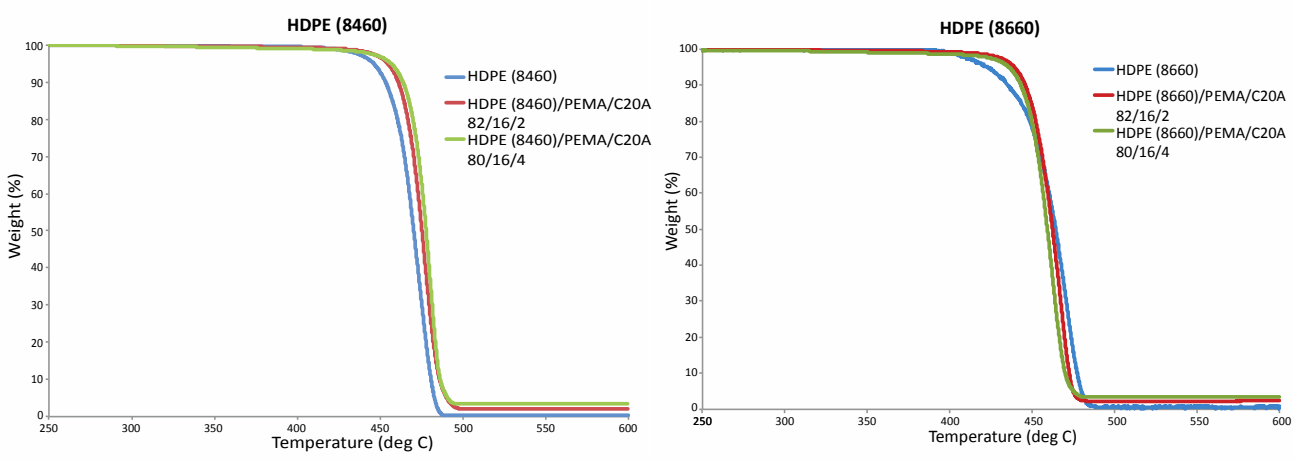

Figure 3-16 – Stress-Strain plot of pure HDPE and HDPE nanocomposite containing different concentrations of nanoclay (Cloisite 20A)

Table 3-4 – $T_{0.9}$ and $T_{0.5}$ obtained from TGA results for pure PE and PE/clay nanocomposite

Sample	TGA	
	$T_{0.9}$ (^{0}C)	$T_{0.5}$ (^{0}C)
LLDPE (8460)	445.4	466.7
LLDPE (8460)/PEMA/ C20A 82/16/2	450.5	469.5
LLDPE (8460)/PEMA/ C20A 80/16/4	452.4	471.1
LLDPE (8555)	447.2	466.7
LLDPE (8555)/PEMA/ C20A 82/16/2	450.9	468.5
LLDPE (8555)/PEMA/ C20A 80/16/4	452.6	469.5
HDPE (6719)	453.3	470.3
HDPE (6719)/PEMA/ C20A 82/16/2	459.7	474.5
HDPE (6719)/PEMA/ C20A 80/16/4	461.2	476.6
HDPE (8660)	434.8	464.2
HDPE (8660)/PEMA/C20A 82/16/2	438.7	462.3
HDPE (8660)/PEMA/C20A 80/16/4	440.8	459.1

3-2-3. Mechanical Test

The mechanical properties of the nanocomposites are associated with the degree of dispersion of the layered silicates and the level of adhesion or interaction between the polymer chain and layered silicates' surface (2). The importance of strong adhesion for enhancing the mechanical properties of the polymer is discussed in many studies (2, 3, 10, 11). Creating a strong interaction with the ingredients in the complex systems, including the PE matrices, compatibilizer and layered silicates, produced by melt mixing remains a challenge (2, 6, 10). Good to excellent miscibility between the compatibilizer and PE matrices is needed, along with a good delamination and dispersion of the layered silicates within the PE matrices (6). Tensile tests, therefore, were carried out on the pure PE and PE/clay nanocomposite samples to study the

effect of the layered silicates on the mechanical properties of the PE matrices and to investigate the adhesion between the components of the nanocomposites. The stress-strain curves of the PE/clay nanocomposite (2 wt % and 4 wt % nanoclay) are plotted in Figure 3-17 and 3-18 for the LLDPE and HDPE nanocomposites, respectively.

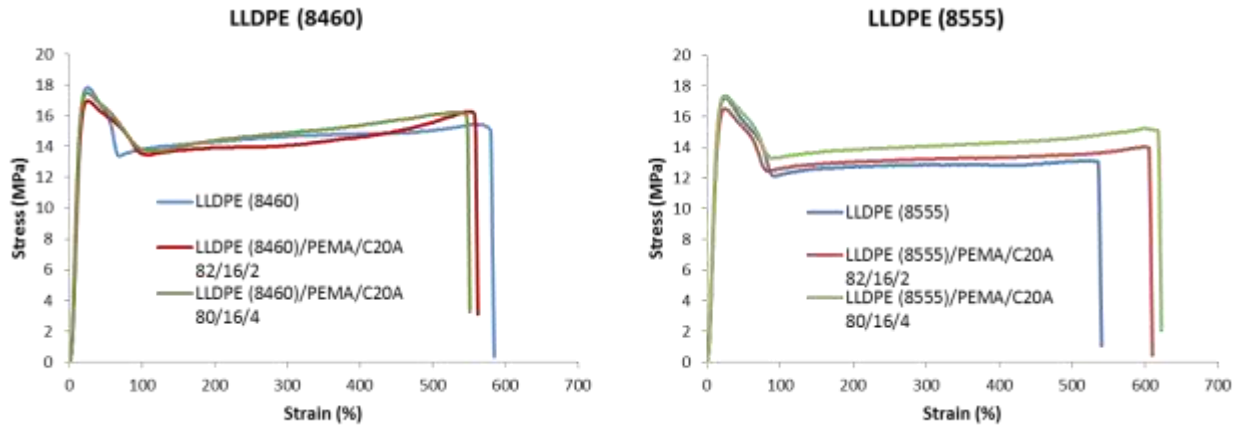

Figure 3-17 – Stress-Strain plot of pure LLDPE and LLDPE nanocomposite containing different concentrations of nanoclay (Cloisite 20A)

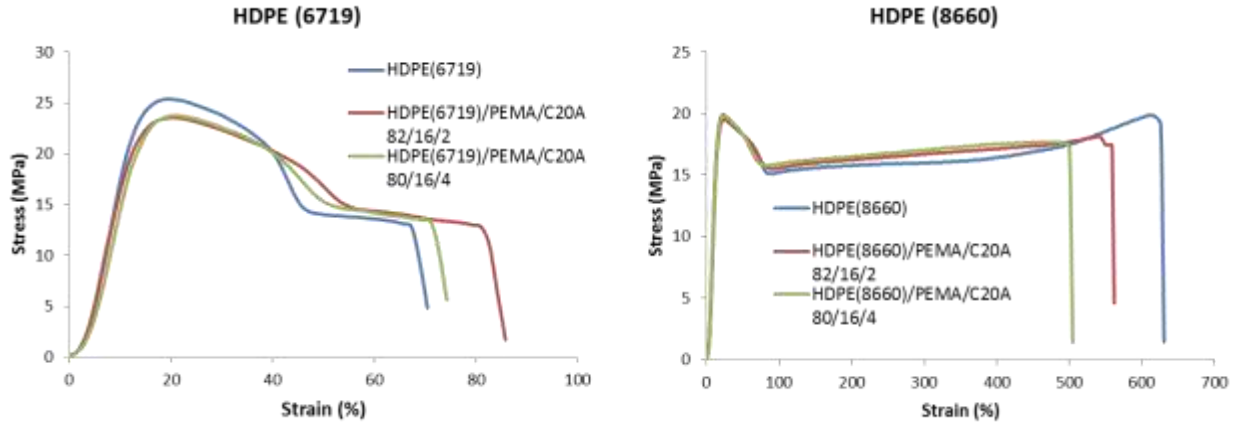

Figure 3-18 – Stress-Strain plot of pure HDPE and HDPE nanocomposite containing different concentrations of nanoclay (Cloisite 20A)

Three important mechanical properties can be extracted from the stress-strain curve. These properties are: *Young's modulus*, *yield strength* and *elongation at break*. Each of these results are presented in an individual plot from Figure 3-19 to 3-21.

Young's modulus is an indicator of the material's stiffness or rigidity and is calculated as the slope of the initial linear part of the stress–strain curve. The linear limits were measured based on the visual evaluation of the curve. The modulus of four pure PE were analyzed as references for comparing the result of the nanocomposite with 2 wt % and 4 wt % loading of Cloisite 20A. The results are shown in Figure 3-19. The error bar indicates the standard deviation of results within each sample. Increasing the molecular weight of the polymer matrix at any clay concentration enhances the stiffness of the polymer/clay nanocomposite. Fornes et al. also supported our data with similar characteristics for N6/nanoclay nanocomposite (3). In this study, the LLDPE (8555) has a low molecular weight (LMW), the LLDPE (8460) has a medium molecular weight (MMW) and the HDPE (8660) has a high molecular weight (HMW). Among all the polyethylenes, HDPE (6719) is an exception. The fact that HDPE (6719) has the lowest molecular weight, but the highest modulus among the other polymer matrices and may be the result of its higher degree of crystallinity, which is cause by fast formation of crystalline phase during cooling in the injection molding. Also the DSC results, as shown previously in Table 3-3 demonstrated a high degree of crystallinity for the HDPE (6719) and HDPE (6719) nanocomposites as compared to other polymer matrices and their nanocomposites.

The modulus decreased in all PE nanocomposites with 2 wt % C20A, as compared with pure PE. The modulus also slightly increased in both the LLDPE samples with 4% C20A nanocomposites. Consequently, it can be concluded that the compatibilizer (LLDPE-g-MA) has a better interaction with the LLDPE matrices than with the HDPE matrices since the base polymer chain (back bone) of this compatibilizer is LLDPE.

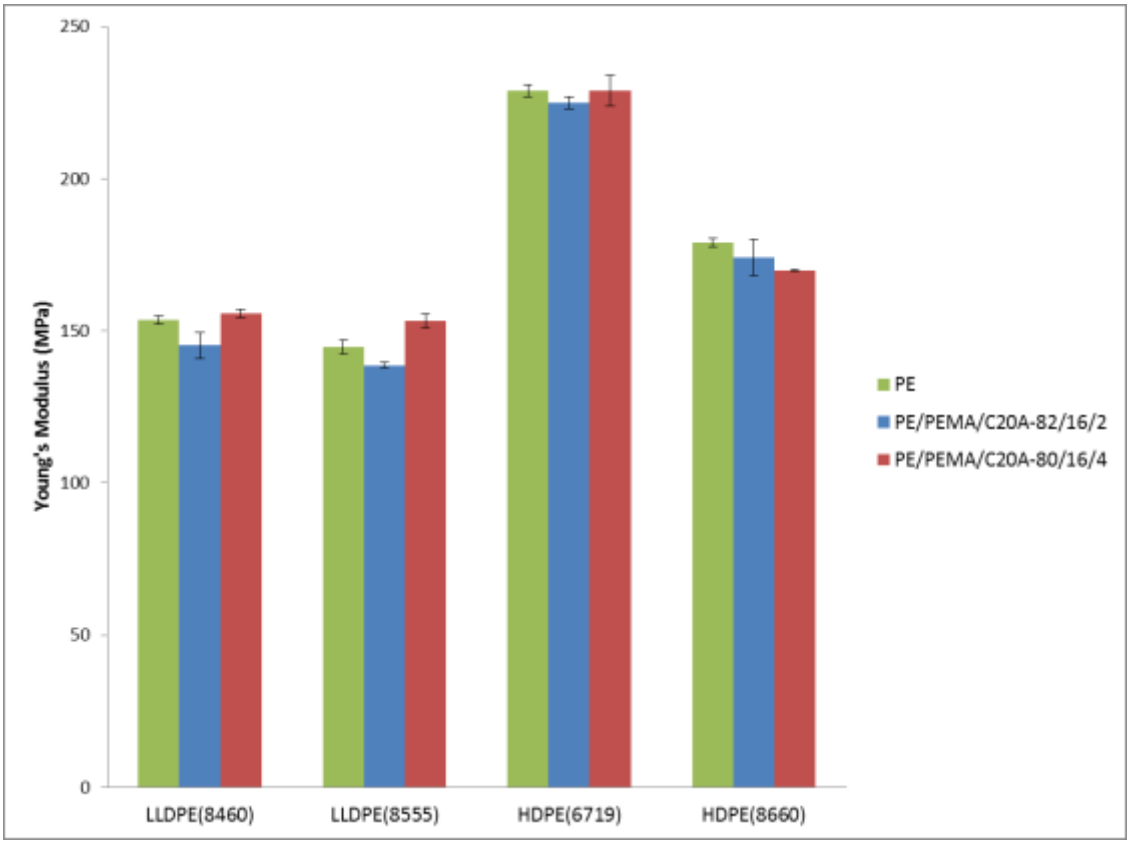

Figure 3-19 – *Young's Modulus* of pure PE and PE nanocomposite containing different concentrations of nanoclay (Cloisite 20A)

The relationship between *yield strength* and *elongation at break* or maximum deformation and nanoclay contents, are shown in Figures 3-20 and 3-21, respectively. *Yield strength* decreased or remained unchanged, within the experimental error, through the incorporation of nanoclay. Another finding has also shown a similar behavior for the strength of polyolefin/clay nanocomposites (10) due to weak interactions between the polymer chain, compatibilizer and layered silicates' surface. These results confirm the higher strength of PE nanocomposites with HMW, as compared to the PE nanocomposites with LMW. Thus the relationship between the molecular weight of polymer and *yield strength* shows the same behavior as *Young's modulus*, which is consistent with the previous study (3).

The nanocomposites with different PE matrices have exhibited inconsistent ductility with the addition of clay even though the compatibilizer (LLDPE-g-MA) shows a better interaction with the LLDPE matrix. Furthermore, the maximum deformation of the HDPE (8660) nanocomposite reduced significantly when nanoclay content was increased due to big clusters as seen in the TEM images (Figure 3-21).

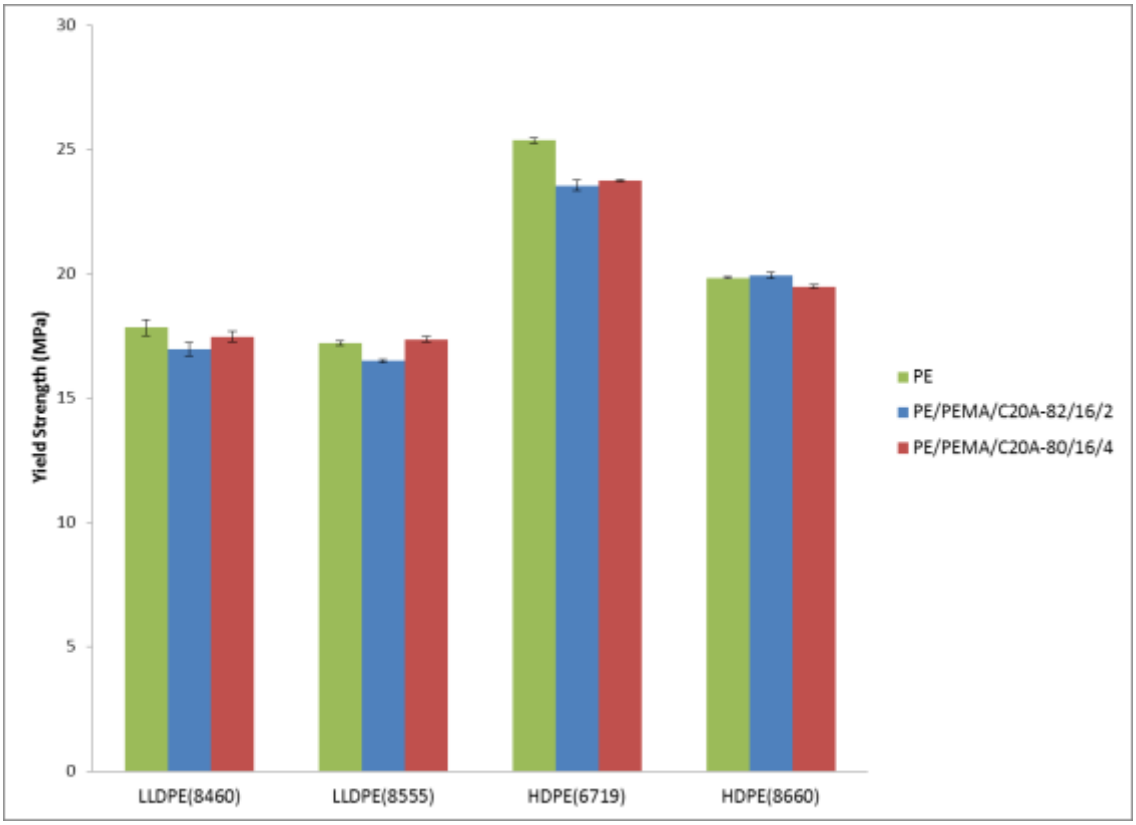

Figure 3-20 – *Yield Strength* of pure PE and PE nanocomposite containing different concentrations of nanoclay (Cloisite 20A)

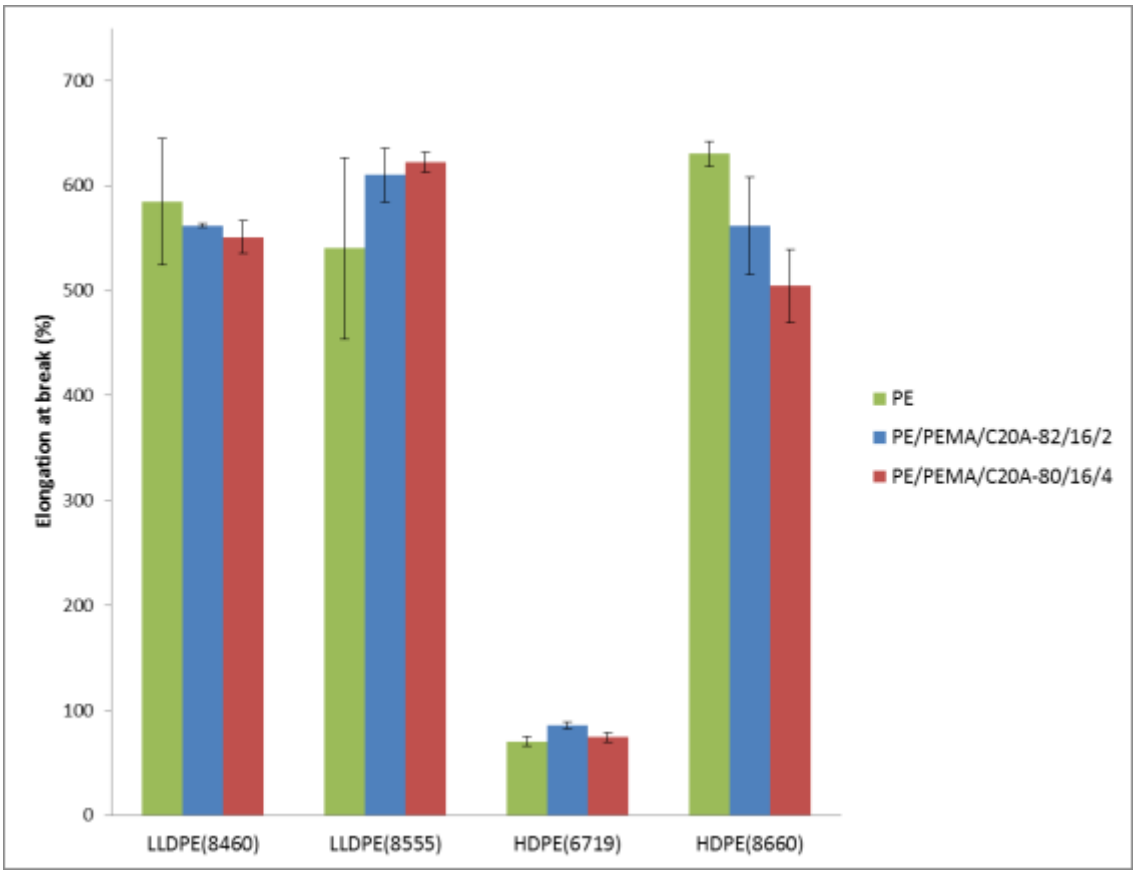

Figure 3-21 – *Elongation at break* of pure PE and PE nanocomposite containing different concentrations of nanoclay (Cloisite 20A)

Overall, the mechanical results were not improved significantly for the PE/clay nanocomposites, as compared to pure PE. As other researcher have shown, the properties of polyolefin/ nanoclay nanocomposites are complex and inconsistent, especially for mechanical properties (10, 11). The mechanical properties improved, however, as the interaction between the PE, compatibilizer and layered silicates increased. For instance, the appropriate compatibilizer (PE-g-MA) or custom organo-modified clay (OMLS) can form a better interaction between the polymer and nanoclay and the stress can transfer more efficiently from the PE matrix to the nanoclay. In addition, we can conclude that a high degree of crystallinity in the HDPE (6719) can affect the modulus and strength enormously by increasing the chain interaction via van der Waals forces. The maximum deformation, however, is impaired for low molecular weight.

3-2-4. Rheology

3-2-3-1. Oscillatory Shear Experiments

Rheology provides fundamental information on the processability of the PE nanocomposite and the effect of the nanoclay and compatibilizer content on zero shear viscosity. Complex viscosity (η*) versus frequency is plotted in Figure 3-22 and 3-23 for LLDPE and HDPE nanocomposites, respectively. The pure PE exhibited the transition from Newtonian behavior at low frequency to a power law (shear-thinning) region at higher frequency. Our results showed that the presence of nanoclay has a significant effect on the complex viscosity of the PE nanocomposite. Previously, our group reported that the maleic anhydride compatibilizer (PE-g-MA) does not have a significant effect on the rheological properties, as compared with the pure PE (6). Thus, the increased complex viscosity is solely affected by the presence of nanoclay at a lower frequency. The liquid-like behavior of the pure polymer changes to solid-like behavior in the nanocomposite. Moreover, the shear-thinning mechanism has an earlier onset for the PE/nanoclay nanocomposite, as compared with the pure PE. By increasing the frequency, the viscosity of the nanocomposite nears to the viscosity of the pure PE at higher frequency. Hyun et al. have suggested that this phenomenon is caused by the alignment of layered silicates in the PE matrix under shear (12). Furthermore, increasing the loading of clay to 4 wt % in the nanocomposite samples increased the complex viscosity of our material.

As mentioned, the compatibilizer can improve the interaction between the PE and layered silicates. Interestingly, in our results, the compatibilizer not only slightly increased the zero shear viscosity of the LLDPE/clay nanocomposites as compared to the neat LLDPE (Figure 3-22) but also provided a better interaction between the LLDPE and nanoclay to create a low viscosity of the LLDPE nanocomposites as compared with the HDPE nanocomposites (Figure 3-23). LLDPE

nanocomposites, therefore, prepared with LLDPE-g-MA as the compatibilizer could be good candidates for "zero-shear" rate processes like rotational molding.

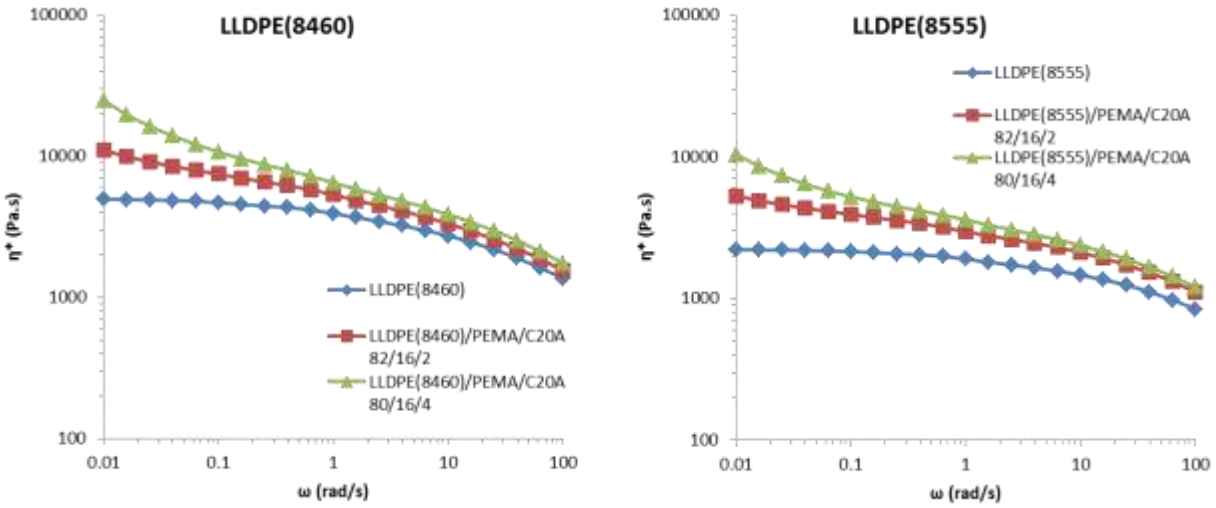

Figure 3-22 – Complex viscosity (η*) versus frequency for pure LLDPE and LLDPE nanocomposite containing different concentrations of nanoclay (Cloisite 20A)

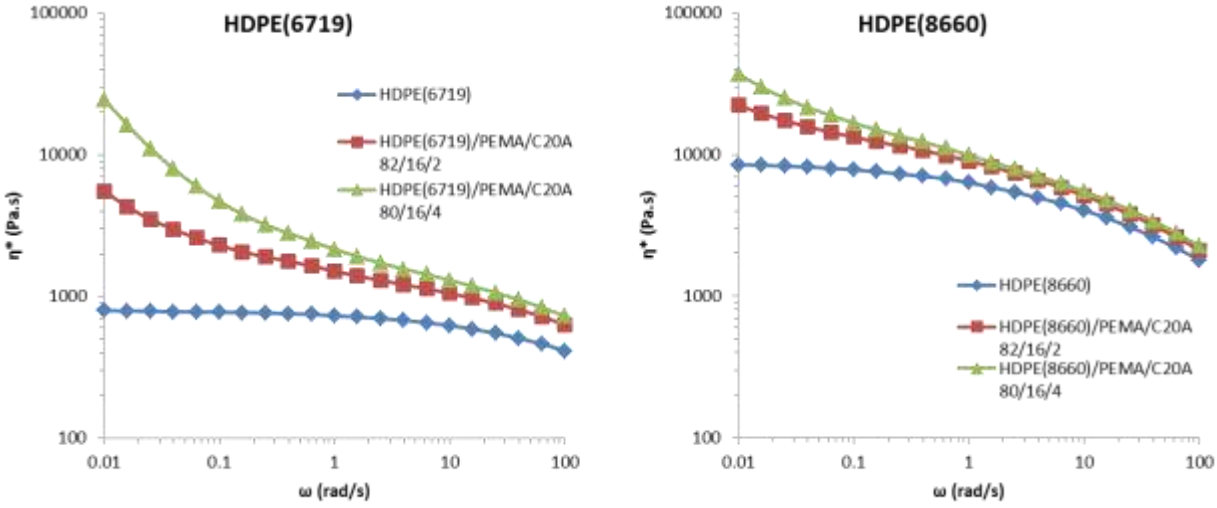

Figure 3-23 – Complex viscosity (η*) versus frequency for pure HDPE and HDPE nanocomposite containing different concentrations of nanoclay (Cloisite 20A)

3-2-3-2. Modulus and Time-Temperature Superposition

The rheological behavior of the PE nanocomposite was measured at different temperatures (160, 180 and 200 ^{0}C) to characterize their behavior over a wide range of frequencies through applying time – temperature superposition principles. As mentioned in Chapter 2, the WLF equation is a method applicable only at testing temperatures close to the glass transition temperature (T_g). Hence, the WLF equation cannot be used for polyethylene since the T_g of all the PE used in this study is less than -100 ^{0}C. The procedure for the calculation of shift factors for different matrices is discussed in the following paragraphs.

In this experiment, the reference temperature (T_S) was considered as 200 ^{0}C. The curves at 200 ^{0}C were kept constant and the other curves, at different temperatures, were shifted horizontally, as shown in Figure 3-24. The shift factor (a_T), which is a function of temperature, is defined as follows:

$$\log a_T = log\, \omega_S/\omega \qquad \text{Eq. 3-3}$$

where ω_s, is the frequency of a point on the curve at T_S with a particular modulus and ω is the frequency of a point with the same modulus on a curve at a different temperature. The calculated horizontal shift factor (a_T) is shown in Figure 3-25 as a function of a different weight percentage of nanoclay.

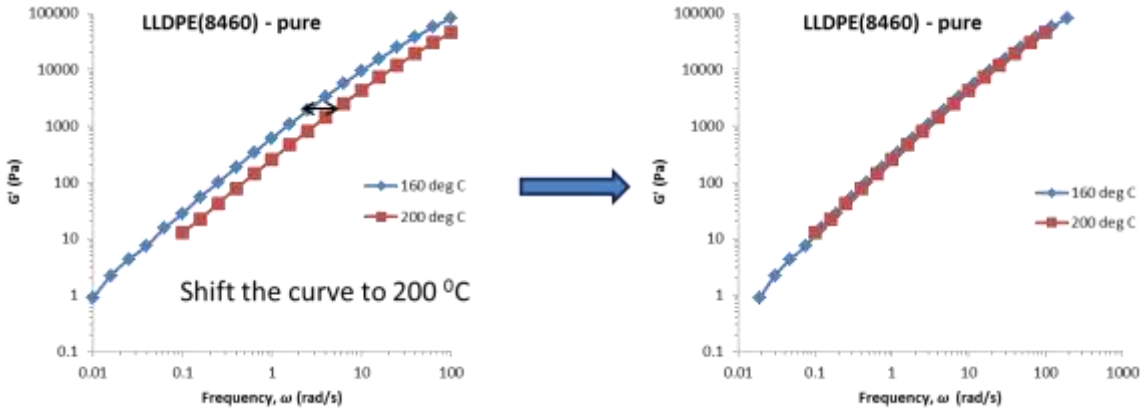

Figure 3-24 – Schematic of horizontal shift of rheological result by applying time-temperature superposition principles

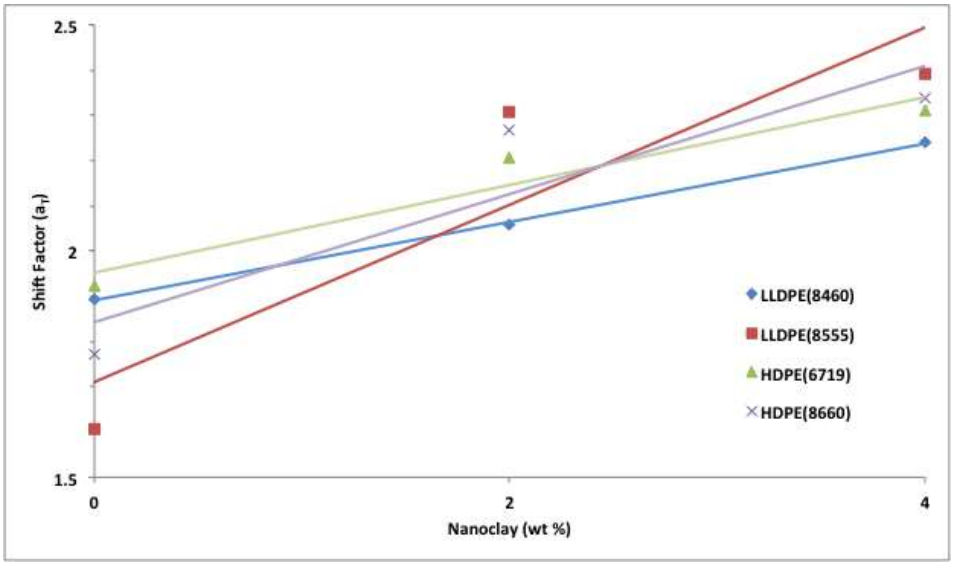

Figure 3-25 – Horizontal shift factors (a_T) of PE and PE nanocomposites containing different concentrations of nanoclay (Cloisite 20A), T_s = 200 ^{0}C

The storage modulus (G') and loss modulus (G") versus frequency are plotted by curve fitting in Figure 3-26 to 3-29. These are the logarithmic graphs for pure PE and PE/clay nanocomposites with 2 and 4 wt % nanoclay. The storage modulus (G') and loss modulus (G") were plotted versus frequency multiplied by the horizontal shift factor (a_T). The values of the storage and loss modulus increased for all the PE nanocomposites as compared to the neat PE. They become independent of frequency at low frequencies, which shows a network formation of

nanoclay in the matrices. Furthermore, both the storage and loss modulus approach the value of the neat PE at a higher frequency.

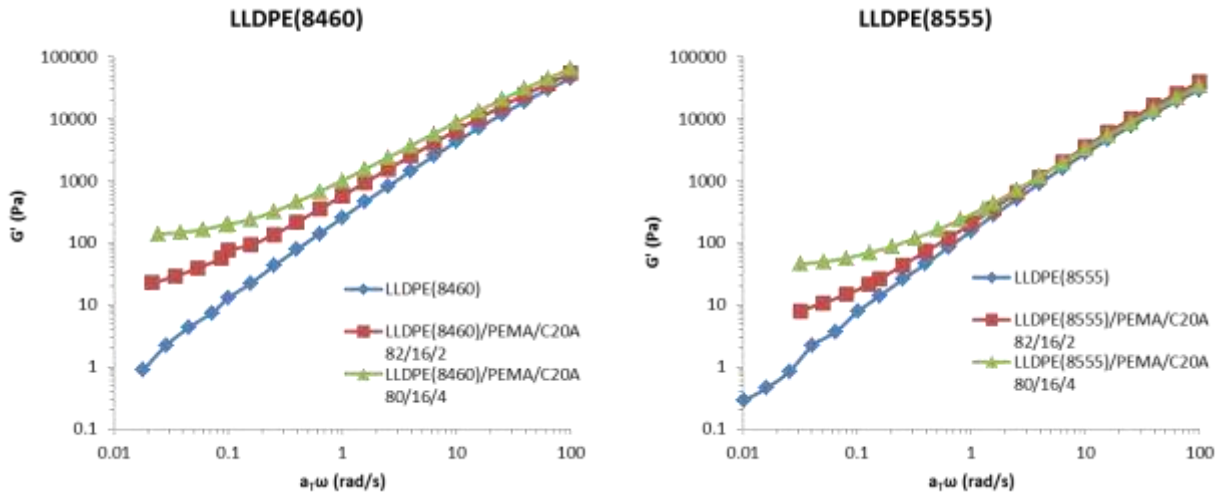

Figure 3-26 – Storage modulus (G') versus frequency for LLDPE and LLDPE nanocomposite containing different concentrations of nanoclay (Cloisite 20A) at T_s = 200 ^{0}C

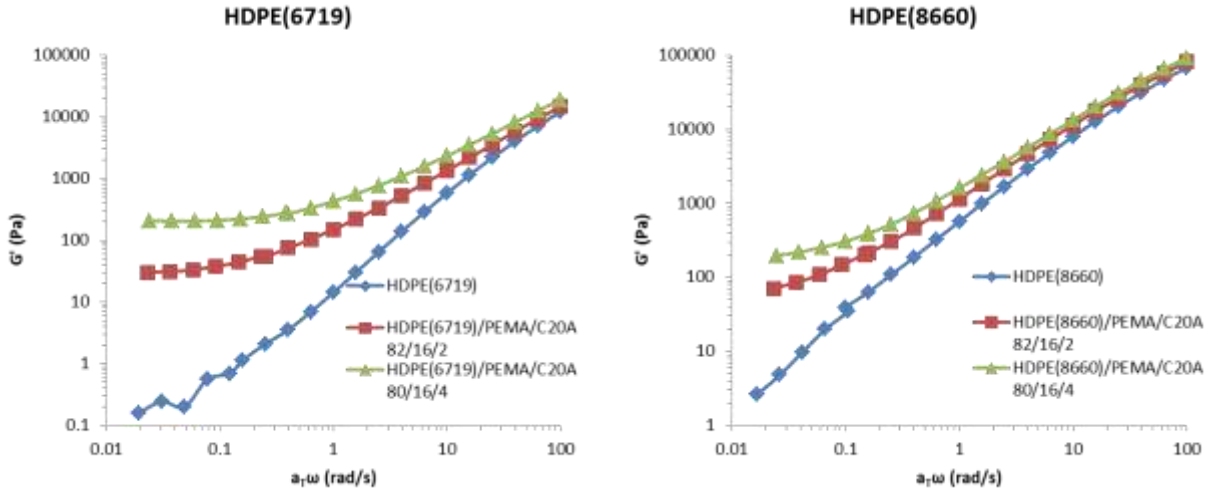

Figure 3-27 – Storage modulus (G') versus frequency for HDPE and HDPE nanocomposite containing different concentrations of nanoclay (Cloisite 20A) at T_s = 200 ^{0}C

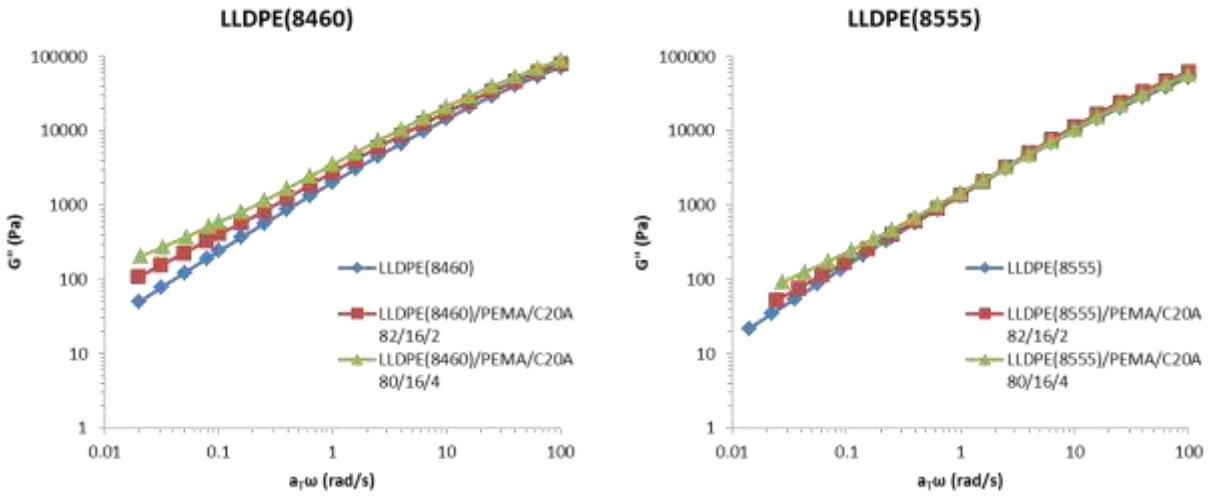

Figure 3-28 – Loss modulus (G") versus frequency for LLDPE and LLDPE nanocomposite containing different concentrations of nanoclay (Cloisite 20A) at T_s = 200 ^{0}C

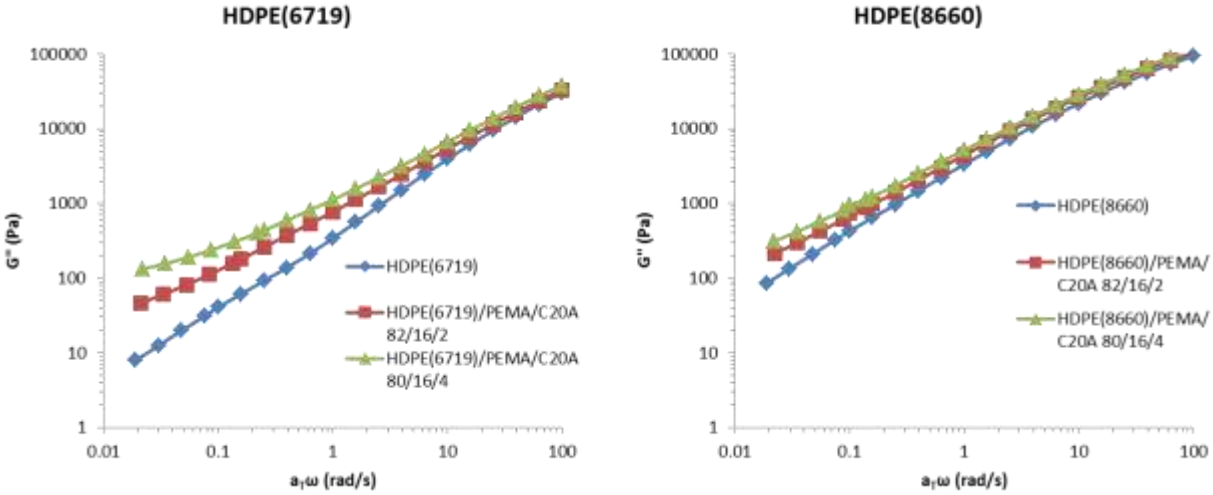

Figure 3-29 – Loss modulus (G") versus frequency for HDPE and HDPE nanocomposite containing different concentrations of nanoclay (Cloisite 20A) at T_s = 200 ^{0}C

3-3. Conclusion

PE/PE-g-MA/clay nanocomposites, with two different nanoclay contents were prepared using a twin-screw extruder. The XRD results and TEM images revealed a uniform dispersion of the layered silicates within the LLDPE nanocomposites with 2 wt % nanoclay as compared to the HDPE nanocomposites with 2 wt % nanoclay. A partially exfoliated structure was also obtained.

On the other hand, the addition of nanoclay at 4 wt % further decreased the basal spacing between the silicate layers. Among all the nanocomposites, the worst dispersion of the layered silicates occurred for the HDPE (8660) matrix. Additionally, the thermal characterization carried out through the DSC and TGA analysis revealed that the addition of the layered silicates had no significant effect on the melting and crystallization temperature of the nanocomposites while it decreased the heat of fusion and enthalpy of crystallization. This suggests that the mobilization of the polymer chains is hindered in the presence of PEMA. In addition, the thermal stability of the nanocomposites increased drastically in the presence of 2 wt % nanoclay, which illustrates a good dispersion of layered silicates in the PE matrices. Moreover, rheological properties exhibited a significantly high storage and loss modulus at low frequencies in the nanocomposites. Complex viscosity also increased; however, for the LLDPE (8555) nanocomposites, there was only a slight increase in viscosity. Furthermore, the rheological behaviors of nanocomposites at low frequencies suggest that they are more dependent on the nanoclay loading contents than the structure of the layered silicates within the nanocomposites. In addition, through studying the mechanical properties of nanocomposites, there was one more important conclusion: the compatibilizer with LLDPE as a backbone has a better interaction with the LLDPE as compared to the HDPE matrices; thus a better interaction between the LLDPE and layered silicates is expected for these nanocomposites.

3-4. References

1. Ray SS. Clay-containing polymer nanocomposites: from fundamentals to real applications: Newnes; 2013.

2. Sinha Ray S, Okamoto M. Polymer/layered silicate nanocomposites: a review from preparation to processing. Progress in polymer science. 2003;28(11):1539-641.

3. Fornes TD, Yoon PJ, Keskkula H, Paul DR. Nylon 6 nanocomposites: the effect of matrix molecular weight. Polymer. 2001;42(25):09929-40.

4. Reichert P, Nitz H, Klinke S, Brandsch R, Thomann R, Mülhaupt R. Poly (propylene)/organoclay nanocomposite formation: influence of compatibilizer functionality and organoclay modification. Macromolecular Materials and Engineering. 2000;275(1):8-17.

5. Picard E, Gauthier H, Gérard JF, Espuche E. Influence of the intercalated cations on the surface energy of montmorillonites: consequences for the morphology and gas barrier properties of polyethylene/montmorillonites nanocomposites. Journal of colloid and interface science. 2007;307(2):364-76.

6. Zhang M, Sundararaj U. Thermal, rheological, and mechanical behaviors of LLDPE/PEMA/clay nanocomposites: effect of interaction between polymer, compatibilizer, and nanofiller. Macromolecular Materials and Engineering. 2006;291(6):697-706.

7. Alamo RG, Graessley WW, Krishnamoorti R, Lohse DJ, Londono JD, Mandelkern L, et al. Small angle neutron scattering investigations of melt miscibility and phase segregation in blends of linear and branched polyethylenes as a function of the branch content. Macromolecules 1997;30:561–6.

8. Kanagaraj, S., et al., Mechanical properties of high density polyethylene/carbon nanotube composites. Composites Science and Technology, 2007. 67(15): p. 3071-3077.

9. Perrin-Sarazin F, Ton-That MT, Bureau MN, Denault J. Micro-and nano-structure in polypropylene/clay nanocomposites. Polymer. 2005;46(25):11624-34.

10. Manias E, Touny A, Wu L, Strawhecker K, Lu B, Chung TC. Polypropylene/montmorillonite nanocomposites. Review of the synthetic routes and materials properties. Chemistry of Materials. 2001;13(10):3516-23.

11. Nam PH, Maiti P, Okamoto M, Kotaka T, Nakayama T, Takada M, et al. Foam processing and cellular structure of polypropylene/clay nanocomposites. Polymer Engineering & Science. 2002;42(9):1907-18.

12. Hyun YH, Lim ST, Choi HJ, Jhon MS. Rheology of poly (ethylene oxide)/organoclay nanocomposites. Macromolecules. 2001;34(23):8084-93.

Chapter 4 – Synthesis and Analysis of Organically Modified Clay

4-1. Introduction

Chapter 4 compares the basal spacing and other properties of an in-house modified nanoclay with a commercial nanoclay, Cloisite 20A. The montmorillonite can be modified with several organic ammonium or phosphonium salts. Each modifier, however, has different effects on the properties of the nanoclay and, consequently, on the final properties of the polymer/clay nanocomposite.

The materials used for the organo-modification of nanoclay are also discussed along with experimental techniques for the modification of nanoclay and nanocomposite preparation. The chapter closes with the presentation of experimental results and analysis.

4-2. Experimental

4-2-1. Materials

Unmodified clay:

Cloisite-Na^+, a natural bentonite, was used in the ion exchange modification process. The cation exchange capacity (CEC) of Cloisite-Na^+ is 92.6 meq/100 g clay and the d-spacing is 1.21 nm, based on X-ray diffraction results (Southern Clay Products Inc.).

Organic modifier:

Dimethyldioctadecylammonium bromide (DDAB), Sigma-Aldrich Co., as an organic modifier was used to modify the natural bentonite, Cloisite-Na^+. Figure 4-1 illustrates the chemical structure of the organic modifier (DDAB). This modifier includes a cationic site for a cation exchange reaction with the montmorillonite (MMT) and long alkyl chains that can

improve the basal spacing between the layered silicates. It may also enhance the compatibility between organo-modified clay (OMLS) and the PE matrices. This modifier was chosen to compare the effect of an in-house modification of nanoclay with commercially available nanoclay. In addition, linear tallow branches make it a good modifier for HDPE.

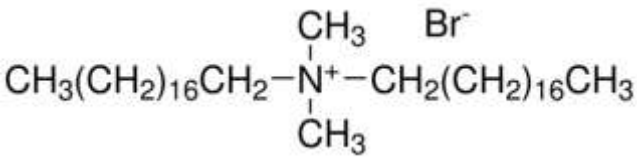

Figure 4-1 – Chemical structure of dimethyl dioctadecyl ammonium bromide (DDAB), Sigma-Aldrich Co.

Polyethylene:

In this experiment, two grades of polyethylene were selected, based on the results from the last chapter, including linear low density polyethylene (LLDPE (8555)) and high density polyethylene (HDPE (8660)). The characteristics of the PEs were presented in Table 3-1. The decision to use these PEs were based on the following: HDPE (8660) had the worst interaction with the components of the nanocomposites, including Cloisite 20A, and the compatibilizer, as compared to the other PE nanocomposites; the layered silicates dispersed nicely within the LLDPE (8555) matrix and could form an intercalated structure. The goals of this experiment, therefore, are to investigate the level of adhesion and interaction between the in-house organo-modified clay (OMLS) and the commercially available nanoclay (Cloisite 20A) with two different types of PE matrices.

4-2-2. Organo modified clay preparation

The steps for the ion exchange modification process of the montmorillonite (MMT) are explained in the following paragraphs and illustrated schematically in Figure 4-2:

1. For the modification of MMT, 1 gram of Cloisite-Na^+ was dispersed in an ethanol-water (4:1, V/V) mixture at 70 ^{0}C. The mixture was stirred for 4 hours to obtain a well-dispersed mixture of nanoclay.
2. The concentration of modifier (DDAB) was set as 0.5, 1.1 and 1.5 × CEC of the corresponding MMT. The modifier was dispersed and stirred in ethanol.
3. The modifier mixture was poured into the MMT dispersion after 4 hours.
4. The ion exchange modification is a rapid process but the mixture was stirred at least 24 hours at 70 ^{0}C to reach equilibrium conditions.
5. The mixture was filtered through a Buchner funnel filtration system; so as to have a bromide ion free suspension water and ethanol were used to wash the retentate. The presence of bromide ion in the nanoclay was also tested with 0.1 N $AgNO_3$.
6. After filtration, the organo-modified clay was dried in a vacuum oven at 70 ^{0}C for 24 hours. The OMLS was ground to particle size less than 64 μm before melt mixing with the polyethylene and compatibilizer.

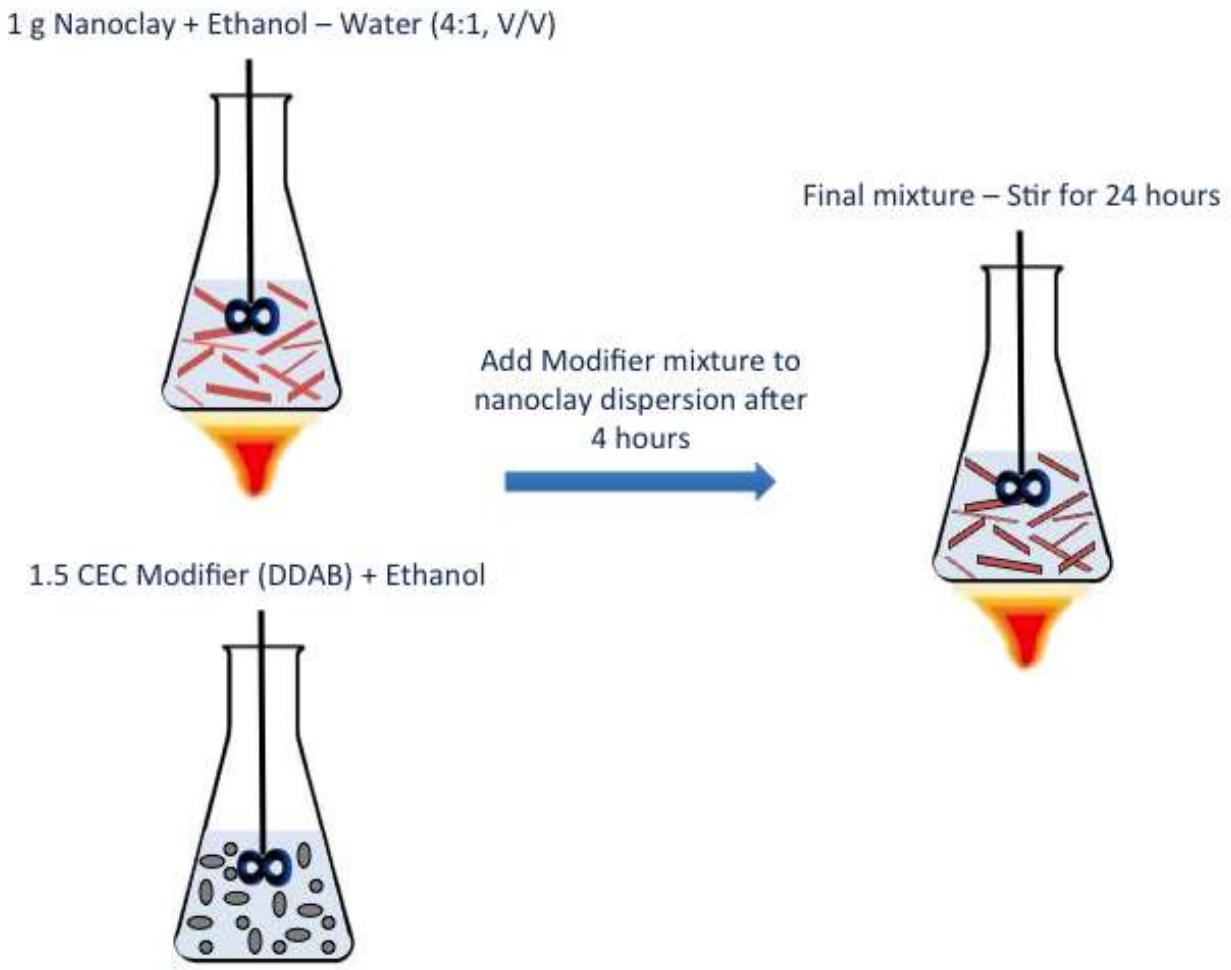

Figure 4-2 – Schematic illustration of preparation method of in-house OMLS

For enhanced understanding, the details of the organo modification of the layered silicates are illustrated in Figure 4-3. In the cation exchange modification process, the alkyl-ammonium salt (DDAB) was replaced by the "intergallery cations", Na^+, and caused the increase in basal spacing between the silicate layers.

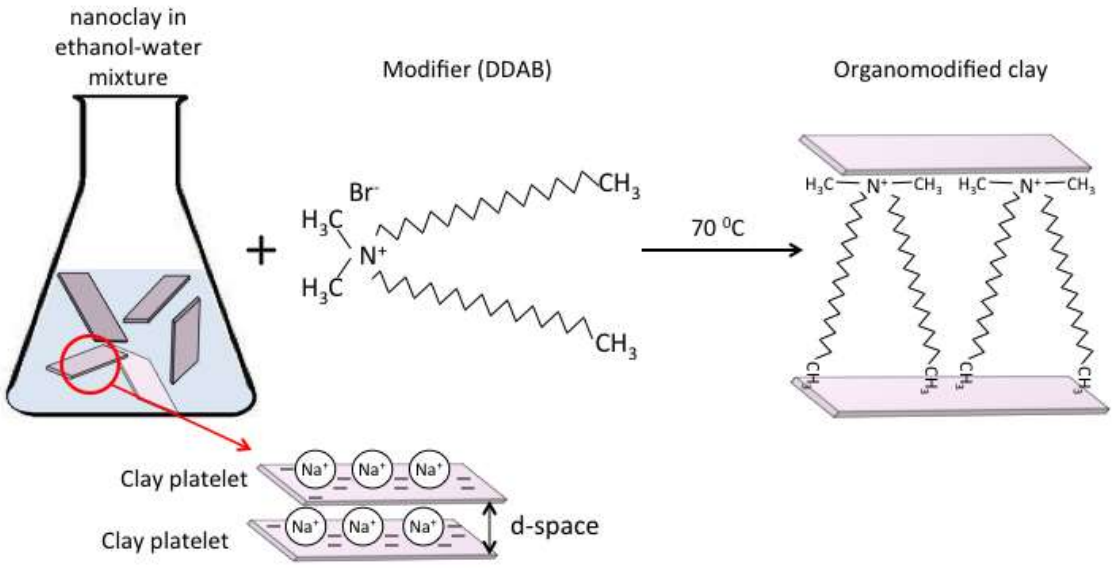

Figure 4-3 – Schematic illustration of the organo modification of nanoclay

4-2-3. Polyethylene/organo-modified clay nanocomposite preparation

Batch mixer:

Polyethylene/organo-modified clay samples were prepared using the Haake Polylab batch mixer connected to the Rheomix 600 mixer equipped with roller blades. The steps of samples' preparation are as follows:

1. In this experiment, each LLDPE (8555) and HDPE (8660) was melt-mixed with compatibilizer (LLDPE-g-MA) in the twin-screw extruder (machine specification is referenced in Chapter 4. The composition of the samples was 50/50 wt % of the PE and compatibilizer. The PE and LLDPE-g-MA pellets were hand mixed and the mixture was transferred to one feeder. The melt compounding was performed at a barrel temperature profile at 170, 170, 180, 180 ^{0}C and a die temperature 190 ^{0}C, with the screw speed of 100 rpm.
2. Melt compounding in the batch mixer was performed at a temperature of 180 ^{0}C and screw speed of 70 rpm for 7 min. The PE/compatibilizer (50/50 wt %) and organo-modified layered silicate were fed to the mixer at once. After 2 minutes, the remaining PE was added to the master batch and the material was mixed for 5 minutes.
3. PE nanocomposite was prepared with both Cloisite 20A and the in-house organo-modified clay (OMLS) to examine the influence of OMLS on the properties of PE, as compared with commercially available organo-modified clay (Cloisite 20A). The composition of the two samples and the preparation conditions are provided in Table 4-1.

Table 4-1 – PE nanocomposite compositions and methods of preparation

Sample Name	Composition				Conditions		
	Polymer Matrix (wt %)	**Compatibilizer (wt %)**	**Nanoclay (wt %)**		**Method of mixing**	**Temperature (^{0}C)**	**RPM**
	LLDPE (8555) or HDPE (8660)	LLDPE-g-MA Orevac (18340)	Cloisite 20A	Organo-modified clay (OMLS)			
LLDPE (8555)/PEMA 50/50	50	50	-	-	Twin-Screw Extruder	170-190	100
LLDPE (8555)/PEMA/C20A 82/16/2	82	16	2	-	Batch mixer	180	70
LLDPE (8555)/PEMA/C20A 80/16/4	80	16	4	-	Batch mixer	180	70
LLDPE (8555)/PEMA/OMLS 82/16/2	82	16	-	2	Batch mixer	180	70
LLDPE (8555)/PEMA/OMLS 80/16/4	80	16	-	4	Batch mixer	180	70
HDPE (8660)/PEMA 50/50	50	50	-	-	Twin-Screw Extruder	170-190	100
HDPE (8660)/PEMA/C20A 82/16/2	82	16	2	-	Batch mixer	180	70
HDPE (8660)/PEMA/C20A 80/16/4	80	16	4	-	Batch mixer	180	70
HDPE (8660)/PEMA/OMLS 82/16/2	82	16	-	2	Batch mixer	180	70
HDPE (8660)/PEMA/OMLS 80/16/4	80	16	-	4	Batch mixer	180	70

4-3. Results and discussions

4-3-1. Thermo Gravimetric Analysis (TGA)

The thermal stability of the organo-modified clay with different amounts of surfactant (DDAB) was determined using TGA (Figure 4-4). The TGA results of pure Cloisite Na^+ and Cloisite 20A were added to the same graph to compare the effect of the in-house modification of nanoclay with unmodified clay and commercially available organo-modified clay. Cloisite Na^+ did not exhibit decomposition at a temperature between 210 to 600 ^{0}C. The resulting weight loss for OMLS is due to the decomposition of surfactant. The thermal decomposition of the organo-modified clays, with different amounts of surfactant, started at 210 ^{0}C while the maximum decomposition occurred at a higher temperature with an increase in the amount of DDAB. The decomposition of OMLS started above 200 ^{0}C; hence, DDAB had a good stability at a normal PE processing temperature.

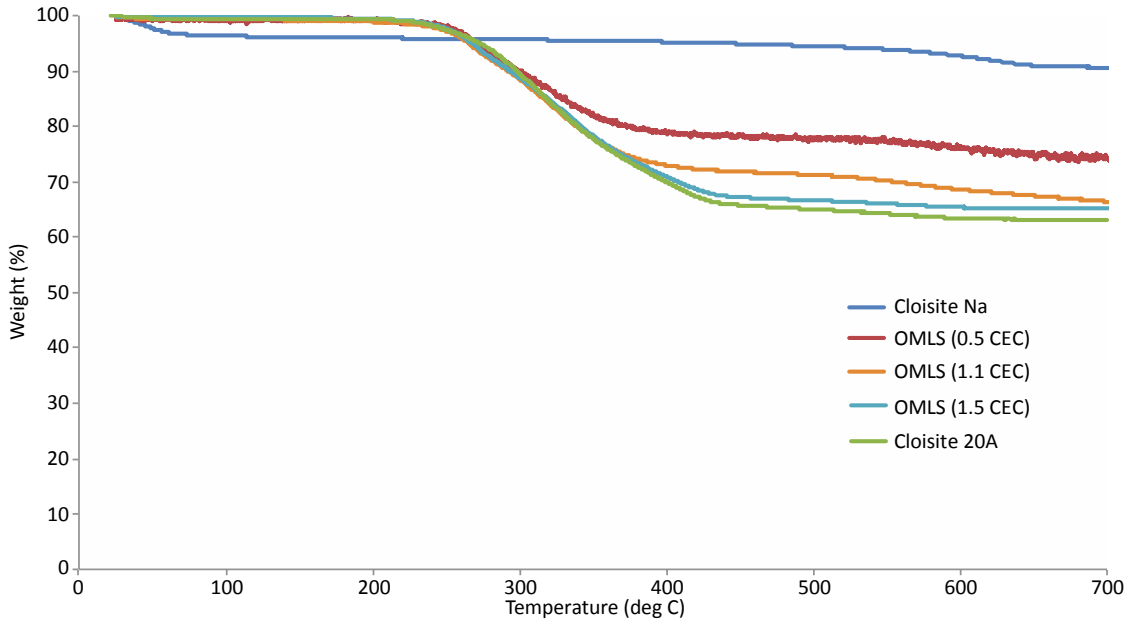

Figure 4-4 – TGA curves of DDAB organoclays with different amounts of added surfactant

Xi et al. have demonstrated that the decomposition of organo-modified clay occurred in four consecutive steps: water desorption, dehydration, desurfactant and dehydroxylation of OMLS.

They also differentiated three different molecular environment types for the surfactant in organo-modified clay: 1. surfactant cations intercalated into the interlayer spaces through a cation exchange and bound to the surface sites via electrostatic interaction; 2. surfactant (cations and/or molecules) physically adsorbed on the external surface of the particles; and 3. surfactant molecules located within the interlayer spaces (1). In Figure 4-4, the peaks - around 280 ^{0}C with high DDAB concentrations - probably occurred due to the thermal decomposition of free surfactant (either type 2 or 3) that had no interaction with the surface of the silicate layers. Thus, the high surfactant concentration did not essentially cause a high basal spacing of layers, while more surfactant intercalated into the layers at a low concentration of surfactant (1, 2). Consequently, these results suggest that OMLS, with a 1.1 CEC concentration, is a good candidate to prepare PE nanocomposite, as compared with PE/C20A nanocomposite.

4-3-2. X-Ray Diffraction (XRD)

X-Ray Diffraction (XRD) of organo-modified clay:

The exfoliated or intercalated structure of nanocomposites can significantly influence the final properties of nanocomposites. Two factors are important in the structure formation of nanocomposites: the degree of dispersion and the quality of interaction quality of the layered silicates with the polymer matrix. Moreover, a large basal spacing of layered silicates, prior to mixing with the polymer, is key to improve the dispersion and interaction between the layered silicates and the polymer matrix. Long alkyl chains of surfactant on the surface of silicate layers

are hypothesized to increase the basal spacing, and hence with improving the dispersion and interaction between the polymer and nanoclay.

In this study, the effects of different concentrations of surfactant (DDAB) on the basal spacing of organo-modified clay were tested using XRD techniques. In Figure 4-5, the XRD results are shown for the in-house organo-modified clay with different surfactant (DDAB) concentrations. Data for pure montmorillonite (Cloisite-Na^+) and commercial organo-modified clay (Cloisite 20A) are also included for comparison.

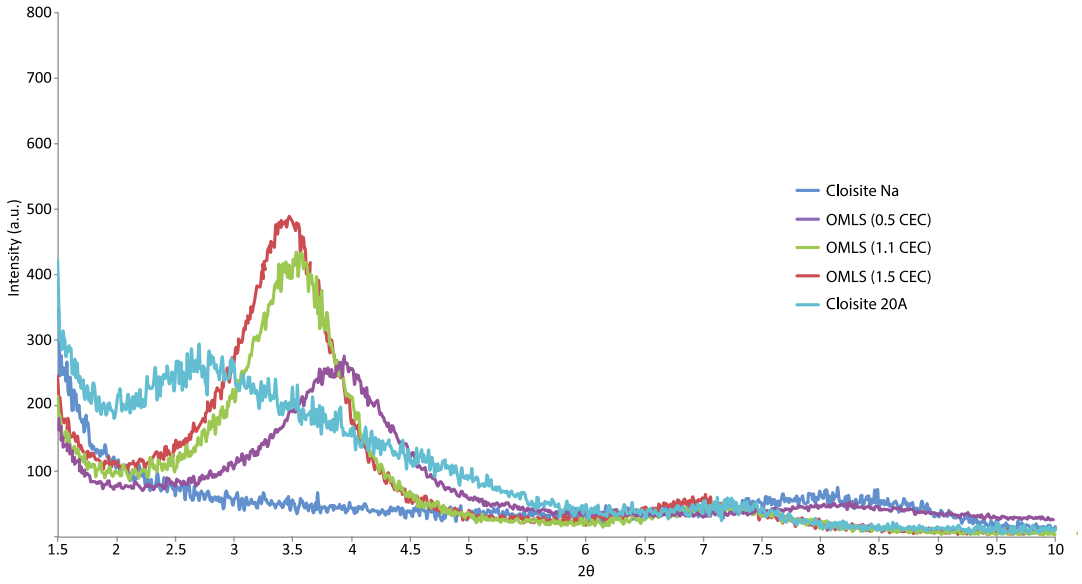

Figure 4-5 – XRD pattern of Cloisite Na^+ treated with alkyl ammonium salt at different CEC concentration

The basal spacing (d_{001}) of the organo-modified clay with different concentrations of DDAB is calculated by utilizing Bragg's law equation. The basal spacing (d_{001}) is equal to 2.61 nm for a 0.5 CEC concentration of surfactant, while the space between layers increased to 2.95 nm for 1.5 CEC concentrations. No significant changes were identified in the basal spacing from 1.1 to 1.5 CEC concentrations, suggesting that the higher concentration of DDAB has no significant effect

on the interlayer distance between the silicate layers. Consistent with other studies researched, we found that the basal spacing increased gradually by increasing the concentration of surfactant until 1.1 CEC (1, 2).

An optimum concentration of surfactant for the modification of layered silicates was found by considering the XRD along with TGA observations. The organo-modified clay, with a 1.1 CEC concentration of alkyl ammonium salts (DDAB), was used to prepare the PE/organo-modified clay nanocomposites and their properties were characterized. The properties of these samples were then compared with the nanocomposites prepared with commercial organo-modified clay (Cloisite 20A).

X-Ray Diffraction (XRD) of PE/organo-modified clay nanocomposite:

The nanocomposites were characterized by XRD and the corresponding basal spacing of the organo-modified clay in the PE nanocomposites was determined from the XRD pattern. Figures 4-6 and 4-7 illustrate the XRD results for the PE nanocomposite with 2 wt % and 4 wt % nanoclay, respectively.

Nanocomposites with 2 wt % OMLS exhibited a better dispersion of layered silicates, as the peaks at the initial angle were broader and shifted to a lower angle. For instance, the basal spacing of the LLDPE (8555) and HDPE (8660)/OMLS nanocomposite increased to 4.22 nm and 4 nm, as compared to the pure OMLS with 2.91 nm basal spacing. In the case of nanocomposite with 4 wt % OMLS, the corresponding peaks were sharper and occurred at a higher angle due to poor dispersion of the layered silicate in PE. In general, PE nanocomposites prepared using OMLS (the in-house organo-modified clay), illustrated a better dispersion of the nanoclay in the

PE matrix than those made with Cloisite 20A since the peaks occurred at a lower diffraction angle.

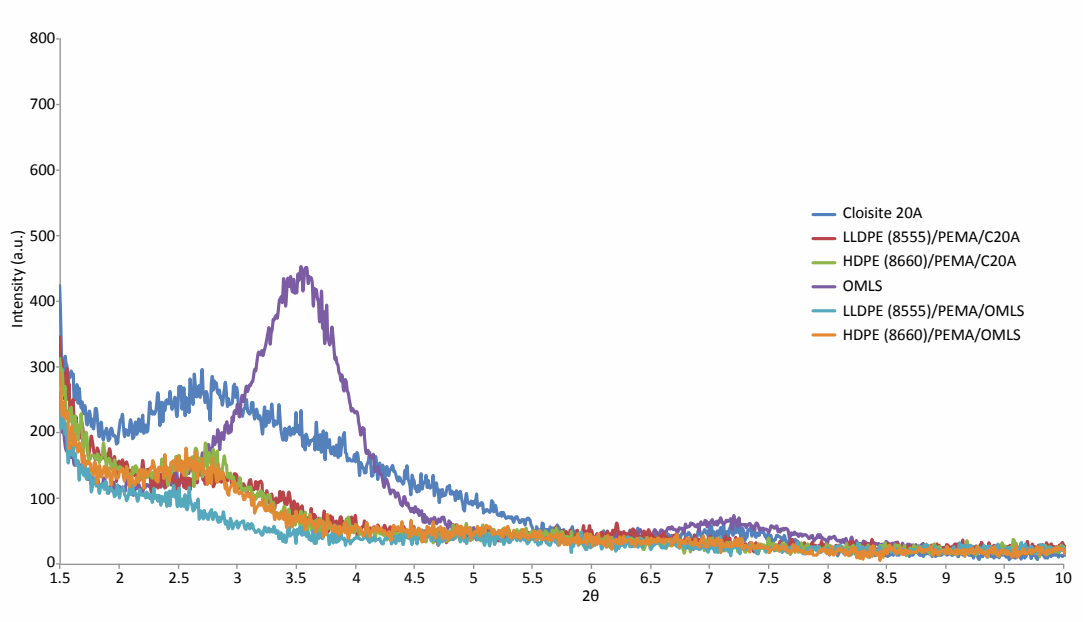

Figure 4-6 – XRD pattern for polyethylene nanocomposite prepared by in-house organo-modified clay and Cloisite 20A (PE/PEMA/clay, 82/16/2 wt %), d_{001} (OMLS, 1.1 CEC) = 2.91 nm

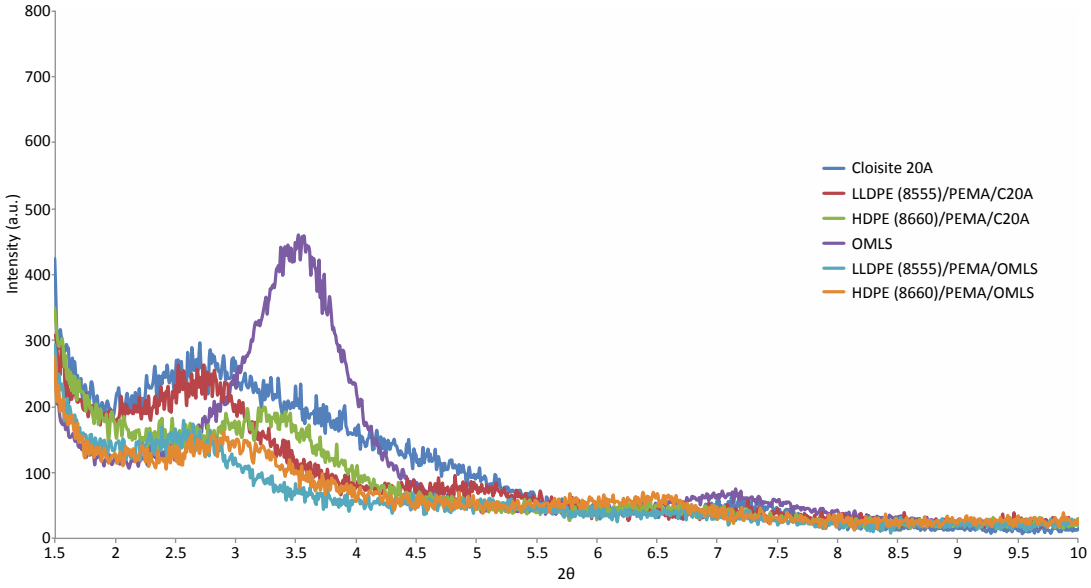

Figure 4-7 – XRD pattern for polyethylene nanocomposite prepared by in-house organo-modified clay and Cloisite 20A (PE/PEMA/clay, 80/16/4 wt %)

4-3-3. Mechanical Test

As mentioned, the mechanical properties of PE/clay nanocomposite are related to the degree of dispersion of layered silicates and the development of adhesion between the layered silicates surface and the polymer chain (3). The stress-strain curves were plotted for the LLDPE (8555) and HDPE (8660) nanocomposite prepared with the in-house organo-modified clay (OMLS) and with the commercial organo-modified clay (Cloisite 20A) (Figure 4-8 and 4-9). The mechanical properties of pure PE were determined from these curves to investigate the effects of different organo-modified clay on the improvement of mechanical properties. To study the mechanical properties, three important properties - *Young's modulus*, *yield strength* and *elongation at break* - were determined, based on stress-strain curves. Results are presented in Figure 4-10 to 4-12.

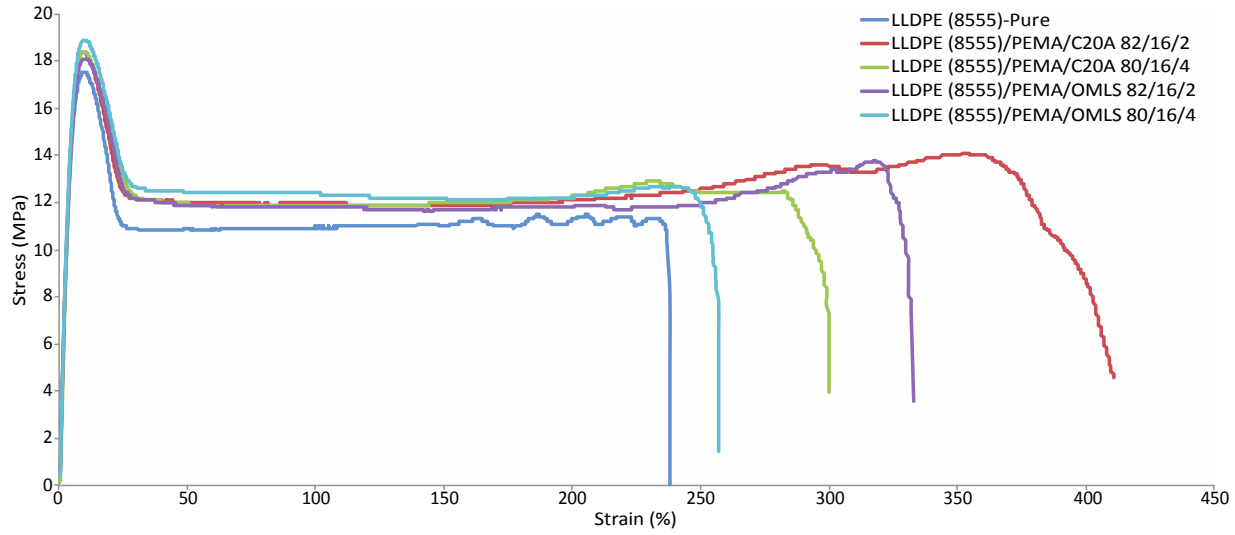

Figure 4-8 – Stress-Strain plot of pure LLDPE and LLDPE nanocomposite prepared by in-house organo-modified clay and Cloisite 20A containing 2 and 4 wt % of nanoclay

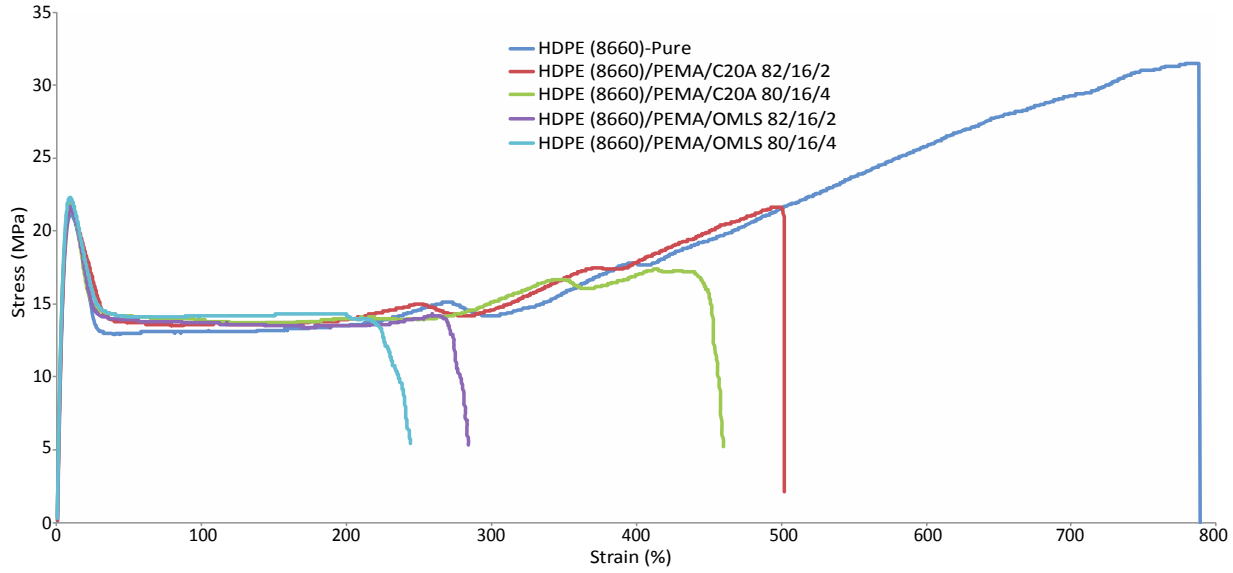

Figure 4-9 – Stress-Strain plot of pure HDPE and HDPE nanocomposite prepared by in-house organo-modified clay and Cloisite 20A containing 2 and 4 wt % of nanoclay

Figure 4-10 shows the *Young's modulus* of the samples as an indication of the material's stiffness or rigidity. *Young's modulus* was calculated as the slope of the initial linear part of the stress–strain curve, based on visual evaluation. Numerous studies illustrated that the clay contributes to the enhancement of modulus in the polymer/clay nanocomposite (3, 4). As the adhesion between the layered silicate surface and polymer chain is improved, the applied stress on the nanocomposite sample can transfer more effectively from the polymer chain to the layered silicate (5). The polyolefin/clay nanocomposites, however, have shown inconsistency in mechanical property measurements, which can be changed by differences in process conditions, organo-modified clay and compatibilizers (5, 6). The modulus of the PE nanocomposites behaved differently with respect to nanoclay concentration, depending on the type of organo-modified clay used. The in-house OMLS brought about the enhancement of the modulus when the nanoclay loading was increased for the LLDPE (8555). Although the modulus of HDPE (8660)/OMLS nanocomposite is inconsistent with increasing the nanoclay content, the modulus

of the HDPE (8660)/OMLS nanocomposite enhanced slightly, as compared to the HDPE (8660)/C20A nanocomposite. The incorporation of the in-house OMLS in both LLDPE and HDPE, therefore, represented a small enhancement in the modulus, over the commercial nanoclay. This may be a consequence of a better compatibility between the in-house OMLS, the LLDPE matrix and the compatibilizer (LLDPE-g-MA).

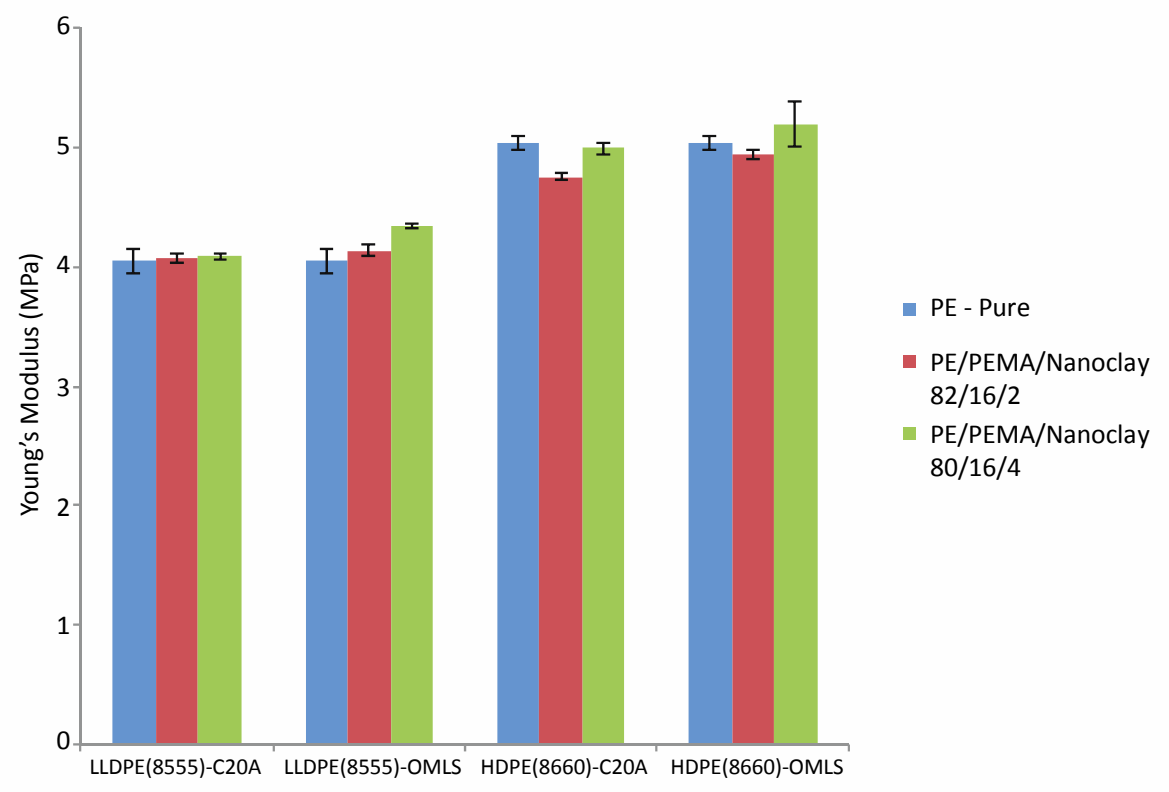

Figure 4-10 – *Young's modulus* of pure PE and PE nanocomposite prepared by in-house organo-modified clay and Cloisite 20A containing 2 and 4 wt % of nanoclay

The strength of the LLDPE nanocomposite with increasing nanoclay concentration slightly increased or remained unchanged (Figure 4-11). The in-house OMLS demonstrated the same behavior as the Cloisite 20A in the LLDPE matrix, due to the poor adhesion of the silicate layers and polymer chains at yield point.

On the other hand, LLDPE with 2 wt % nanoclay showed a drastic increase in the maximum deformation, following with a reduction at higher clay content (Figure 4-12). Comparatively, the maximum deformation of the HDPE nanocomposite showed a continuous deterioration as the nanoclay content increased, again due to the poor adhesion between the layered silicate surface and HDPE chain. These results confirmed that LLDPE-g-MA has a stronger incorporation with the LLDPE matrix than with the HDPE matrix as would be expected due to chemical similarity of LLDPE-g-MA and LLDPE.

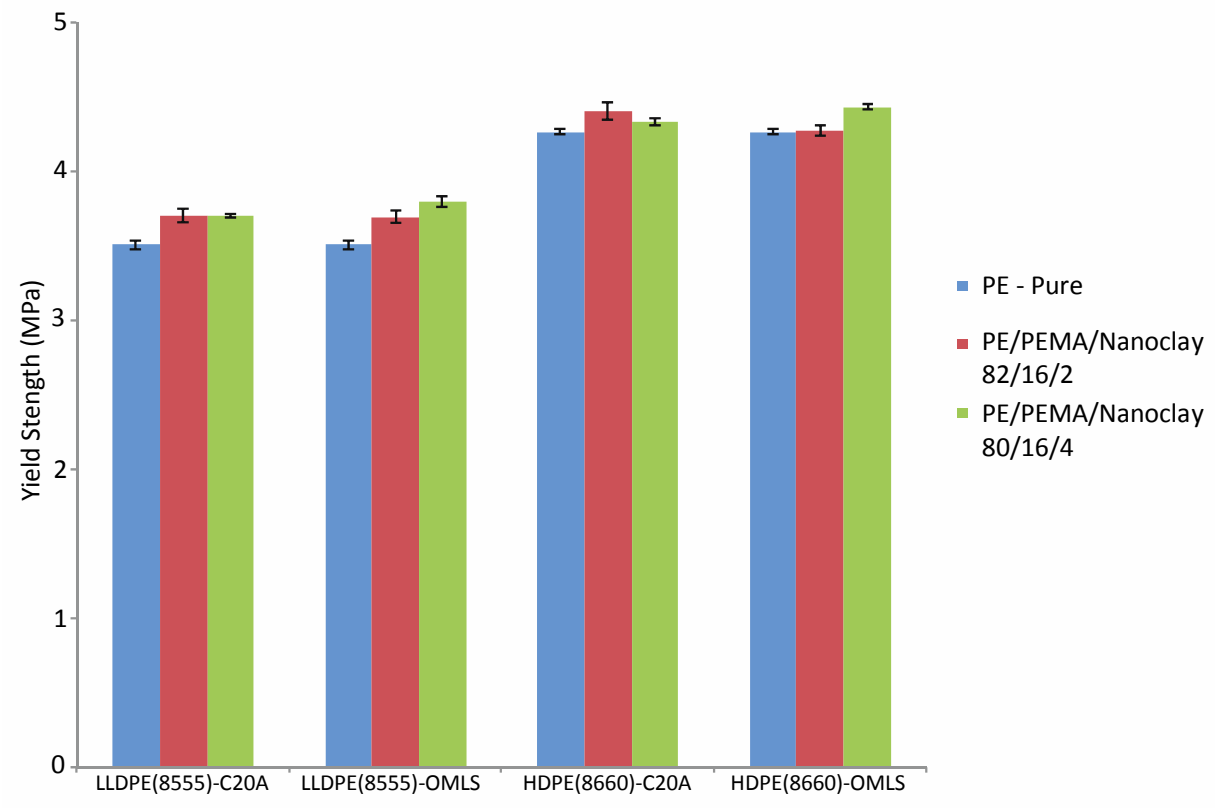

Figure 4-11 – *Yield strength* of pure PE and PE nanocomposite prepared by in-house organo-modified clay and Cloisite 20A containing 2 and 4 wt % of nanoclay

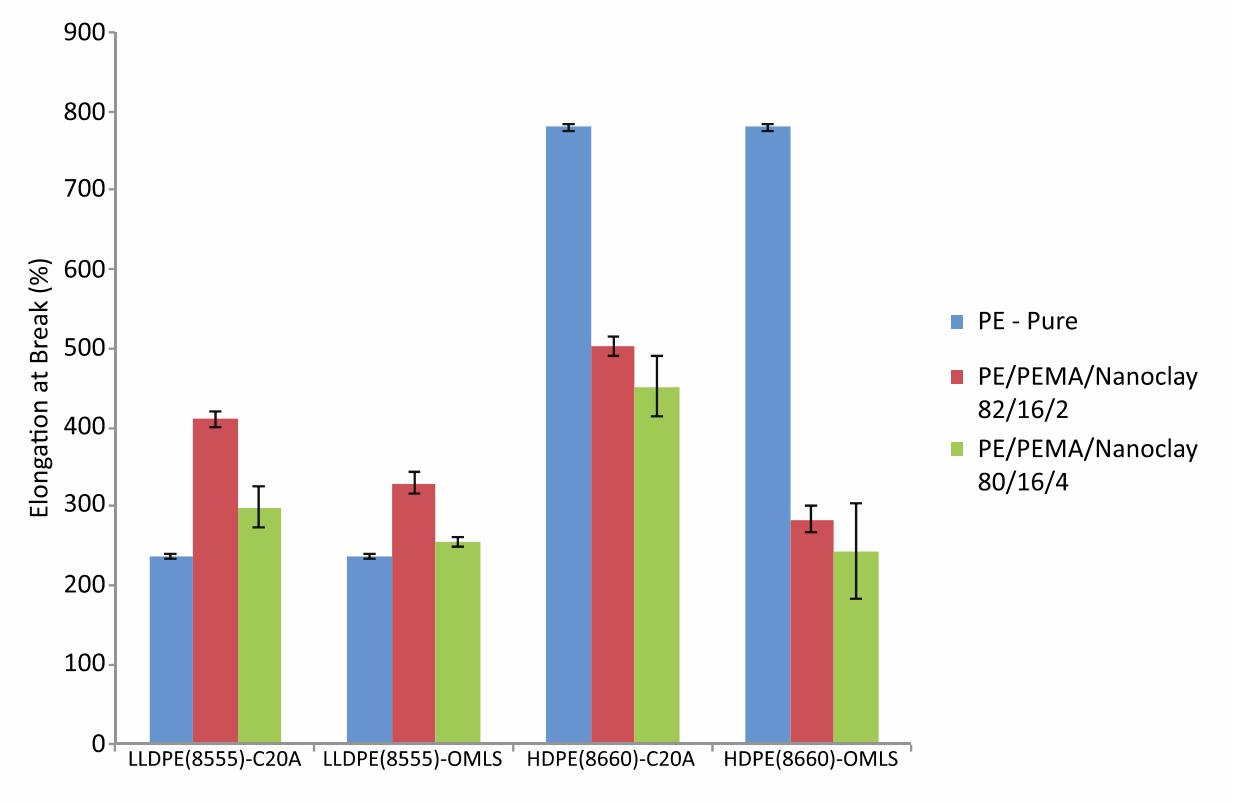

Figure 4-12 – *Elongation at break* of pure PE and PE nanocomposite prepared by in-house organo-modified clay and Cloisite 20A containing 2 and 4 wt % of nanoclay

4-3-4. Rheology Test

The rheological properties of the melt-mixed nanocomposite with the commercial nanoclay (Cloisite 20A) and the in-house organo-modified nanoclay (OMLS) are plotted in Figure 4-13 to 4-18. The flow behavior of the LLDPE (8555) and HDPE (8660) nanocomposites varied considerably from the corresponding pure matrices (Figure 4-13 and 4-14). The in-house OMLS nanocomposites revealed very strong non-Newtonian behavior in both the LLDPE and HDPE matrices; this is more pronounced at low frequencies. The solid-like response of the nanocomposite is strongly influenced by the presence of nanoclay at a low frequency (7). At a high frequency, the behavior of the nanocomposites approaches that of the pure matrices, which corresponds to the domination of the matrix rheology at high frequency. The difference at the

terminal zone, however, may be due to the extent of the dispersion of the nanoclay in the polymer matrices (8). Galgali et al. have suggested that the solid-like behavior of nanocomposites at a low frequency is completely independent of the structure of the layered silicate in nanocomposites; rather, it depends upon the amount of clay loading in the nanocomposites. They confirmed that this rheological behavior stems from the frictional interactions between the layered silicate and is not due to the immobilization of the confined polymer chains (7).

The storage modulus (G') and loss modulus (G") of the LLDPE (8555) and HDPE (8660) versus frequency are plotted in Figure 4-15 to 4-18. The slope of the log-log curve of G' and G" versus frequency are smaller for the nanocomposite prepared with the in-house OMLS, even for a small amount of layered silicates, and is due to the formation of a network structure in the molten state (9). Meaningful improvements in the elastic and viscous modulus of the in-house OMLS nanocomposites are seen, which are further augmented at higher clay loading at all frequencies.

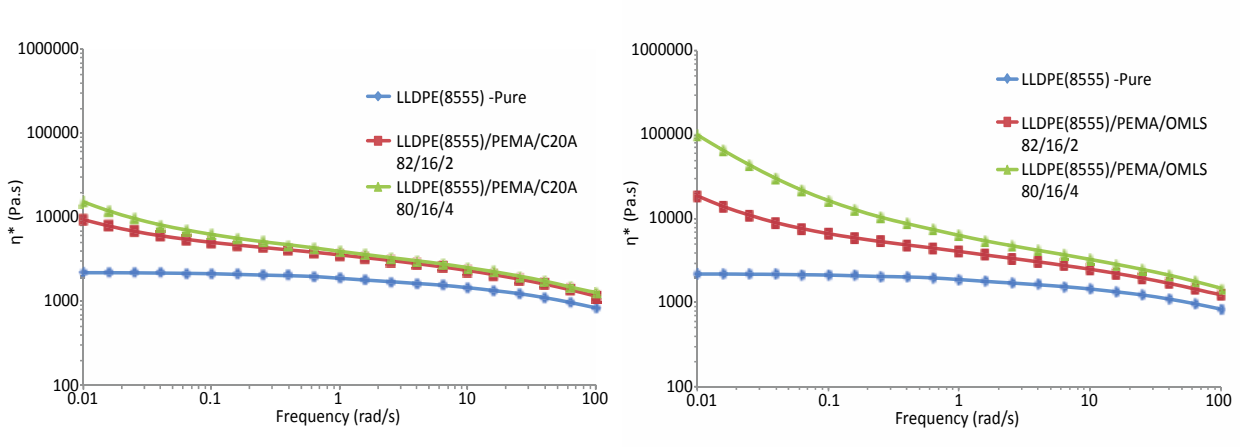

Figure 4-13 – Complex viscosity (η*) versus frequency for LLDPE (8555) and LLDPE (8555) nanocomposite prepared by in-house organo-modified clay and Cloisite 20A containing 2 and 4 wt % of nanoclay

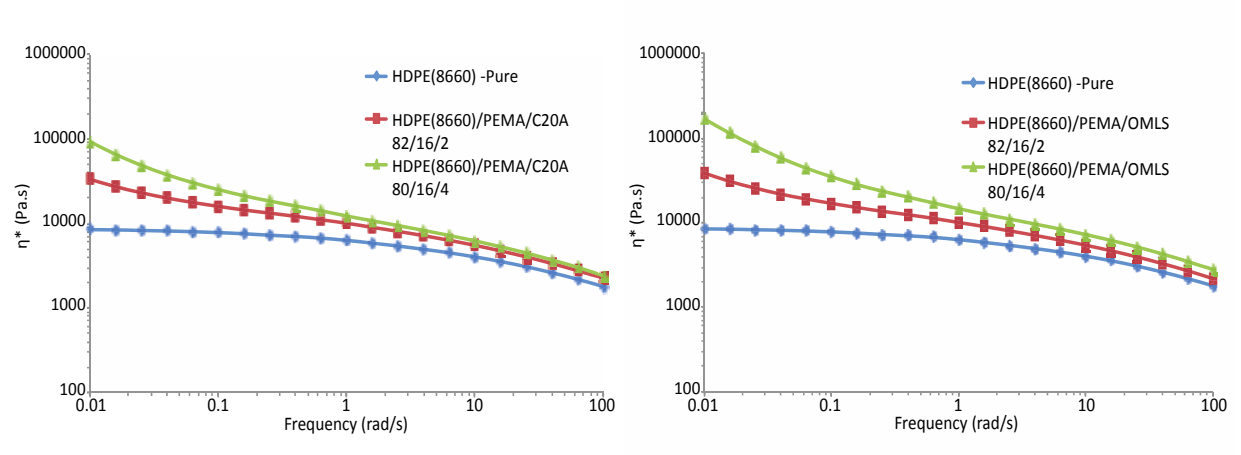

Figure 4-14 – Complex viscosity (η*) versus frequency for HDPE (8660) and HDPE (8660) nanocomposite prepared by in-house organo-modified clay and Cloisite 20A containing 2 and 4 wt % of nanoclay

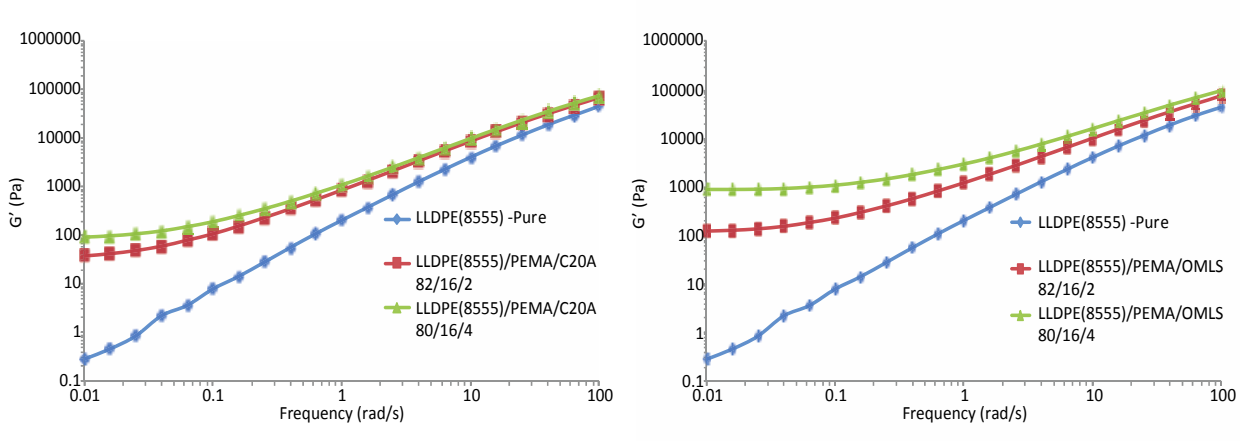

Figure 4-15 – Storage modulus (G') versus frequency for LLDPE (8555) and LLDPE (8555) nanocomposite prepared by in-house organo-modified clay and Cloisite 20A containing 2 and 4 wt % of nanoclay

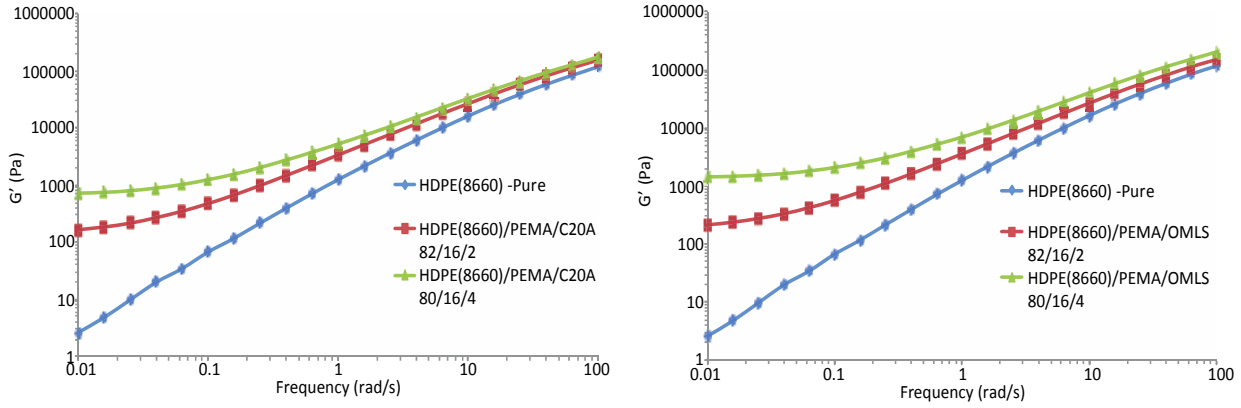

Figure 4-16 – Storage modulus (G') versus frequency for HDPE (8660) and HDPE (8660) nanocomposite prepared by in-house organo-modified clay and Cloisite 20A containing 2 and 4 wt % of nanoclay

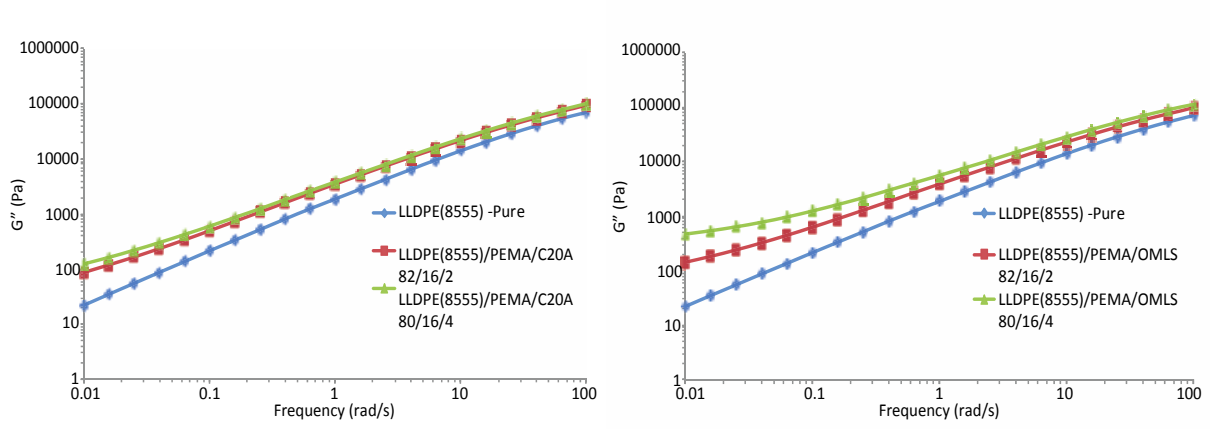

Figure 4-17 – Loss modulus (G") versus frequency for LLDPE (8555) and LLDPE (8555) nanocomposite prepared by in-house organo-modified clay and Cloisite 20A containing 2 and 4 wt % of nanoclay

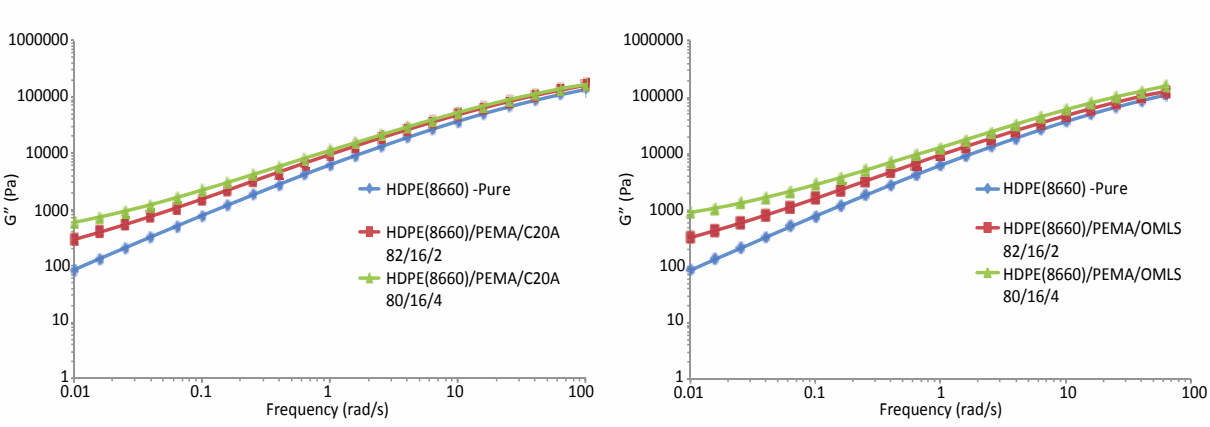

Figure 4-18 – Loss modulus (G") versus frequency for HDPE (8660) and HDPE (8660) nanocomposite prepared by in-house organo-modified clay and Cloisite 20A containing 2 and 4 wt % of nanoclay

4-4. Conclusion

An alkyl ammonium salt (DDAB), was used as a surfactant to increase the basal spacing of the layered silicates, enhanced the dispersion of the layered silicate in the PE matrix. Organo-modified layered silicates exhibited a higher thermal stability and also higher basal spacing of layered silicates with increased surfactant concentration. An optimum of surfactant concentration

is required to enhance properties, as found by the XRD and TGA characterization of the in-house organo-modified clay nanocomposites. Furthermore, the organo-modified clay with the optimum surfactant concentration must be used for melt mixing with the LLDPE and HDPE matrices and compatibilizer in the batch mixer. The same conditions were used for the preparation of commercially available organo-modified clay. The observations indicated that the in-house organo-modified clay was dispersed perfectly in the matrix, as compared to Cloisite 20A at a lower nanoclay loading. Modified clay, however, was dispersed into aggregates without a significant increase in the basal spacing of the PE nanocomposites with higher nanoclay content. As a result, the mechanical properties and modulus of the LLDPE/OMLS nanocomposites slightly improved in comparison to the LLDPE/C20A nanocomposite. Further investigation into the mechanical properties of all nanocomposites prepared by OMLS and C20A have shown that the compatibilizer used in this study has a better incorporation with the LLDPE compared to the HDPE since, as this compatibilizer has LLDPE as its backbone.

4-5. References

1. Xi Y, Frost RL, He H, Kloprogge T, Bostrom T. Modification of Wyoming montmorillonite surfaces using a cationic surfactant. Langmuir. 2005;21(19):8675-80.

2. Seyidoglu T, Yilmazer U. Production of modified clays and their use in polypropylene‐based nanocomposites. Journal of Applied Polymer Science. 2013;127(2):1257-67.

3. Sinha Ray S, Okamoto M. Polymer/layered silicate nanocomposites: a review from preparation to processing. Progress in polymer science. 2003;28(11):1539-641.

4. Kojima Y, Usuki A, Kawasumi M, Okada A, Fukushima Y, Kurauchi T, et al. Mechanical properties of nylon 6-clay hybrid. Journal of Materials Research. 1993;8(05):1185-9.

5. Manias E, Touny A, Wu L, Strawhecker K, Lu B, Chung TC. Polypropylene/montmorillonite nanocomposites. Review of the synthetic routes and materials properties. Chemistry of Materials. 2001;13(10):3516-23.

6. Reichert P, Nitz H, Klinke S, Brandsch R, Thomann R, Mülhaupt R. Poly (propylene)/organoclay nanocomposite formation: influence of compatibilizer functionality and organoclay modification. Macromolecular Materials and Engineering. 2000;275(1):8-17.

7. Galgali G, Ramesh C, Lele A. A rheological study on the kinetics of hybrid formation in polypropylene nanocomposites. Macromolecules. 2001;34(4):852-8.

8. Fornes TD, Yoon PJ, Keskkula H, Paul DR. Nylon 6 nanocomposites: the effect of matrix molecular weight. Polymer. 2001;42(25):09929-40.

9. Hoffmann B, Dietrich C, Thomann R, Friedrich C, Mülhaupt R. Morphology and rheology of polystyrene nanocomposites based upon organoclay. Macromolecular rapid communications. 2000;21(1):57-61.

Chapter 5 – Powder Sintering of Polymer/Clay Nanocomposite

5-1. Introduction

Several studies discussed different aspects of rotational molding (1-3). One of the dominant areas of investigation is the coalescence of two particles, also called sintering, in a biaxially rotating heated mold (1). Sintering happens when two powder particles, at a high temperature and/or pressure, form a homogenous melt (4). The sintering process controls a major part of the final properties of the molded part. For instance, the mechanical properties of the final molded part can improve with a full powder particle coalescence, and consequently, complete disappearance of bubbles (2, 3). Understanding the sintering behavior of polymer powders can illustrate a fundamental knowledge of the rotomoldability of these materials.

Although polyethylene/clay nanocomposites were extensively studied for high-pressure industrial plastic processes, such as extrusion and injection molding (5, 6), the properties and the behaviors of these nanocomposites have not been investigated in low-shear processes, such as rotational molding. In general, adding nanoclay to the polymer matrix can cause a drastic increase in the zero shear viscosity of these materials, which is unfavorable for powder sintering and, consequently, also for the mechanical properties of the molded parts (7). In this study, the effects of PE properties and the addition of nanoclay on the sintering behavior are investigated using a microscopic approach under closely controlled conditions. Typically, coalescence occurs in a pool of polymer particles in rotational molding (1); however, this experiment studied the coalescence of two individual particles. The results can be used to explain the role of polymer nanocomposites' sintering behavior in rotational molding.

5-2. Powder Sintering Experiment

5-2-1. Powder Characterization

The sintering behavior of pure LLDPE (8555) and HDPE (8660) were compared with their nanocomposites (the compositions are presented in Table 3-2). The powder particles were only used to perform the sintering experiments; for this, the samples were sent to Imperial Oil, Canada (Sarnia, ON) for grinding nanocomposite to powder particles. The ground samples has the typical size used in rotational molding process.

5-2-2. Powder Sintering Experiment

The sintering experiments were performed using a METTLER FP82 hot stage, controlled by a METTLER FP90 central processor. The sintering process was observed using a CCD camera (Olympus DP80) connected to an Olympus (BX60) optical microscope. Pictures of the sintering sequence were taken at fixed time intervals and saved in an electronic format using cellSens digital imaging software. The sintering experiments were carried out at a constant temperature, with two particles of approximately equal diameter (~ 300 - 400 μm) placed on a glass slide. The isothermal experiments were performed at 130^0C, which is consistent with the sintering conditions of LLDPE and HDPE (1). Prior to placing the samples inside the hot stage, the temperature of the hot stage was set below the melting temperature of the samples (100^0C). The temperature was increased rapidly to the sintering condition (steady state occurred in 15 to 20 seconds). Isothermal conditions were chosen in this study, since the viscosity of materials and surface tension are not expected to vary during the experiment and the sintering behavior of the pure polyethylene and their nanocomposites can be more easily compared (1).

5-3. Powder Sintering Results and Discussions

A schematic of the sintering sequence for the two idealized particles is represented in Figure 5-1 where a_0, a, a_f and y are the initial particle radius, particle radius, final particle radius and neck radius, respectively. The ratio of the sintering neck radius (y) and average radius of the two particles (a) represent the dimensionless sintering neck growth (y/a) (1). As the sintering process continues, the two quantities, y and a, become equal and one single particle forms; consequently, the value of (y/a) approaches to one.

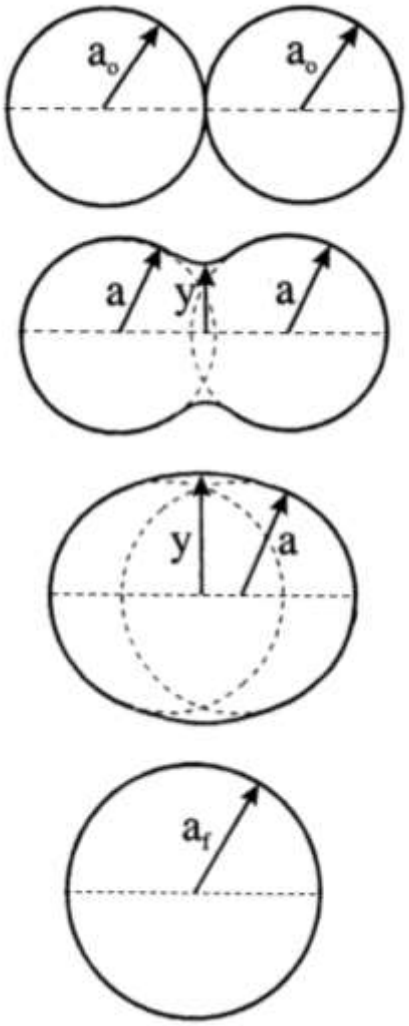

Figure 5-1 – Schematic of sintering sequence for two idealized particles, reproduced from (1)

Bellehumeur et al. illustrated that the shape of powder particles (irregular powder or cylinder) has no significant effect on the coalescence rate of the LLDPE and HDPE (1). In addition, the effect of the particle size has not been considered as only irregular powder particles, with approximately similar size, were used in the present study. A minimum of three experiments was carried out for each sample to ensure good reproducibility and to minimize the effect of particle shape on the sintering results. We expected that the addition of layered silicates in the PE matrix might have an impact on the sintering process. Consequently, the sintering experiments were performed on our PE nanocomposites with two different nanoclay loadings (2 wt % and 4 wt %), along with pure PE, to investigate the difference in their sintering behavior. The sintering neck radius (y) and average radius of the two particles (a) were measured using the image analysis software ImageJ. The dimensionless sintering neck growth (y/a) versus time for the pure PE and PE/clay nanocomposites is plotted in Figure 5-2 and 5-3. The average diameter of the particles in the sintering experiments is also reported on the same graph for clarity and completeness.

In all sintering experiments, the particles are in contact with the surface. Viscosity and adhesion forces become important. A previous study showed that the sintering process is derived mainly by the viscosity and surface tension of the particles. Viscous dissipation occurs over the volume of the sintering particles, while the surface tension acts only on the surface of the sintering system (1). Thus, the results for complex viscosity at zero shear rate are used in this study to elucidate the sintering behavior of our samples. The complex viscosity at low shear viscosity of our materials, represented in Figure 3-11 and Figure 3-12, revealed that pure HDPE (8660) has a higher viscosity than pure LLDPE (8555). This is due to the higher molecular weight of the HDPE (8660) as compared with that of LLDPE (8555) (Table 3-1). The sintering rate, therefore, was found to decrease when the zero shear viscosity (or molecular weight)

increased. This outcome is consistent with our expectations and previous studies (1). Furthermore, adding nanoclay increased the zero shear viscosity of the HDPE (8660) significantly (Figure 3-12). The sintering rate of nanocomposites exhibited drastic reductions with an increase in the amount of nanoclay loading (Figure 5-3). Interestingly, in our results, the complex viscosity of the LLDPE (8555)/clay nanocomposites only slightly increased (Figure 3-11) and the sintering rate of these materials demonstrated only a modest reduction as compare to pure matrix (Figure 5-2). Hence, nanocomposites prepared with LLDPE (8555) could be good candidates for the rotational molding process and further properties characterization is warranted.

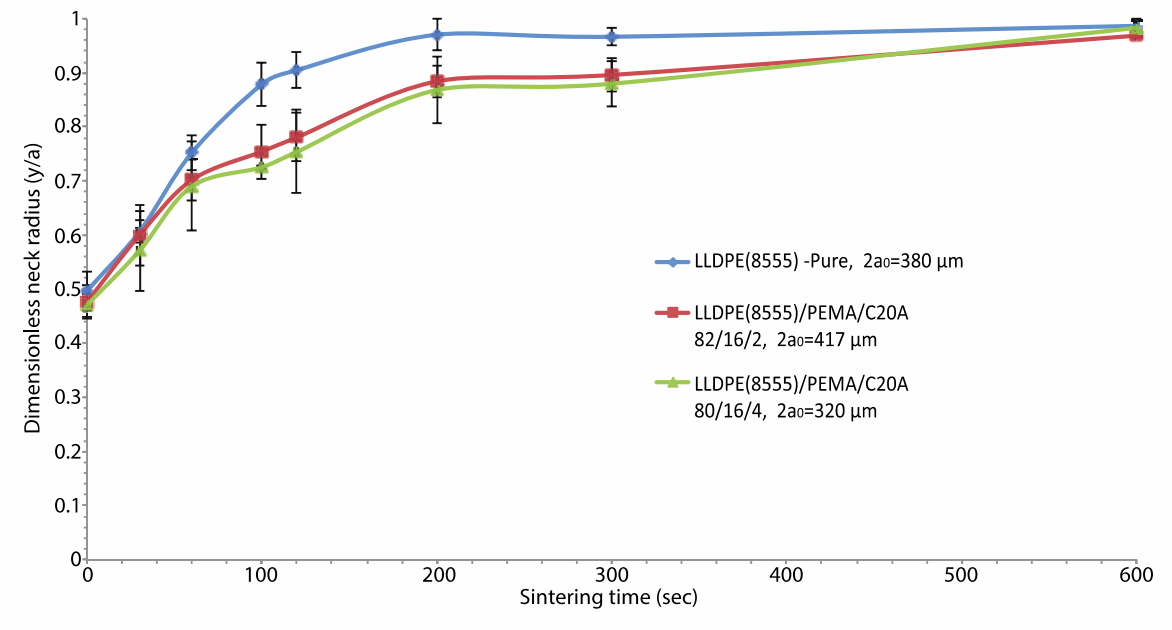

Figure 5-2 – Sintering of pure LLDPE (8555) and LLDPE (8555) nanocomposite containing different concentrations of nanoclay (Cloisite 20A)

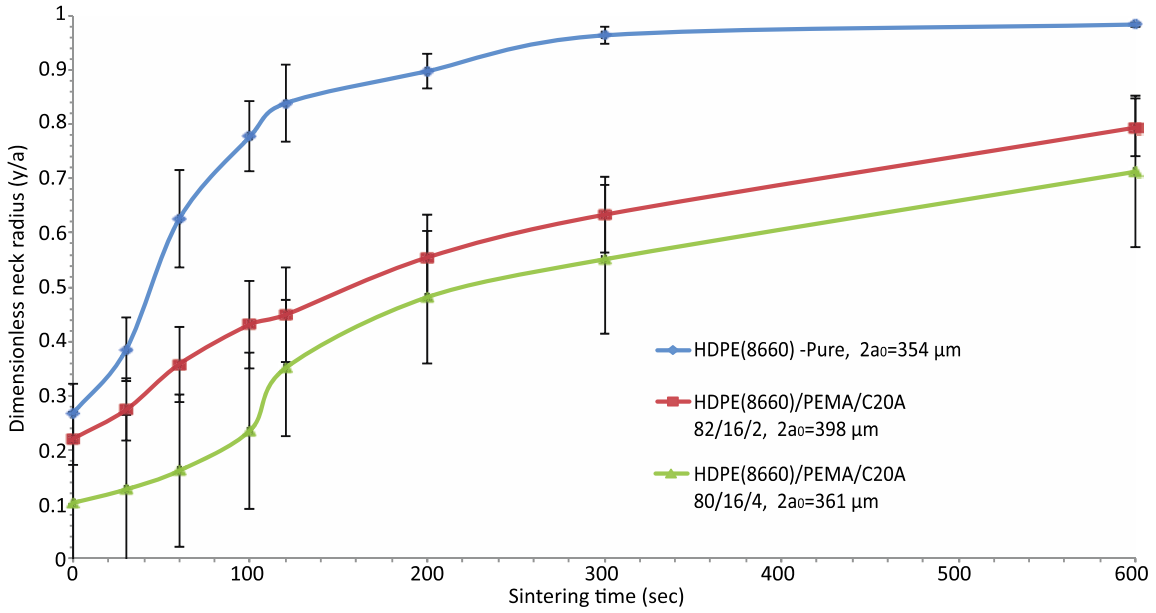

Figure 5-3 – Sintering of pure HDPE (8660) and HDPE (8660) nanocomposite containing different concentrations of nanoclay (Cloisite 20A)

The typical sintering sequence for pure LLDPE (8555) and HDPE (8660), at the temperature of 130^0C, are presented in Figure 5-4 (a) and Figure 5-5 (a), respectively. In addition, the sintering sequences of the PE nanocomposites are presented to visualize the effect of the nanoclay on the sintering behavior (2 wt % nanoclay in Figure 5-4 and 5-5 (b) and 4 wt % nanoclay in Figure 5-4 and 5-5 (c)). Based on the images, the pure polymer powder particles melt, as time increased, and the contour of the particles developed into a smooth and circular shape; and, the sintering process terminated after 600 seconds. On the other hand, the important difference between the pure PE and PE nanocomposites can be observed in the contour evolution of these samples. The interaction of the layered silicates with compatibilizer and the PE in the molecular level can result in variations of surface energy or adhesion properties of the powder particles (8). In addition, other parts of this work identified that the thermal behavior changed and specifically there was a reduction in the rate of the thermal degradation by adding layered silicates. The improvement in the thermal behavior of PE, however, can cause a lower sintering

rate, which is unfavorable for the rotational molding process. Hence, an optimum should be found between an improvement of thermal behavior and the sintering rate of nanocomposites.

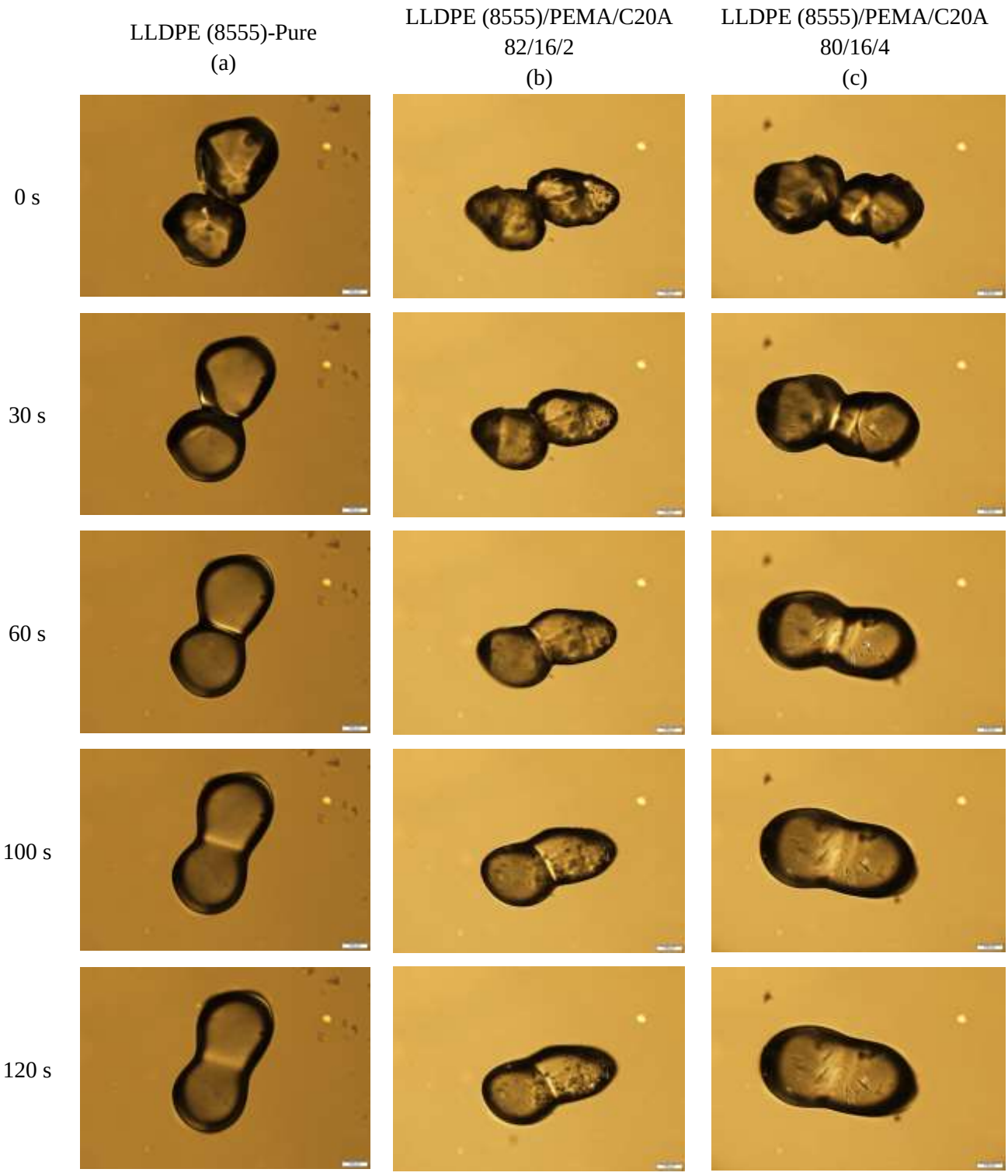

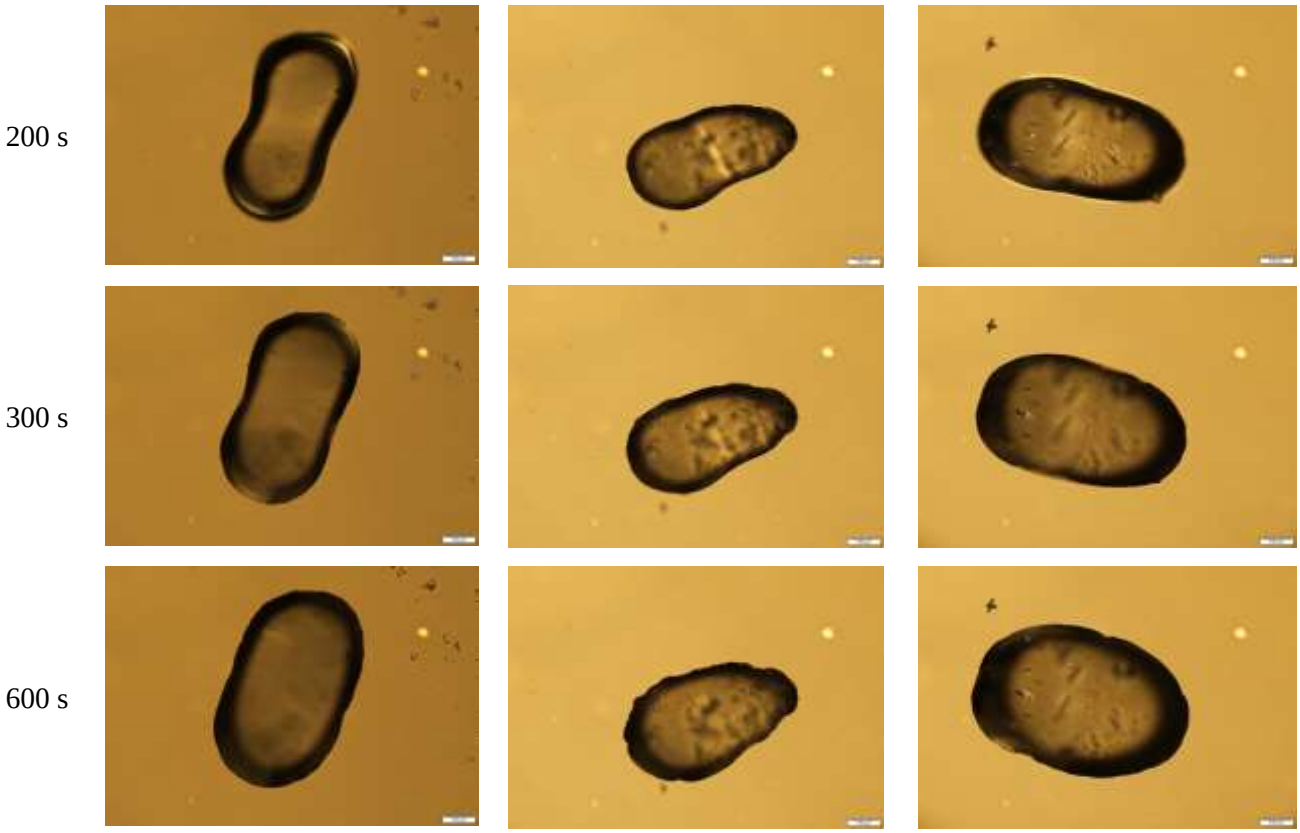

Figure 5-4 – Sintering sequence for pure LLDPE (8555) and LLDPE (8555) nanocomposite containing different concentrations of nanoclay (Cloisite 20A), powder particles at 130 ^{0}C, the scale bars indicate 100 μm

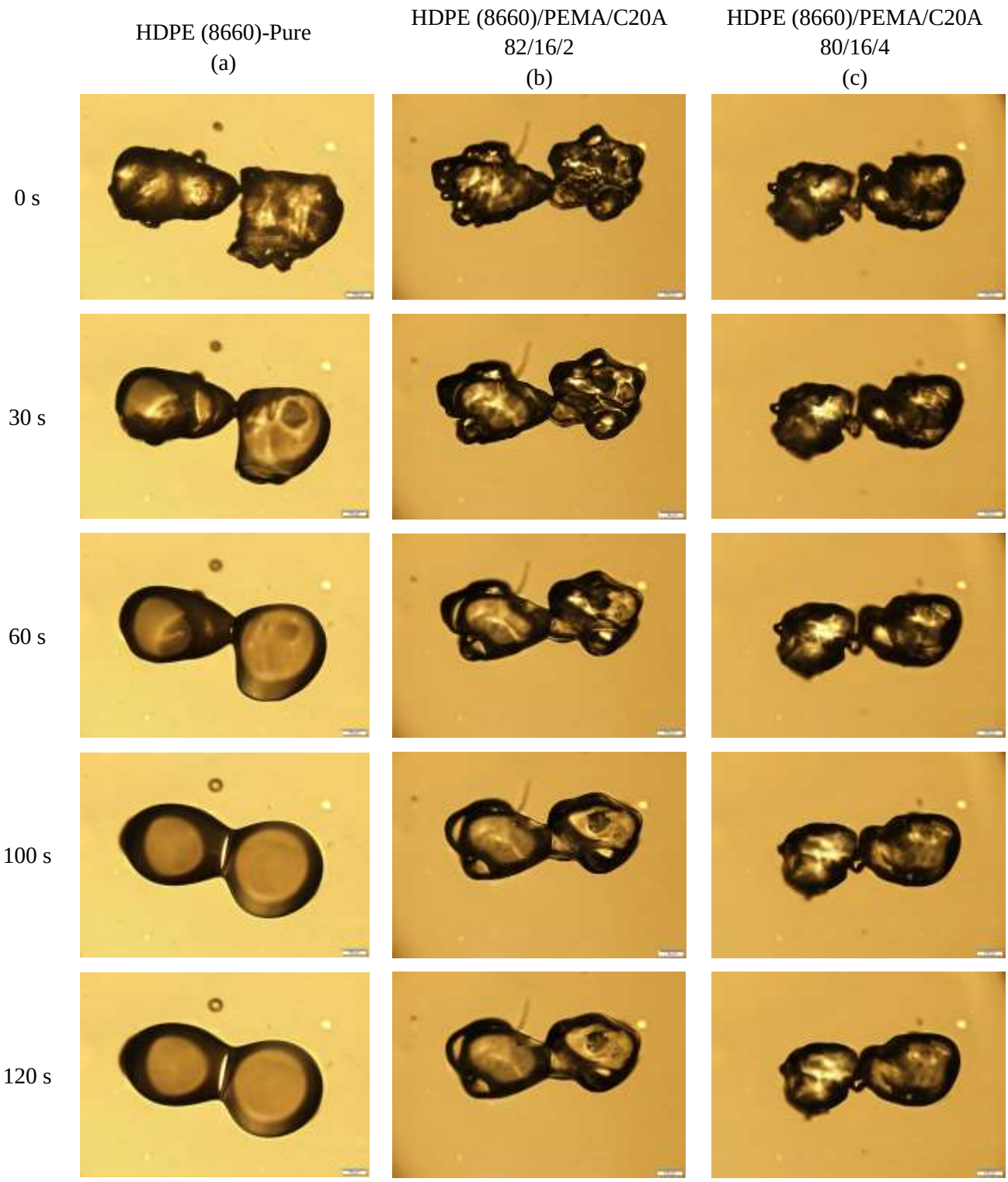
HDPE (8660)-Pure
(a)
HDPE (8660)/PEMA/C20A
82/16/2
(b)
HDPE (8660)/PEMA/C20A
80/16/4
(c)
0 s
30 s
60 s
100 s
120 s

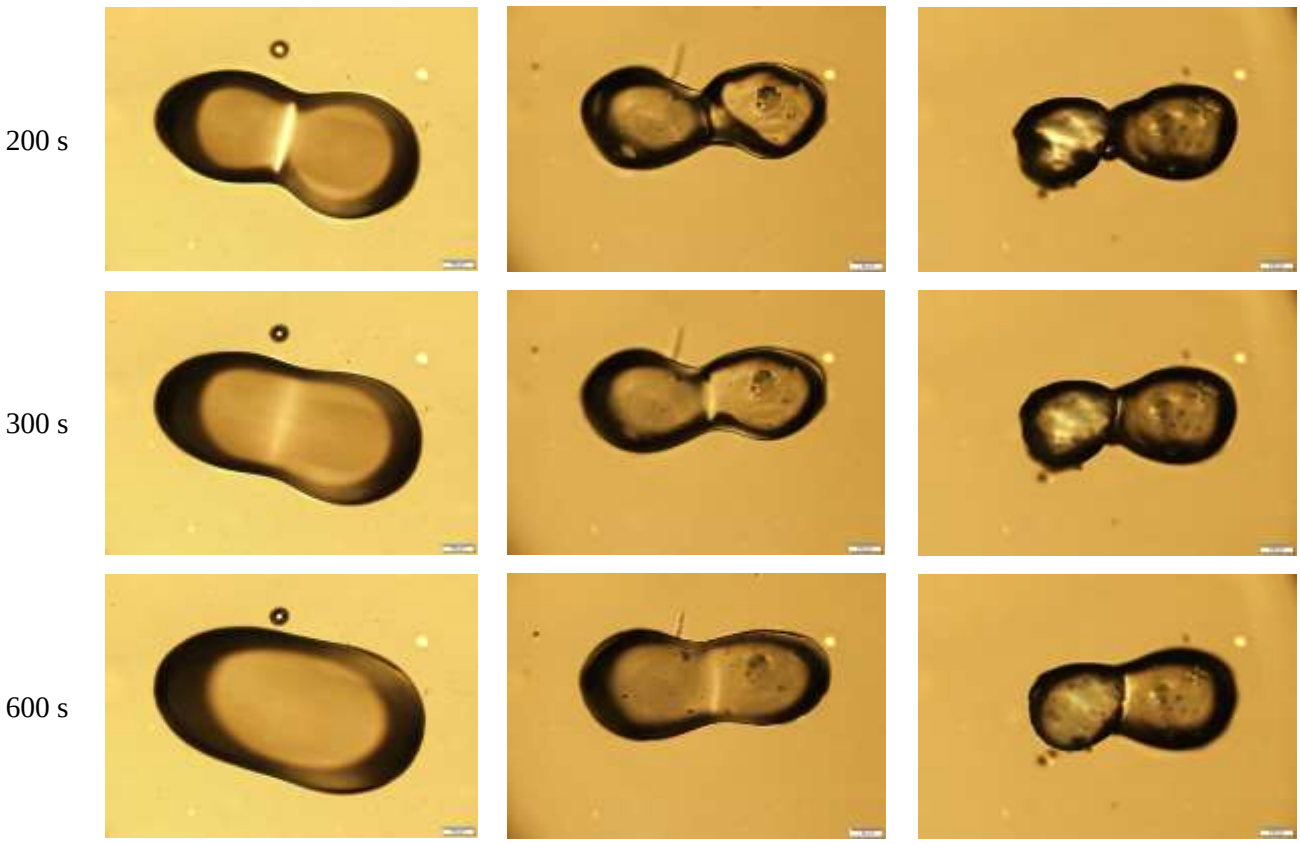

Figure 5-5 –Sintering sequence for pure HDPE (8660) and HDPE (8660) nanocomposite containing different concentrations of nanoclay (Cloisite 20A), powder particles at 130 ^{0}C, the scale bars indicate 100 μm

5-4. Conclusion

In this chapter, sintering experiments were conducted with powder particles of pure LLDPE, HDPE, and their nanocomposites, to investigate the sintering behavior of these materials. The experimental results showed that viscosity is an important factor in the sintering rate of polyethylene. Through our results, we found that high viscosity had a negative influence on the sintering rate. This effect was expected: as the molecular weight of the pure PE elevates, the viscosity also increases, and high molecular weight represents a resistance to the mobilization of the macromolecular chains. Furthermore, as the molecular weight and, consequently, the viscosity increase, the sintering rate decreases. This phenomenon is more pronounced with the addition of nanoclay, since the viscosity of the nanocomposites increases with the incorporation

of nanoclay. Nevertheless, the LLDPE nanocomposites prepared in this work showed only a slight reduction in the sintering rate. The results reveal that these materials may be good candidates for the rotational molding process and require further properties' characterizations.

5-5. References

1. Bellehumeur CT, Bisaria MK, Vlachopoulos J. An experimental study and model assessment of polymer sintering. Polymer Engineering & Science. 1996;36(17):2198-207.

2. Nugent PJ, Crawford RJ, Xu L. Computer prediction of cycle times during rotational molding of plastics. Advances in Polymer Technology. 1992;11(3):181-91.

3. Rao MA, Throne JL. Principles of rotational molding. Polymer Engineering & Science. 1972;12(4):237-64.

4. Bellehumeur CT, Kontopoulou M, Vlachopoulos J. The role of viscoelasticity in polymer sintering. Rheologica acta. 1998;37(3):270-8.

5. Zhang M, Sundararaj U. Thermal, rheological, and mechanical behaviors of LLDPE/PEMA/clay nanocomposites: effect of interaction between polymer, compatibilizer, and nanofiller. Macromolecular Materials and Engineering. 2006;291(6):697-706.

6. Shah RK, Paul DR. Organoclay degradation in melt processed polyethylene nanocomposites. Polymer. 2006;47(11):4075-84.

7. Martin D, Halley P, Truss R, Murphy M, Jackson O, Kwon OY. Polyethylene-layered silicate nanocomposites for rotational moulding. Polymer international. 2003;52(11):1774-9.

8. Wang WQ, Kontopoulou M. Effect of molecular structure on the rotational molding characteristics of ultra-low-density ethylene-α-olefin copolymers. Polymer Engineering & Science. 2004;44(3):496-508.

Chapter 6 – Conclusions and Future Work

6-1. Highlights and Conclusions

The aim of this study was to investigate the effect of layered silicates in polyethylene (PE) nanocomposites properties. Two grades of LLDPE and HDPE resins, with different characteristics, such as, molecular weight and density, were studied with the intent to support and verify some of the hypotheses that arose during this research. Most of the resins studied were of rotational molding grades, since this work is part of a project focused on the rotational molding process. The melt mixing method, which is both industrially and environmentally friendly was used to prepare the nanocomposites with compatibilizer and different nanoclay loadings. Subsequently, the nanocomposites were characterized using XRD, TEM images and mechanical and rheological techniques. The XRD results, parallel to the TEM images, revealed a uniform dispersion of the layered silicates within the LLDPE nanocomposites at small nanoclay loadings (2 wt %). Through other characterization techniques, the results illustrate that the thermal resistance and rheological properties of the PE/clay nanocomposites were enhanced through the incorporation of layered silicates. In addition, the molecular characteristics of the PE/clay nanocomposites, such as crystallinity, affected the analysis of the mechanical properties; however, a simple trend could not be identified for the mechanical properties of the nanocomposites. Overall, through analyzing some important properties of the nanocomposites, we found that the compatibilizer with LLDPE as a backbone has a compatibility with LLDPE as compared to HDPE.

In this study, the in-house organo-modified layered silicates were prepared by an ion exchange reaction, with an alkyl ammonium salt as the cationic surfactant. Through this reaction, the hydrophilic silicate was modified to become an organophilic one and thus, the cohesive

forces among layered silicates decreased. The organo-modified clay with the optimum surfactant concentration found with the TGA and XRD analysis was then used for melt mixing with the LLDPE and HDPE matrices and compatibilizer. Thereafter, the properties of the nanocomposites prepared with in-house organo-modified clay and commercial organo-modified clay were investigated through XRD, mechanical and rheological techniques. Our observations, through the XRD, illustrated that the in-house organo-modified clay was dispersed very well in the LLDPE matrix as compared to the commercially available nanoclay at lower nanoclay loading. As a result, the mechanical properties and modulus of the LLDPE nanocomposites, prepared by in-house OMLS, were higher than those of other nanocomposites.

At the end, the shear viscosity results obtained from the rheological characterization technique, combined with sintering experiments, were used to study the sintering behavior of pure PE and to determine how the addition of nanoclay to PE nanocomposite affected sintering behavior. The sintering experiments were carried out at isothermal conditions using powder particles. The sintering observations, along with rheological characterization, provided information about the effect of the pure polymer characteristics on the sintering process. Essentially, increasing the molecular weight was found to increase the zero shear viscosity and, consequently, had a negative effect on the sintering phenomenon. Furthermore, the sintering rate decreased due to the addition of nanoclay to the PE matrices. This behavior was predicted based on the solid-like behavior of the nanocomposites observed at the zero shear viscosity. Interestingly, this study found that the LLDPE nanocomposites prepared in this work showed only a slight reduction in the sintering rate, which reveals that these materials, with our formulation, are viable candidates for the rotational molding process and further properties characterization.

6-2. Future work

1. Employ different process conditions to take advantages of applied shear on the layered silicates and in turn, on the morphology of nanocomposites.
2. Investigate different compatibilizers and compositions to obtain a better dispersion of nanoclay and a stronger interaction between the nanocomposites' components.
3. Incorporate other surfactants for the organo-modification of the layered silicates to obtain a desired thermal stability and basal spacing. Alternative surfactant would include alkyl phosphonium salts and surfactants with different alkyl chain structures.
4. Consider other molecular characteristics, such as molecular weight distribution, on the sintering rate, using a wider range of pure PE resins.
5. Compare the results of sintering experiments against the results of the actual rotational molding process. The investigation of the sintering behavior of only two powder particles might not represent the sintering behavior of a pool of powder particles.
6. Perform the lab-scale rotational molding on the nanocomposites and analyze the mechanical and permeability measurements of the final products.

Appendix – Error Analysis

1. Error analysis for tensile test measurements

Here are some examples of average properties and standard deviation calculation for tensile properties and sintering experiment Figures in this Master dissertation:

Figure 3-19 – *Young's Modulus* of LLDPE (8555)/clay nanocomposite containing 2 wt % of nanoclay (Cloisite 20A).

Young's Modulus (MPa)	Average *Young's Modulus* (MPa)	Standard Deviation
136.87, 140.06, 139.05	138.66	1.63

Figure 3-20 – *Yield Strength* of LLDPE (8555)/clay nanocomposite containing 4 wt % of nanoclay (Cloisite 20A).

Yield Strength (MPa)	Average *yield Strength* (MPa)	Standard Deviation
17.59, 17.35, 17.24	17.36	0.181

Figure 3-21 – *Elongation at break* of LLDPE (8555)/clay nanocomposite containing 4 wt % of nanoclay (Cloisite 20A).

Elongation at break (%)	Average *elongation at break* (%)	Standard Deviation
656.93, 622.39, 642.93	622.39	27.37

Figure 5-2 – Sintering of LLDPE (8555)/clay nanocomposite containing 4 wt % of nanoclay (Cloisite 20A) at 30 sec.

Dimensionless neck radius	Average dimensionless neck radius	Standard deviation
0.33, 0.57, 0.53	0.48	0.13